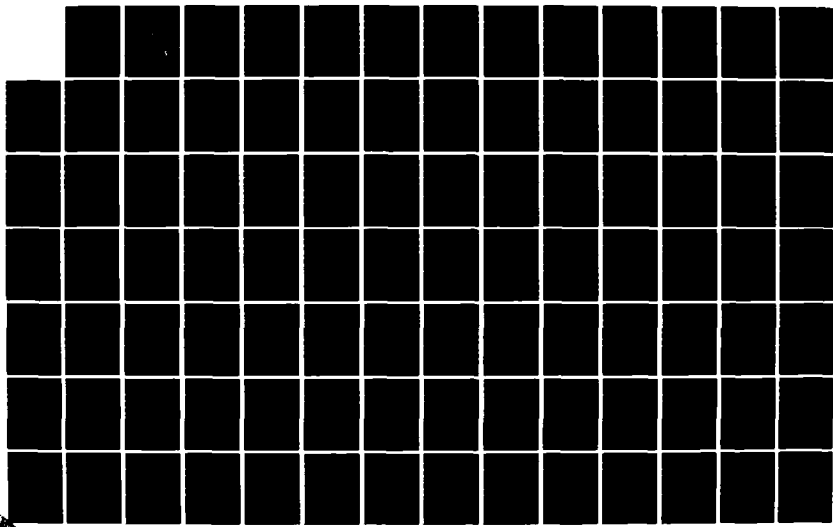


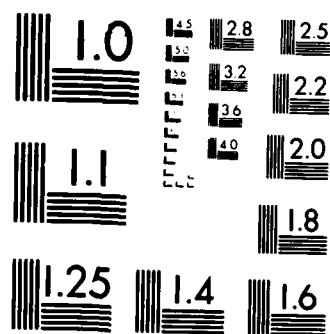
AD-R150 781 OBSERVATIONS OF THE CALIFORNIA COUNTERCURRENT (U) NAVAL
POSTGRADUATE SCHOOL MONTEREY CA R L HARROD JUN 84 1/2

UNCLASSIFIED

F/G 8/3

NL





MICROCOPY RESOLUTION TEST CHART
NATIONAL BUREAU OF STANDARDS-1963-A

AD-A150 781

NAVAL POSTGRADUATE SCHOOL

Monterey, California



THESIS

OBSERVATIONS OF THE
CALIFORNIA COUNTERCURRENT

by

Robert L. Harrod

June 1984

Thesis Advisors:

J. B. Wickham
S. P. Tucker

DTIC
SELECTED

MAR 4 1985

S D
D

AMC FILE COPY

Approved for public release; distribution unlimited.

UNCLASSIFIED

SECURITY CLASSIFICATION OF THIS PAGE (When Data Entered)

REPORT DOCUMENTATION PAGE		READ INSTRUCTIONS BEFORE COMPLETING FORM	
1. REPORT NUMBER	2. GOVT ACCESSION NO.		
AD-A150781			3. RECIPIENT'S DATA CODE NUMBER
4. TITLE (and Subtitle)	5. TYPE OF REPORT & PERIOD COVERED		
Observations of the California Countercurrent	Master's Thesis June 1984		
7. AUTHOR(s)	6. PERFORMING ORG. REPORT NUMBER		
Robert L. Harrod	8. CONTRACT OR GRANT NUMBER		
9. PERFORMING ORGANIZATION NAME AND ADDRESS	10. PROGRAM ELEMENT PROJECT TASK AREA & WORK UNIT NUMBERS		
Naval Postgraduate School Monterey, California 93943			
11. CONTROLLING OFFICE NAME AND ADDRESS	12. REPORT DATE		
Naval Postgraduate School Monterey, California 93943	June 1984		
14. MONITORING AGENCY NAME & ADDRESS (if different from Controlling Office)	13. NUMBER OF PAGES		
	147		
	15. SECURITY CLASS. FOR THIS REPORT		
	UNCLASSIFIED		
	16. DECLASSIFICATION/DOWNGRADING SCHEDULE		
16. DISTRIBUTION STATEMENT (of this Report)	Accession For <input checked="" type="checkbox"/> NTIS GRA&I <input type="checkbox"/> DTIC TAB <input type="checkbox"/> Unannounced <input type="checkbox"/> Justification		
Approved for public release; distribution unlimited.			
17. DISTRIBUTION STATEMENT (of the abstract entered in Block 20, if different from Report)	By _____ Distribution/ Availability Codes		
18. SUPPLEMENTARY NOTES	Avail and/or Dist Special R-1 .		
19. KEY WORDS (Continue on reverse side if necessary and identify by block number)			
California Countercurrent, California Undercurrent, Davidson Current, California Current, Eastern boundary currents, metered currents.			
20. ABSTRACT (Continue on reverse side if necessary and identify by block number)	Results from moored current meters, 150-350 m, are described for a region over the continental slope off Cape San Martin, from January 1979 to April 1980. Current vector time series were constructed from the data and compared to the local coastal upwelling index. Progressive vector diagrams were also constructed, and spectrum analysis was performed for alongshore		

UNCLASSIFIED

SECURITY CLASSIFICATION OF THIS PAGE (When Data Entered)

and cross-slope currents.

The California Countercurrent was found to be present in the study area during the entire period. Seasonally, the countercurrent was substantially stronger during the spring. Frequent current reversals and oscillations occurred between equatorward and poleward flow, less often at the nearshore station. Preferred low frequency energy peaks were found at periods of about 10 days. The intensity of the countercurrent increased with increasing coastal upwelling index, and the cross-slope flow also appeared to be related to the local coastal upwelling index.

02-114-6601

2

UNCLASSIFIED

SECURITY CLASSIFICATION OF THIS PAGE (When Data Entered)

Approved for public release; distribution unlimited.

Observations of the
California Countercurrent

by

Robert L. Harrod
Lieutenant Commander, United States Navy
B.S., Oregon State University, 1975

Submitted in partial fulfillment of the
requirements for the degress of

MASTER OF SCIENCE IN METEOROLOGY AND OCEANOGRAPHY

from the

NAVAL POSTGRADUATE SCHOOL
June 1984

Author:

Robert L. Harrod

Approved by:

Jacob B. Wicksom

Thesis Co-Advisor

Stevens P. Tucker

Thesis Co-Advisor

T. M. Dyer / Chairman
Chairman, Department of Oceanography

J. M. Dyer
Dean of Science and Engineering

ABSTRACT

Results from moored current meters, 150 - 350 m, are discussed for a region over the continental slope off Cape San Martin, California from January 1979 to April 1981.

Current vector time series were constructed from the data and compared to a local upwelling index. Progression vector diagrams of the data were also constructed, and spectrum analysis was performed for alongshore and cross-slope currents.

The California Countercurrent was found to be present in the study area during the entire period. Seasonally, the countercurrent was substantially stronger during the spring. Frequent current reversals and oscillations occurred between equatorward and poleward flow, less often at the nearshore station. Preferred low frequency energy peaks were found at periods of about 10 days. The intensity of the countercurrent increased with increasing coastal upwelling index, and the cross-slope flow also appeared to be related to the local coastal upwelling index.

TABLE OF CONTENTS

I.	INTRODUCTION AND BACKGROUND -----	12
II.	DIRECT CURRENT OBSERVATIONS -----	20
	A. DATA COLLECTION -----	20
	B. DATA PROCESSING -----	21
III.	STUDY OBJECTIVES -----	24
IV.	DESCRIPTION AND ORGANIZATION OF GRAPHICS -----	25
V.	ANALYSIS -----	28
	A. RELATION BETWEEN CURRENT AND LOCAL WIND FORCING -----	28
	1. Analysis at Station 2 -----	29
	2. Analysis at Station 7 -----	31
	3. Comparison of Stations 2 and 7 -----	32
	B. SPECTRUM ANALYSIS -----	34
	C. INFERENCES FROM PROGRESSIVE VECTOR DIAGRAMS -----	36
	D. CROSS-SLOPE CURRENT -----	41
	E. TIME SERIES -----	41
VI.	CONCLUSIONS -----	43
APPENDIX A:	TIME SERIES PLOTS -----	71
APPENDIX B:	SPECTRUM ANALYSES OF ALONGSHORE FLOW AND ON/OFFSHORE FLOW -----	75
APPENDIX C:	PROGRESSIVE VECTOR DIAGRAMS -----	91
APPENDIX D:	COMPUTER PROGRAM LISTINGS -----	107
LIST OF REFERENCES -----		143
INITIAL DISTRIBUTION LIST -----		146

LIST OF TABLES

TABLES	PAGE
I. Comparison of high energy peaks-----	37
II. Comparison of mean current and temperature-----	38

LIST OF FIGURES

FIGURES	PAGE
1. The study area-----	45
2. Chronology of current meter deployment-----	46
3. Vertical section showing representative locations of current meters off Cape San Martin, California-----	47
4. Current meter array-----	48
5. Mean onshore currents-----	49
6. Mean temperatures at Station 2-----	50
7. Mean temperatures at Station 7-----	51
8. Point Sur Upwelling Index and stickplots of hourly current vectors for the current meters at Station 7 deployed on 5 January 1979-----	52
9. U component, V component, and temperature plots versus time for the current meter at 152 m depth at Station 7 deployed on 5 January 1979-----	53
10. U component, V component, and temperature plots versus time for the current meter at 223 m depth at Station 7 deployed on 5 January 1979-----	54
11. Point Sur Upwelling Index and stickplots of hourly current vectors for the current meters at Station 2 deployed on 23 April 1979-----	55
12. U component, V component, and temperature plots versus time for the current meter at 169 m depth at Station 2 deployed on 23 April 1979-----	56
13. U component, V component, and temperature plots versus time for the current meter at 241 m depth at Station 2 deployed on 23 April 1979-----	57
14. Point Sur Upwelling Index and stickplots of hourly current vectors for the current meters at Station 7 deployed on 7 July 1979-----	58
15. U component, V component, and temperature plots versus time for the current meter at 158 m depth at Station 7 deployed on 7 July 1979-----	59

16.	U component, V component, and temperature plots versus time for the current meter at 131 m depth at Station 7 deployed on 7 July 1979-----	61
17.	U component, V component, and temperature plots versus time for the current meter at 356 m depth at Station 7 deployed on 7 July 1979-----	61
18.	Point Sur Upwelling Index and stickplots of hourly current vectors for the current meters at Station 2 deployed on 21 July 1979-----	62
19.	U component, V component, and temperature plots versus time for the current meter at 165 m depth at Station 2 deployed on 21 July 1979-----	63
20.	U component, V component, and temperature plots versus time for the current meter at 237 m depth at Station 2 deployed on 21 July 1979-----	64
21.	Point Sur Upwelling Index and stickplots of hourly current vectors for the current meters at Station 7 deployed on 7 October 1979-----	65
22.	U component, V component, and temperature plots versus time for the current meter at 127 m depth at Station 7 deployed on 7 October 1979-----	66
23.	U component, V component, and temperature plots versus time for the current meter at 200 m depth at Station 7 deployed on 7 October 1979-----	67
24.	Point Sur Upwelling Index and stickplots of hourly current vectors for the current meters at Station 2 deployed on 24 November 1979-----	68
25.	U component, V component, and temperature plots versus time for the current meter at 194 m depth at Station 2 deployed on 24 November 1979---	69
26.	U component, V component, and temperature plots versus time for the current meter at 265 m depth at Station 2 deployed on 24 November 1979-----	70
27.	Point Sur Upwelling Index and stickplots of hourly current vectors for the current meters at Station 7 deployed on 3 March 1980-----	71
28.	U component, V component, and temperature plots versus time for the current meter at 113 m depth at Station 7 deployed on 3 March 1980-----	72

19. U component, V component, and temperature plots versus time for the current meters at 187 m depth at Station 7 deployed on 3 March 1980----- 73
30. U component, V component, and temperature plots versus time for the current meter at 311 m depth at Station 7 deployed on 3 March 1980----- 74
31. Energy density spectrum of current meter at 152 m depth at Station 7 deployed on 5 January 1979----- 75
32. Energy density spectrum of current meter at 223 m depth at Station 7 deployed on 5 January 1979----- 76
33. Energy density spectrum of current meter at 169 m depth at Station 2 deployed on 23 April 1979----- 77
34. Energy density spectrum of current meter at 241 m depth at Station 2 deployed on 23 April 1979----- 78
35. Energy density spectrum of current meter at 152 m depth at Station 7 deployed on 7 July 1979----- 79
36. Energy density spectrum of current meter at 231 m depth at Station 7 deployed on 7 July 1979----- 80
37. Energy density spectrum of current meter at 356 m depth at Station 7 deployed on 7 July 1979----- 81
38. Energy density spectrum of current meter at 165 m depth at Station 2 deployed on 21 July 1979----- 82
39. Energy density spectrum of current meter at 237 m depth at Station 2 deployed on 21 July 1979----- 83
40. Energy density spectrum of current meter at 127 m depth at Station 7 deployed on 7 October 1979----- 84
41. Energy density spectrum of current meter at 200 m depth at Station 7 deployed on 7 October 1979----- 85
42. Energy density spectrum of current meter at 194 m depth at Station 2 deployed on 24 November 1979--- 86
43. Energy density spectrum of current meter at 265 m depth at Station 2 deployed on 24 November 1979--- 87
44. Energy density spectrum of current meter at 113 m depth at Station 7 deployed on 3 March 1980----- 88

45. Energy density spectrum of current meter at 127 m depth at Station 7 deployed on 3 March 1980----- 89
46. Energy density spectrum of current meter at 311 m depth at Station 7 deployed on 3 March 1980----- 90
47. Progressive vector diagram for the current meter at 127 m depth at Station 7 from 9 January to 28 February 1979----- 91
48. Progressive vector diagram for the current meter at 223 m depth at Station 7 from 9 January to 28 February 1979----- 92
49. Progressive vector diagram for the current meter at 109 m depth at Station 2 from 24 April to 13 June 1979----- 93
50. Progressive vector diagram for the current meter at 241 m depth at Station 2 from 24 April to 12 June 1979----- 94
51. Progressive vector diagram for the current meter at 158 m depth at Station 7 from 9 July to 30 August 1979----- 95
52. Progressive vector diagram for the current meter at 231 m depth at Station 7 from 9 July to 29 August 1979----- 96
53. Progressive vector diagram for the current meter at 356 m depth at Station 7 from 9 July to 30 August 1979----- 97
54. Progressive vector diagram for the current meter at 109 m depth at Station 2 from 13 July to 13 September 1979----- 98
55. Progressive vector diagram for the current meter at 237 m depth at Station 2 from 23 July to 13 September 1979----- 99
56. Progressive vector diagram for the current meter at 127 m depth at Station 7 from 9 October to 29 November 1979----- 100
57. Progressive vector diagram for the current meter at 200 m depth at Station 7 from 9 October to 29 November 1979----- 101

58. Progressive vector diagram for the current meter
at 109 m depth at Station 2 from 27 November 1979
to 16 January 1980----- 112
59. Progressive vector diagram for the current meter
at 266 m depth at Station 2 from 27 November 1979
to 18 January 1980----- 113
60. Progressive vector diagram for the current meter
at 311 m depth at Station 7 from 4 March to
15 April 1980----- 114
61. Progressive vector diagram for the current meter
at 186 m depth at Station 7 from 4 March to
12 April 1980----- 115
62. Progressive vector diagram for the current meter
at 311 m depth at Station 7 from 4 March to
19 April 1980----- 116

I. INTRODUCTION AND BACKGROUND

Eastern boundary currents are the subject of scientific investigation for a variety of reasons, particularly the impact of these currents on the fishing industry. Ryther (1969) concluded certain fishing grounds such as those off Peru, California, northwest and southwest Africa, Somalia, and the Arabian coast are so fertile, that they supply over half of the world's fish harvest, yet constitute less than one percent of the oceans. These fishing grounds are invariably located close to shore, and their great fertility is due to frequent replenishment of near-surface nutrients from a few hundred meters deep in the open ocean offshore. The primary process for this is coastal upwelling, which in the Western Hemisphere is associated most markedly with the eastern boundary currents off North and South America. The economic need to understand these currents is made evident by the devastation of the coastal regions of Ecuador and Peru in 1982-1983 by the sudden influx of warm water termed El Niño. The socioeconomic effects included; flooding, landslides, destruction of transportation facilities, huge agricultural losses, disturbance of coastal fisheries, and loss of life (Halpern et al., 1983). This warm water influx takes place from

time-to-time, and recovery from a severe occurrence may take several years (Smith 1983).

Off the North American west coast, the eastern boundary flow regime is known as the California Current System. A comprehensive summary of the present knowledge of this system is given by Hickey (1978). The California Current System includes the southward flowing California Current, and a number of manifestations of a counter-flow: the California Undercurrent, the Davidson Current, and the Southern California Countercurrent. This system is part of the general circulation of the North Pacific Ocean which is dominated by an oceanwide, clockwise circulation known as the North Pacific Gyre. The eastern limb of the gyre is the California Current System, which extends along the North American continent from southern Canada to Mexico. The system includes both poleward and equatorward flows which vary on many time-scales. There are, for example, inter-annual variations such as El Niño, seasonal variations, and large variations with periods associated with weather systems. The California Current is a slow and broad equatorward surface flow, branching from the North Pacific Current, and marked by cold subarctic water type. The waters of the various countercurrents may be characterized by their admixture with water of equatorial origin which has relatively high levels of temperature, salinity and phosphate, and relatively low dissolved

oxygen. During the winter months a surface current with poleward flow occurs in nearshore regions off the west coast of the United States. This current, inshore of the California Current, is known as the Davidson Current and is ordinarily found north of Point Conception. The Davidson Current may be a surface manifestation of the California Undercurrent. The Southern California Countercurrent is the name applied to the poleward flow from San Diego to Point Conception; during winter months, this nearshore flow is sometimes continuous with the Davidson Current.

The study of eastern boundary currents is of both theoretical and practical interest. Dynamical models with features of observed eastern boundary currents have been developed since the turn of the century. Ekman (1905) described the effects of a steady wind blowing on an ocean, and stated the concepts now known as the Ekman spiral and the Ekman transport. Sverdrup, Johnson, and Fleming (1941) provided some understanding of the dynamics of the upwelling process. Munk (1950) computed the mass transports in a wind-driven ocean from the curl of the estimated wind stress.

Recent models include the two-dimensional and three-dimensional upwelling models, and sea breeze produced upwelling models reviewed by O'Brien (1977). These models considered the influences of horizontal boundaries, bottom topography, and the variability of wind stress on the

ocean. The first numerical model of coastal upwelling was constructed by O'Brien and Hurlburt (1972); this two-layer model successfully predicted the observed equatorward jet but failed to produce a poleward undercurrent. Suginohara (1974) used a model with a straight coast and a bottom topography which did not vary in a coastwise direction. His model succeeded in developing a poleward flow in the lower layer. A later review of models is given by Allen (1980). These models permit inferences, such as the effects of shelf width and coastal winds, to be made about shelf-flow motions which have time scales like those of the atmospheric weather systems which drive them. Irregularities of the coastline and bottom topography force three-dimensional motions. However, there has been little theoretical work in this area until recently. An important conclusion from the models is that the currents arise from and are maintained by both local and remote atmospheric forcing. Significantly improved models of coastal upwelling include more realistic wind stress and finer resolution of bottom topography, especially the shelf break and steep bottom slopes.

Complementing models are field experiments which provide the basis for their motivation and verification. Two recent comparisons of models to field observations are Hickey (1980) and Janowitz (1980). Hickey used the two-dimensional, baroclinic, time-dependent model of

Hamilton (1978) and found it to be effective for time periods as long as fifteen days in predicting the displacement of isopycnals off the Oregon coast. Janowitz's comparison of a model of time-dependent quasi-geostrophic upwelling to moored meter data concluded tentatively that the model may have some validity, but further comparisons and verification should be undertaken.

Early observational studies of the California Current System emphasized relatively large-scale motions. Sverdrup and Fleming (1941) utilized T-S relationships to define the origins of water of two sorts (in northern hemispheric eastern boundary flows): northern water with increasing salinity as temperature decreases with depth and southern water with relatively constant salinity as temperature decreases. That the warmer water was a northward-flowing current was also demonstrated by Sverdrup and Fleming (1941) utilizing geostrophy; later, Reid, et al. (1958) showed that geo-strophic shear of the flow at the 200-dbar surface with respect to the 500 and the 1000-dbar surfaces indicates a northward flowing undercurrent. During the fifties and early sixties most Lagrangian current measurements were limited to drift bottle estimates of surface currents. One important exception was the tracking (for a few days) of deep drogues by Reid (1962), which also indicated a northward-flowing undercurrent off the central California coast. It is in the last decade that moored

current meters have provided a means to examine details of the flow over long time-periods. Moored current meters can be positioned to give direct measurements of the currents over extended periods (approximately two months for the Aanderaa meter, if a ten-minute sampling interval is used). Moored meters provide an excellent means for detailed local studies to elucidate better the properties, relationships, and interactions of the several portions of the California Current System. Studies of the California Current System during the 1960's using moored meters were primarily of the coastal waters off Oregon and Washington. While few current measurements have been made in the California Current and reliable wind stations are sparse, continuing studies off Washington and Oregon by Hickey (1979, 1980) and Huyer et al. (1979) show a significant relationship between local wind forcing and currents. Hickey stated that the seasonal variation of the nearshore region of strong flow appears to be related to the seasonal variation of the alongshore component of wind stress at the coast. Huyer et al. show that the transition from the predominantly northward surface currents of the winter oceanographic regime to the predominantly southward surface currents of the spring oceanographic regime over the Oregon continental shelf occurs within a period of several days during a strong southward wind event. Recent work for waters off the central region of the California

coast includes descriptive studies by Wickham (1975), Coddington (1979) and Dreves (1980). Wickham (1975) made salinity-temperature-depth (STD) sections, and parachute drogue observations off Monterey Bay. Wickham found the California Countercurrent to be present 15 km off the coast in August 1972 and in August 1973. Coddington (1979) compared direct current measurements from an array moored off Cape San Martin to indirect measurements from geostrophy. Coddington found the California Countercurrent to be present during the study period from November 1978 to February 1979. Dreves (1980) studied the relationship between local sea level gradient and alongshore flow for the same study period as Coddington. Dreves found that current and sea level gradient energy distributions were in close agreement, showing high energy concentration at the low frequency end of the spectrum.

The region of the central California coast off Cape San Martin (Figure 1) was chosen for study for several reasons: there is relatively little ship traffic or fishing and, consequently, less risk of current meter damage or loss; the bottom topography is relatively devoid of complications, consisting of an extremely narrow shelf, sharp shelf break, and depth contours approximately parallel to the coast; additionally, the close proximity of the study area to Monterey was a logistical convenience.

The current meter data used by Coddington and Dreves,

some six sets of current meter observations spanning six months from 25 July 1978 until 22 January 1979, have been augmented as part of the continuous monitoring of the countercurrent off Cape San Martin. An observational data base of direct current measurements of more than one year's duration now exists.

The objective of this study is to provide a preliminary analysis of current meter data for the period January 1979 to April 1980.

II. DIRECT CURRENT OBSERVATIONS

A. DATA COLLECTION

The data for this study were collected using Aanderaa Model RCM-4 recording current meters, which are self-recording and intended to be anchored in the ocean below the wind wave zone; they record current speed and direction and water temperature.

The meters were deployed off Cape San Martin, California, from August 1978 until July 1980 (see Figure 2). The station locations are shown in Figure 3. The present study covers the period from January 1979 to May 1980.

Coddington (1979) and Dreves (1980) have discussed data collected during the period from April 1978 to January 1979. Deployment of the arrays was accomplished with the Naval Postgraduate School's research vessel ACANIA. Each mooring of several meters was launched by being strung out behind the ship, the uppermost meter and flotation devices first and the anchor last. The array's descent was slowed by a small drogue about two meters in diameter attached to the anchor. An array of three meters was used at Station 2 ($35^{\circ} 52.16'N$, $121^{\circ} 33.76'W$) and four meters at Station 7 ($35^{\circ} 51.4'N$, $121^{\circ} 46.54'W$). They were arranged approximately as depicted in Figure 4. The anchor consisted of

one or two railroad wheels attached to an AMF-Sealink Model 242 acoustic release. Benthos 17-inch glass spheres in plastic hard hats (55 pounds net buoyancy each) were used to provide wire tension, with two spheres directly above each current meter and six above the release. The entire array was moored below the region of strong surface wave action and was recovered by acoustically activating the release. Upon recovery the meters were returned to the laboratory for maintenance prior to subsequent redeployment.

B. DATA PROCESSING

The data were recorded on three-inch reels of 1/4-inch audio tape (Scotch Brand number 295) at ten-minute sampling intervals. Conversion of the data from the tapes recorded by the RCM-4 meters into a computer-acceptable format was accomplished with a Hewlett-Packard 9845 computer and an Andoria tape translator. The 1/4-inch tape was played back on a Wollensach audio deck and an oscilloscope was used to give a visual confirmation that data were present and of appropriate amplitude. The data were then translated from long and short to high and low voltage pulses and recorded on IBM-compatible 9-track tape on a Kennedy 9-track tape recorder. The Hewlett-Packard 9345 computer was also used to plot and print portions of the data.

Five different programs were used with the Naval Postgraduate School's IBM 360 computer in processing the data. They are listed in Appendix D. The initial program reads in the raw data from the 9-track magnetic tape, allows an initial look at the data if desired, and stores the data in mass storage for quicker, more efficient utilization. The second program applies temperature, speed, and direction calibrations to the data for each current meter. The third program reads in the calibrated output from program two, identifies missing records, and uses established cut-off parameters to suppress noise. Temperatures greater than 12°C, and less than 5°C are discarded, along with current speeds in excess of 100 cm-s^{-1} . Discarded and missing records are filled in by the following process: upon encountering a faulty value, searching continues until a value is found that meets the acceptance criteria. Linear interpolation is used to obtain fill-in values. Initial looks at the data revealed only minimal gaps in the records. Program three, by means of a binomial, converts the data record from ten-minute values to hourly values and then produces four plots. Currents are presented in the form of stickplots, and three other plots display U and V components of the current (respectively, eastward and northward for positive values), and temperature as functions of time. The fourth program reads in the output of program two, fills in missing and

faulty records, and then performs a spectrum analysis of the data. Its output consists of two plots of frequency versus power density for onshore and alongshore components of current. The fifth program uses the hourly records produced in program three to construct progressive vector plots. Two of the current meters used in the study were very noisy and gave unrealistically high indications of the speed. These noisy data are not shown here.

III. STUDY OBJECTIVES

The objective of this study is to provide a preliminary analysis of the current meter data. Questions to be considered are:

1. Do the data reveal seasonal variations of the flow?
2. Do the data reveal differences or similarities in the flow between Stations 2 and 7?
3. Are there indications of mesoscale events?
4. Are such mesoscale events coherent with respect to depth and/or position?
5. Is there a generalization about variation with depth that can be made?
6. How do the currents appear to be related to Bakun's coastal upwelling index (Bakun, 1980)?

IV. DESCRIPTION AND ORGANIZATION OF GRAPHICS

To highlight the salient features of the variations, and to examine them in the framework of Section III the data are presented in several ways. There are seven different graphical representations in Appendices A, B, and C. These plots are:

1. Time series of Bakun's coastal upwelling index (Bakun, 1980).
2. Time series of current vectors.
3. Time series of eastward components of the current vectors.
4. Time series of northward components of the current vectors.
5. Time series of temperature.
6. Spectrum analyses of alongshore flow and on/offshore flow.
7. Progressive vector diagrams.

The plots are organized chronologically according to deployment date of the meters, beginning 5 January 1979 and ending in March 1980.

In Appendix A there are sets of time series. For example, Figure 8 and those like it contain time series of Bakun's coastal upwelling index (UI), and current series

(stickplots), in this case for the meters deployed on 5 January 1979 at Station 7, permitting visual comparison of one aspect of local forcing and the associated motions. The coastal upwelling indices are indicative of onshore-offshore Ekman transport, as estimated from wind stress at the position in the vicinity of Point Sur indicated in Figure 1. The procedure for calculating upwelling indices is presented in detail by Bakun (1973). The stickplots are graphical depictions of current speed and current direction. Time-scales are indicated along the top and bottom of Figure 5, and the units of measurement for the ordinates are shown on the left side of the figure. Pertinent information on the figures of this type include: station number, date of deployment, meter serial number, and depth of meter deployment.

Another type is represented by Figures 6 and 7. They depict U, V, and T for the two current meter records represented in Figure 8, where U (positive) is the eastward component of the current vector, V (positive) is the northward component of the current vector, and T is the temperature. Again, time scales and pertinent station information are given in the figure. The time series of these variables are complementary to the progressive vector diagrams found in Appendix C since they accentuate higher frequency events such as inertial and tidal oscillations.

The figures in Appendix B contain spectrum analyses of

alongshore flow and on/offshore flow for each current meter. The abscissa (frequency) and the ordinate (power density function) are clearly labeled, and each figure also lists station number, meter serial number, meter deployment depth, and date of deployment. The spectrum analyses indicate regions of high energy in the frequency domain and suggest forces at work.

Appendix C contains the progressive vector diagrams (PVD). The vertical and horizontal scales are equal (kilometers), and true North is indicated. Crosses are positioned at 3-day intervals, and the letter "F" indicates the final plotted position. In addition to station number, meter number, meter depth, and period of computation, the mean speed and mean direction for the entire period are indicated. The PVD's depict well the low frequency variations, so-called "events", such as eddies.

Appendix D contains the listings of the computer programs used to process and plot the current meter data.

V. ANALYSIS

A. RELATION BETWEEN CURRENT AND LOCAL WIND FORCING

The coastal mountains of California tend to deflect the low level winds so that they blow equatorward parallel to the coast. Consequently, the average Ekman transport is offshore (Stewart 1967). In the simple Ekman model, the offshore flow lies generally above the level at which our current meters are moored. But there are strong vertical motions (up-and-downwelling) and other intense mesoscale exchange mechanisms in the area of study which negate the application of the simple Ekman model to observed cross-slope flow and suggest the possibility of a deeper "virtual" Ekman layer extending well into the pycnocline.

In this section qualitative relations between current and local wind forcing are examined through use of the time series of stickplots and upwelling index and also by referring to Figure 5. These relations will first be examined separately at each mooring station, and then for the time period July - August 1979, when current meters were deployed at both Station 2 and Station 7. Finally, seasonal and geographical variations will be considered.

I. Analysis at Station 2

The corresponding UI and current velocity for Station 2, the inshore station, are shown in Figure 11 for the period from 23 April to mid-June. There are event-scale (ca. one week) changes in current direction and speed that appear to be coherent with depth. The upwelling index is positive all during the months of May and June with nearly periodic episodes of great intensity. It is reasonable that there be upwelling in this period of strong positive upwelling index ($UI=+138$). The mean cross slope flow (\bar{U}') for this period (Table II) is small and positive, which indicates that the meters are below the Ekman layer. The poleward alongshore flow shown by the stickplots indicates the presence of a countercurrent at 169 and 241 m. Strong equatorward winds (positive UI) seem to correlate well with strong poleward flow of the countercurrent during this time period, especially at the level nearest the surface. Also, very large drops in the index are associated with a slightly lagging decrease in the poleward current speed, and increased variability in current direction during intervals centered on 21 May, 1 June, and 9 June (Figure 11).

Continuing at Station 2 in the period 21 July - 12 September 1979 (Figure 18), there is also an overall tendency for poleward flow associated with positive upwelling index especially at the level nearest the surface. The mean cross-slope flow (Table II) for this

period of strong upwelling index ($\overline{UI}=+125$) is noted; if an extended Ekman layer is postulated, this cross-slope flow can be interpreted as lying within a layer which includes both meters. The magnitude of UI declines during the latter part of this period. On a shorter time-scale (about 9 days) the rise and fall of the upwelling index is accompanied throughout the record, beginning about 10 August, by poleward currents during periods of high upwelling index, and equatorward or diminished poleward currents during periods of reduced upwelling index. Thus, decreases in the upwelling index clearly relate to decreases in, or disappearance of, the counter current on these time scales (ca. 9 days), especially at the greater depth, 237 m.

In the following period, 24 November 1979 through 18 January 1980, as shown in Figure 24, the upwelling index is further reduced ($\overline{UI}=-20$), becoming dominantly negative after mid December. The meter at 194 m (Figure 24) is suspect due to lack of direction changes. This could be the result of a stuck vane, or a malfunction in the sensor. The alongshore current at depth 266 m alternates between poleward and equatorward flows with durations between three and ten days. There is a marked change in currents after 23 December; they become weak and variable following a strong surge in the downwelling index at that time.

1. Analysis at Station 7

First consider the winter period January - February 1979, illustrated in Figure 8. The mean flow at both levels (152 m and 223 m) is predominantly poleward; but there are important event-scale variations. There are also alternating periods of positive and negative upwelling index during this period. The significant current variations and the upwelling index changes do not seem correlated. For example, from 5 to 10 January 1979 the currents at both depths were toward the southwest and during the next 15 to 17 days rotated clockwise. While the upwelling index varied erratically about zero, a similar rotation of the currents and unrelated variation of the upwelling index continued until about mid-February, when predominantly poleward flow again resumed, and the currents flowed in this direction for the remainder of the record, approximately twelve days. A fair conclusion for this period, when wind forcing is inconsistent and weak, is that there is no simple relation between the local upwelling index and the observed behavior of the currents on time scales of tens of days, and that some other mechanism than local forcing is involved.

During July and August 1979 (Figure 14), the index is positive and the flow at Station 7, is also predominantly poleward at 158, 231, and 356 m, especially in July. Large events involving reversals in the currents can be seen on

about 7 August and 24 August at all three observed levels. These events appear to occur at all depths almost simultaneously, which suggests that they are not directly related to the local wind.

During October and November 1979 (Figure 21) there is again a period of generally weak upwelling index when that index has no obvious relation to the currents. These currents were equatorward from 12 until to 3rd October, followed by a reversal to become poleward from 1 through 21 November while the upwelling index again varied erratically near zero.

During the period 3 March through 12 April 1980 (Figure 27) poleward and equatorward flow alternate until about mid-March, while the upwelling index remains low. Following a rise in the upwelling index at that time (mid-March) and its persistence at high levels for nearly three weeks, predominantly poleward flow begins and persists for the remainder of the recorded period, some three weeks.

The meter at 113 m (Figure 27) is suspect due to lack of direction changes and small magnitude, and its data will be ignored.

3. Comparision of Stations 2 and 7

Current meter arrays were deployed at both Stations 2 and 7 during the period from 21 July to the end of August, providing an opportunity for examining horizontal

variations. As mentioned above, the currents at Station 2 (depicted in Figure 18) appear to respond with little or no lag to local forcing for this entire period. The response of the currents to local winds is not so clear at Station 7 (Figure 14). The currents at Station 7 may respond differently to local winds than currents at Station 2 because of the increased distance from the controlling boundary (coast). It is also possible that the response of the currents at Station 7 to local forcing may be masked by other influences. Certainly, there is no longer a nearly in-phase response of the current (note, for example, that on 27 August flow at Station 2 is predominantly poleward while flow at Station 7 is predominantly equatorward). If flow at Station 7 is being driven by local winds, the response must lag the wind.

Seasonally, the countercurrent was strongest during the spring months of 1979 at Station 2 (Figure 11). Geographically, the major discernable difference is the closer correlation between the current and the local forcing at Station 2 (inshore) than at Station 7 (offshore).

In summary, there are four important conclusions to the analysis of the currents and their relation to the upwelling index:

1. The entire record from January 1979 to April 1980 indicates currents are predominantly poleward at both stations, especially while Bakun's coastal upwelling index is high and positive.

2. Throughout the period, many events with time scales of tens of days occur at all recorded depths.

3. Current response to local forcing is more apparent at Station 2.

4. The countercurrent runs most strongly during the periods of high upwelling index at the nearshore station (Station 2).

B. SPECTRUM ANALYSIS

The current meter data are subjected to spectrum analysis in order to identify regions of high energy in the frequency domain, and consequently suggest forces at work in the study area.

The information from spectrum analysis, in this case via a program using Fast Fourier Transform (FFT), depends upon the record length and the sampling interval. The parameters used in the spectrum analysis program are:

Record length	= TR = 1024 h
Sampling interval	= $\Delta t = 1$ h
No. of points per record	= N = 1024
Resolution	= $\Delta f = .0098$ h ⁻¹
Nyquist frequency	= $f_N = .5$ h ⁻¹
No. of frequencies resolved	= M = $f_N/\Delta f = 512$
No. of degrees of freedom	= N/M = 2

The records available are typically about 50 days (1200 h) long; the maximum resolution attainable by FFT is, therefore, obtained from data sets of length 1024 hours.

For a fixed record length, however, high resolution is paid for at the expense of stability. The resolution with no averaging of spectral estimates over frequency is $\Delta f = 1024^{-1} \text{ h}^{-1}$; and for single spectra (with no ensemble averaging) the estimates of variance have only two degrees of freedom (and are thus uncertain indicators of the variance distribution).

For time series defined at equal time-intervals Δt , the highest frequency component discernable is given by $N_f = (2\Delta t)^{-1}$, the "Nyquist frequency". The variance of frequencies higher than this are attributed, spuriously, to lower frequencies. Such misread ("aliased") variance is thought to be of minor concern in the data sets of this study except for those few (discarded) with high frequency instrumental noise. Among forces known to be at work in the ocean which are likely to contribute to energetic currents are tidal and (possibly) inertial forces. Some of the most important components are the semi-diurnal tide-producing forces (Sverdrup, et al., 1942):

Name	Symbol	Period(h)	Frequency(h^{-1})
Principal lunar	M_2	12.42	.0805
Principal solar	S_2	12.00	.0833
Luni-solar	K_2	11.97	.1833

The inertial frequency and period, calculated with the average latitude (35.8°) of Station 2 and Station 7, are $f(i) = .0487 \text{ h}^{-1}$, and $T(i) = 20.5 \text{ h}$.

The spectral estimates consistently indicate energetic components at tidal and inertial frequencies as well as at periods of approximately 10 days. The dominant tidal components present are the semi-diurnal, with the most significant peaks appearing to be the luni-solar. In Table I are shown the approximate values of the low frequency, inertial, and semi-diurnal tidal peaks for both alongshore, and onshore/offshore motion. These values in Table I are taken from the spectrum analysis plots to show what, if any, relation there is between high energy and depth, season, and proximity of the shore. In general the spectra indicate greater energy for tidal, inertial, and low frequencies at the upper meters. It appears that motions at these frequencies are also more energetic in winter than in summer. Finally, tidal and low frequency energy are greater near shore, while energy in the inertial frequency is greater offshore.

C. INFERENCES FROM PROGRESSIVE VECTOR DIAGRAMS

The PVD's are helpful in observing low frequency variations and the mean currents which are summarized in Table II. As a meander, eddy, or wave in the countercurrent moves through a station's position the boundary between the poleward flow and equatorward flow moves about, with the current meters alternating between either side of that boundary. Such an occurrence is reflected in the PVD's as a current reversal.

TABLE I
COMPARISON OF HIGH ENERGY PEAKS (1000 CM. SQ. HOUR)

STATION	START DATE	DEPTH	LOW FREQ. (10 DAY)		INERTIAL		S.D. TIDAL	
			ALONG SHORE	ON/OFF SHORE	ALONG SHORE	ON/OFF SHORE	ALONG SHORE	ON/OFF SHORE
2	23 APR 79	169	5.3	0.5	1.0	0.5	8.0	6.5
		241	4.0	SMALL	1.0	0.5	11.0	5.0
2	21 JUL 79	165	17.0	0.5	1.0	0.3	3.0	1.7
		237	8.0	0.5	SMALL	0.2	3.0	1.2
2	24 NOV 79	194*	0.3	0.5	SMALL	SMALL	SMALL	0.1
		266	45.0	1.0	2.0	1.0	11.0	17.0
7	5 JAN 79	152	6.8	7.0	1.8	2.3	1.8	2.0
		223	1.5	5.4	0.6	0.5	1.4	0.8
7	7 JUL 79	158	2.6	17.0	0.2	SMALL	1.6	2.0
		231	2.0	5.1	0.4	SMALL	1.3	1.8
7	7 OCT 79	127	1.0	1.6	4.5	3.4	3.7	3.8
		200	1.3	1.1	2.0	2.3	3.0	2.6
7	3 MAR 80	113*	0.2	0.1	0.1	0.1	0.3	0.1
		186	1.8	1.1	1.4	1.5	2.6	2.0
		311	0.9	0.2	1.8	1.8	5.0	1.2

S.D. = Semi-Diurnal
* = Meter is suspect

TABLE II
COMPARISON OF MEAN CURRENT AND TEMPERATURE

STATION	TIME PERIOD	DEPTH	(azim. °T)	(cm/sec)	(° cent.)	(cm/sec)	(cm/sec)
2	23 APR 79	169	3411.2	16.0	8.5	+ 16.0	+ 0.34
	thru 16 JUN 79	241	3400.4	11.1	8.0	+ 11.1	+ 0.08
2	21 JUL 79	165	3255.1	6.1	9.0	+ 5.89	- 1.57
	thru 13 SEP 79	237	3141.3	1.5	8.5	+ 1.35	- 0.65
2	24 NOV 79	194*	2799.8	6.2	9.0	+ 3.08	- 5.38
	thru 18 JAN 80	266	0033.1	2.7	8.0	+ 2.48	+ 1.06
7	9 JAN 79	152	3544.8	4.6	9.4	+ 4.58	+ 0.39
	28 FEB 79	223	16.6	4.3	8.6	+ 3.84	+ 1.93
7	9 JUL 79	158	3122.2	4.5	8.7	+ 3.56	- 2.76
	thru 30 AUG 79	231	3306.6	5.8	8.3	+ 5.47	- 1.93
7	9 OCT 79	127	68.1	5.1	9.3	+ 1.05	+ 4.99
	thru 29 NOV 79	200	70.6	4.1	8.4	+ 0.67	+ 4.05
7	4 MAR 80	1113*	3105.5	4.4	9.0	+ 3.40	- 2.80
	thru 15 APR 80	186	3287	3.4	8.0	+ 3.17	- 1.24
		311	8.2	2.7	7.0	+ 2.56	+ 0.84

\bar{U}' = Mean cross-slope current
 \bar{V}' = Mean alongshore current
* = Meter is suspect

Exhibiting features readily seen in the progressive vector diagrams Figures 47 through 62, are current reversals of long duration, and the mean current for the duration of the mooring. The mean current direction (θ), given as azimuth, speed (V), cm-s^{-1} , and temperature (T), degrees Celsius, for each current meter for the entire study period are shown in Table II; and they are also shown on the individual plots. Also shown in Table II are the mean onshore and alongshore current components respectively. The alongshore direction in this case is defined as 340° T for Station 2, and 350° T for Station 7, which represent the azimuths of the mean contours at those sites.

For both Stations 2 and 7 over the entire period, the seasonal and depth variations will be considered. The mean alongshore current is always poleward at all observed levels (from 127 m to 356 m) and at both stations. Mean alongshore current speeds were greater nearshore at Station 2, than offshore at Station 7. Mean alongshore current speed at the upper levels appears to vary only slightly seasonally at both stations, approximately 4 to 6 cm-s^{-1} , with the exception of the upper meter at Station 2, 23 April to mid-June, i.e., the counter current appears weak at observed depths, except in late spring.

The PVD's indicate predominantly unidirectional flow at the near-surface levels of Station 2, while at the deeper,

lower meters there were often current reversals and oscillations possibly associated with meanders, waves, and eddies. Current reversals occurred in greater numbers and were present at all depths at Station 7 which may possibly be due to Station 7 being near a boundary between north and south currents. The semidiurnal components of the currents are at times apparent in the PVD's as for example in Figures 49 and 57.

Shorter term variations are also indicated by the PVD's, in particular reversals. No apparent current reversals are present at the upper meter of Station 2, 24 April to mid-June (Figure 49), and only two minor reversals can be seen near the end of the record for the lower meter (Figure 50). At the same station from 23 July to mid-September, two current reversals of short duration are evident at the upper layer (Figure 54); and more than half a dozen current reversals of from three to twelve days in duration can be seen for the current at greater depth (Figure 55). Current reversals are not present at the upper level of Station 2 (Figure 58), 27 November 1979 to mid-January 1980, but several current reversals of approximately three to nine days duration can be seen at depth (Figure 59).

A single current reversal is present at both meters of Station 7 (Figures 47 and 48), 9 January to the end of February 1979. At the same station, 9 July to the end of

August 1979, three current reversals are apparent at the upper two meters (Figures 51 and 52), and two reversals can be seen in the lower meter (Figure 53). These reversals all appear to be of a relatively long duration, 15 to 20 d. Two current reversals are present at both meters of Station 7 (Figures 56 and 57), 9 October to 29 November 1979. For the period 4 March to 15 April 1980 at the same station, no reversals are seen in the upper meter (Figure 60), but several oscillations and reversals are seen in the two lower meters (Figures 61 and 62).

D. CROSS-SLOPE CURRENT

The mean cross-slope currents from Table II are plotted against time in Figure 5. The dominant feature of these currents is an annual variation with onshore flow in winter months and offshore in spring and summer. This annual variation correlates with the strong upwelling occurring in the spring and summer, and the weak upwelling index in the winter.

Qualitatively, the relation between the upwelling index and the cross-slope current means is consistent with a thick layer influenced by a modified surface Ekman regime.

E. TIME SERIES

The time series plots of U (positive-east) and V (positive-north) components were primarily used as an aid in interpreting the stickplot data. They are also useful for their resolution of high frequency variations. The

semidiurnal components of the currents are evident as well as the larger scale current oscillations indicated in the stickplots.

The temperature versus time plots also indicate the semidiurnal components and large-scale oscillations found in the stickplots. Approximate mean temperatures for the current meters at Station 2 and 7 throughout the record are shown in Table II. The temperature decreased with depth at all stations. The mean temperatures at Station 2 at all depths (Figure 6) became increasingly warmer during the period from April 1979 to January 1980, while the mean temperatures at Station 7 at all depths (Figure 7) became increasingly cooler. This is consistent with existing wind stresses, which would tend to uplift the isotherms at the nearshore station (Station 2) in the spring (strong upwelling index) and depress them in winter (weak upwelling index). The cooling continues at Station 7 at all depths from December 1979 until April 1980, and no simple explanation is apparent.

IV. CONCLUSIONS

A northward flowing current was found for the entire period of this study. It was strongest at the upper levels, roughly between 100 and 200 m. Seasonally, this countercurrent was strong during spring and substantially weaker during winter. The speed and direction of the countercurrent at any given time may differ markedly from the average flow. There were events on scales of tens of days which appeared to be qualitatively coherent between stations and also between depths at a given station. Frequent current reversals and oscillations occurred, consistent with the weak, poorly defined, broad flows associated with eastern boundary currents.

Bakun's coastal upwelling index is an indicator of possible wind-driven coastal upwelling. The coastal upwelling index is, in the mean, consistent with the observations of a deep cross-slope flow (Ekman layer), a large upwelling index corresponding to thickening of the Ekman layer. The countercurrent is present during the entire study, and the low frequency alongshore current is never equatorward.

Relatively high-energy peaks at semidiurnal tidal frequencies and inertial frequencies occurred in the

majority of the current records. Additionally, low frequency energy peaks were found at periods of about 10 d.

At Station 2, (nearshore), the alongshore component of these three frequencies tends to be greater than the on/offshore component, and generally speaking, the low frequency energy peak ($T = 10$ d) is dominant. At Station 7 (offshore), the on/offshore component of these three frequencies is noticeably greater, but there is no obvious pattern to the energy distribution.

The countercurrent was present at the study site, but it was not possible to unequivocally identify and correlate local forcing with the countercurrent. The vertical migration of the frontal boundary between equatorward and poleward flow was observed at both stations, but less often at the nearshore Station 2 than at Station 7. Hydrographic data from the study area for this time period were not examined at all, and deserve future consideration. Correlation of currents and wind or upwelling index, comparision of observed currents with predictions of various models, and the relation of metered currents to those inferred from hydrographic data are recommended for future studies.

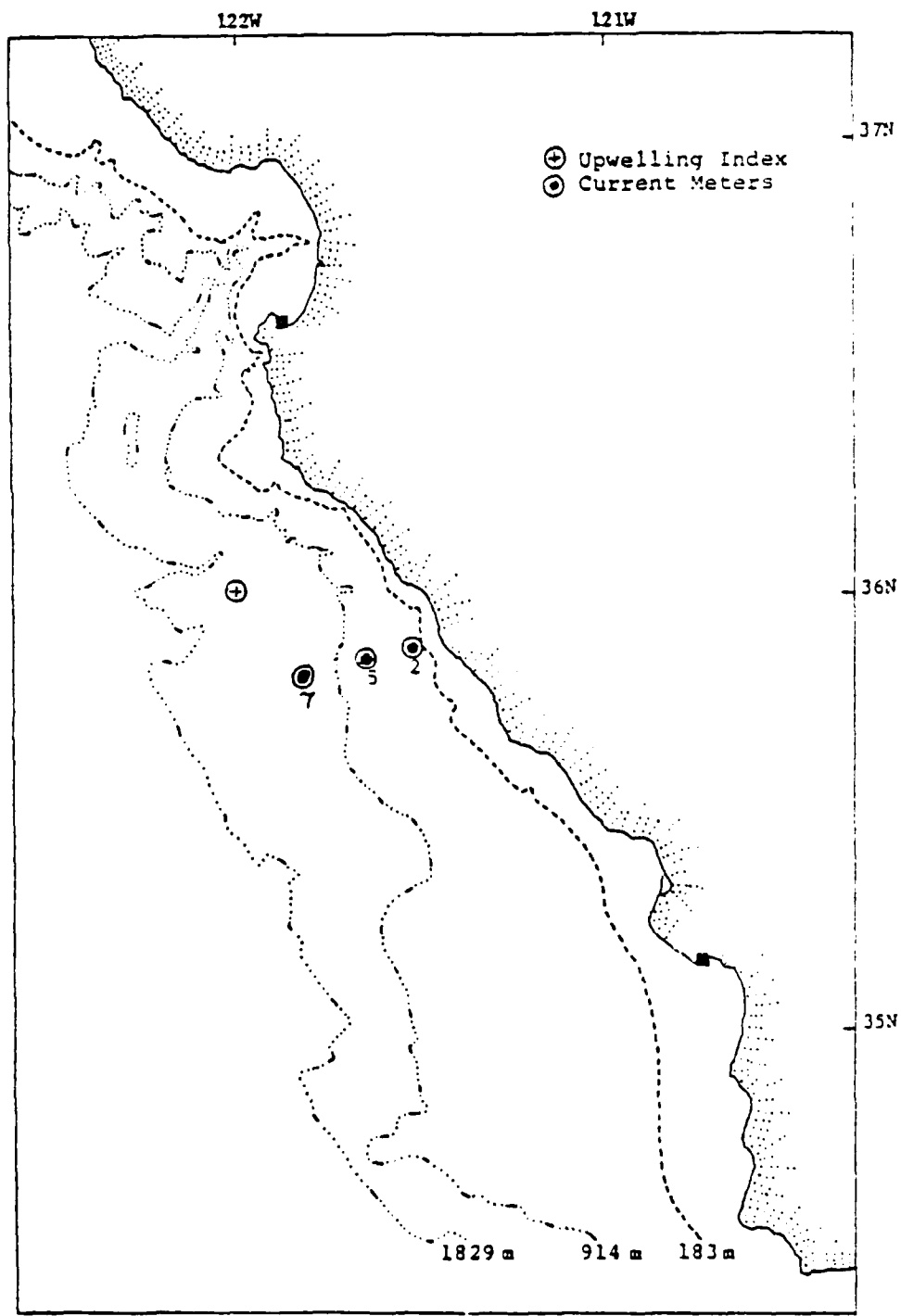


Figure 1. The study area.

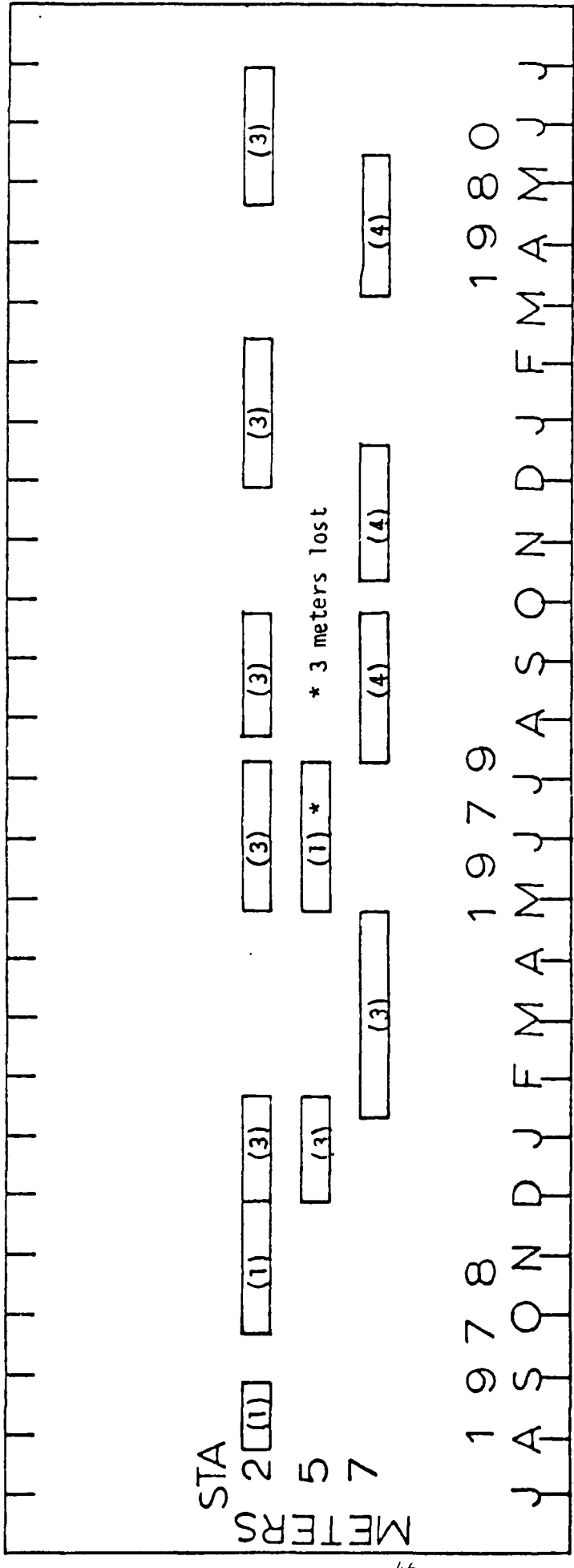


Figure 2. Chronology of current meter deployment.

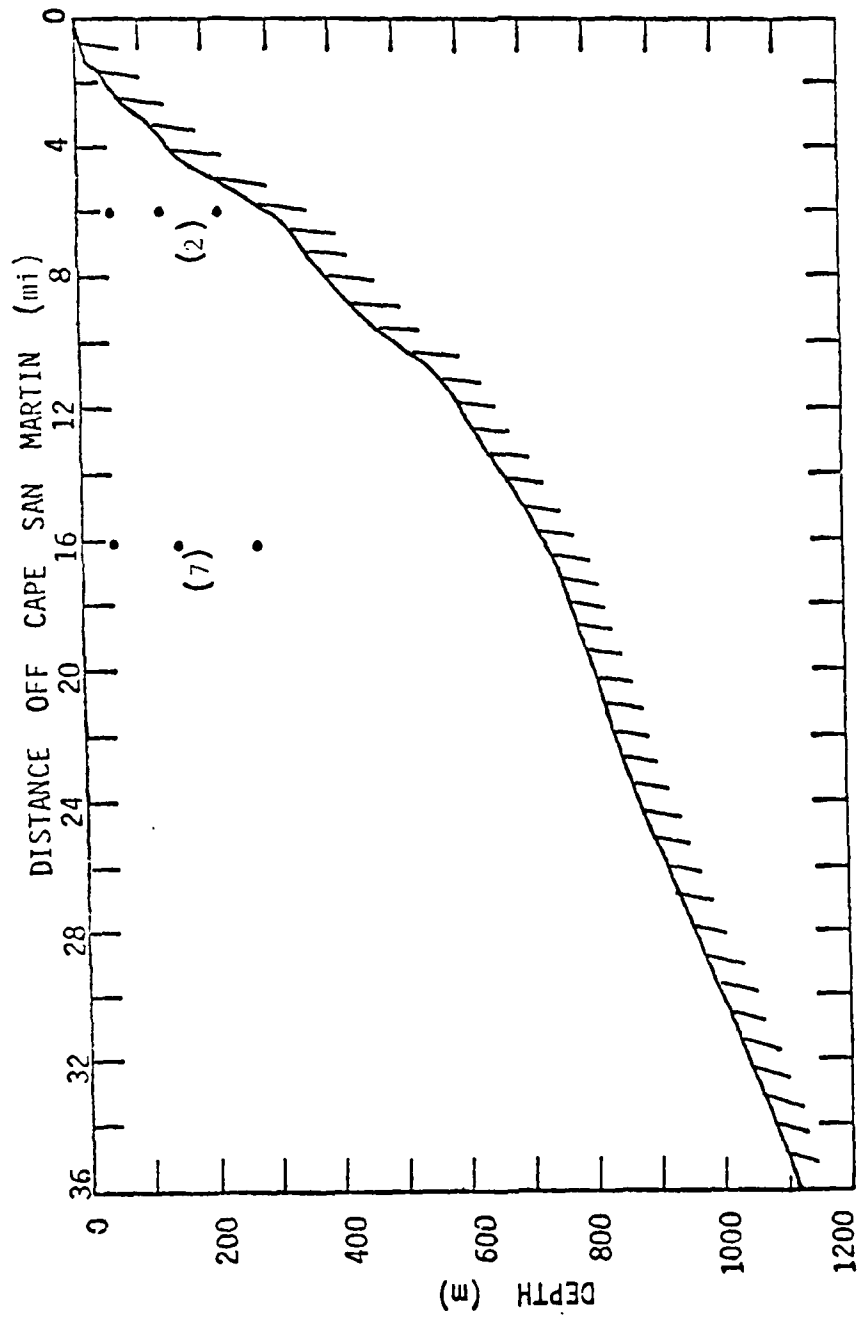


Figure 3. Vertical section showing representative locations of current meters off Cape San Martin, California.

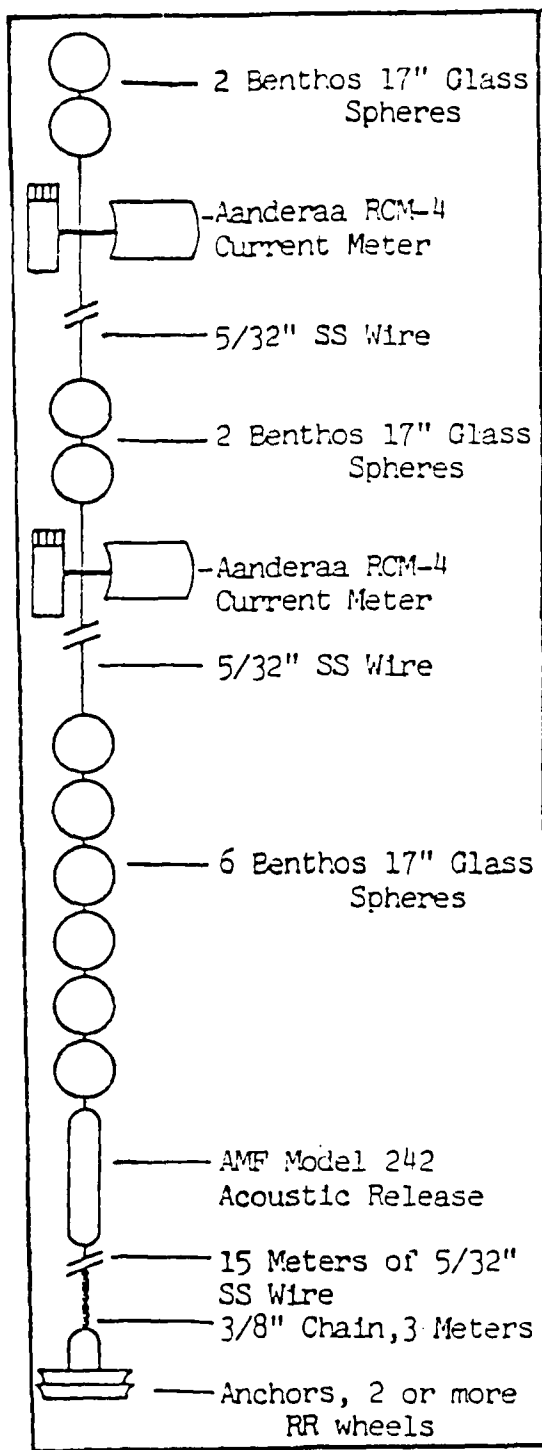


Figure 4. Current meter array.

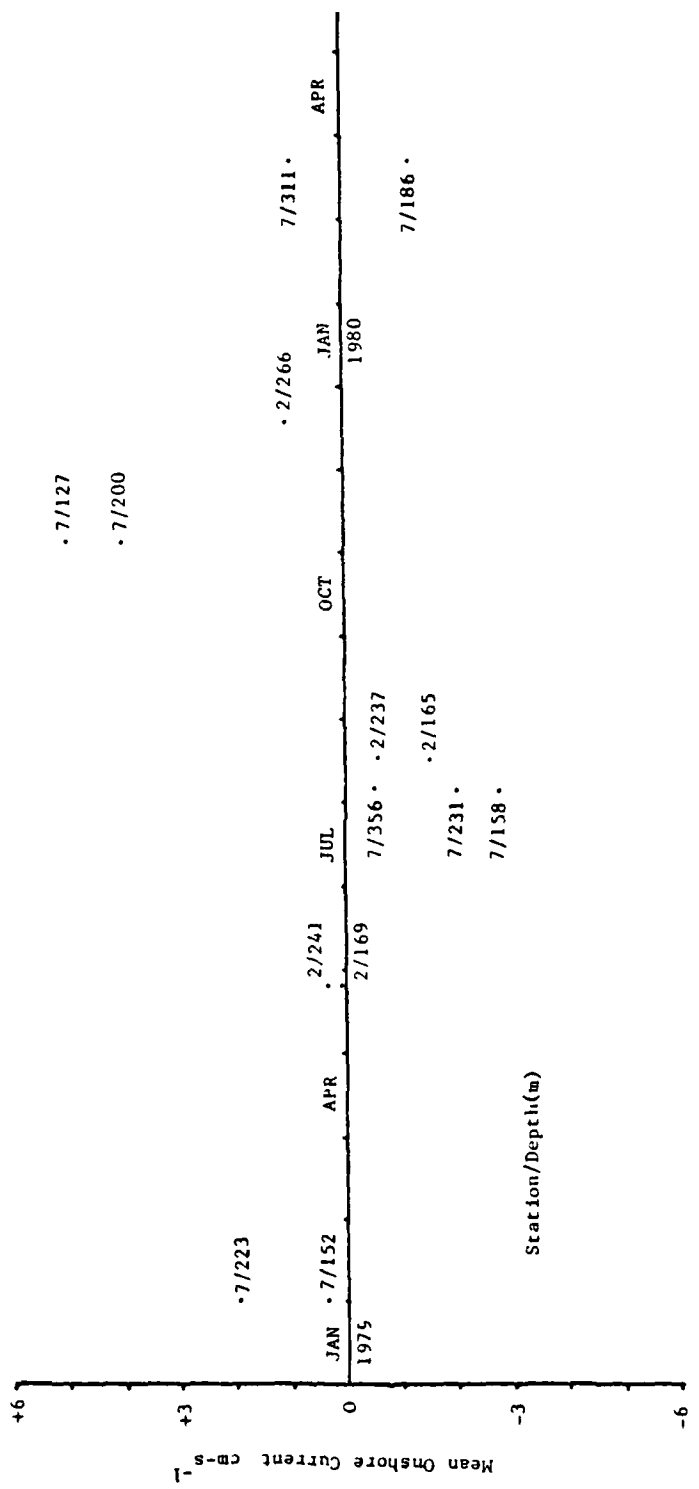


Figure 5. Mean onshore currents.

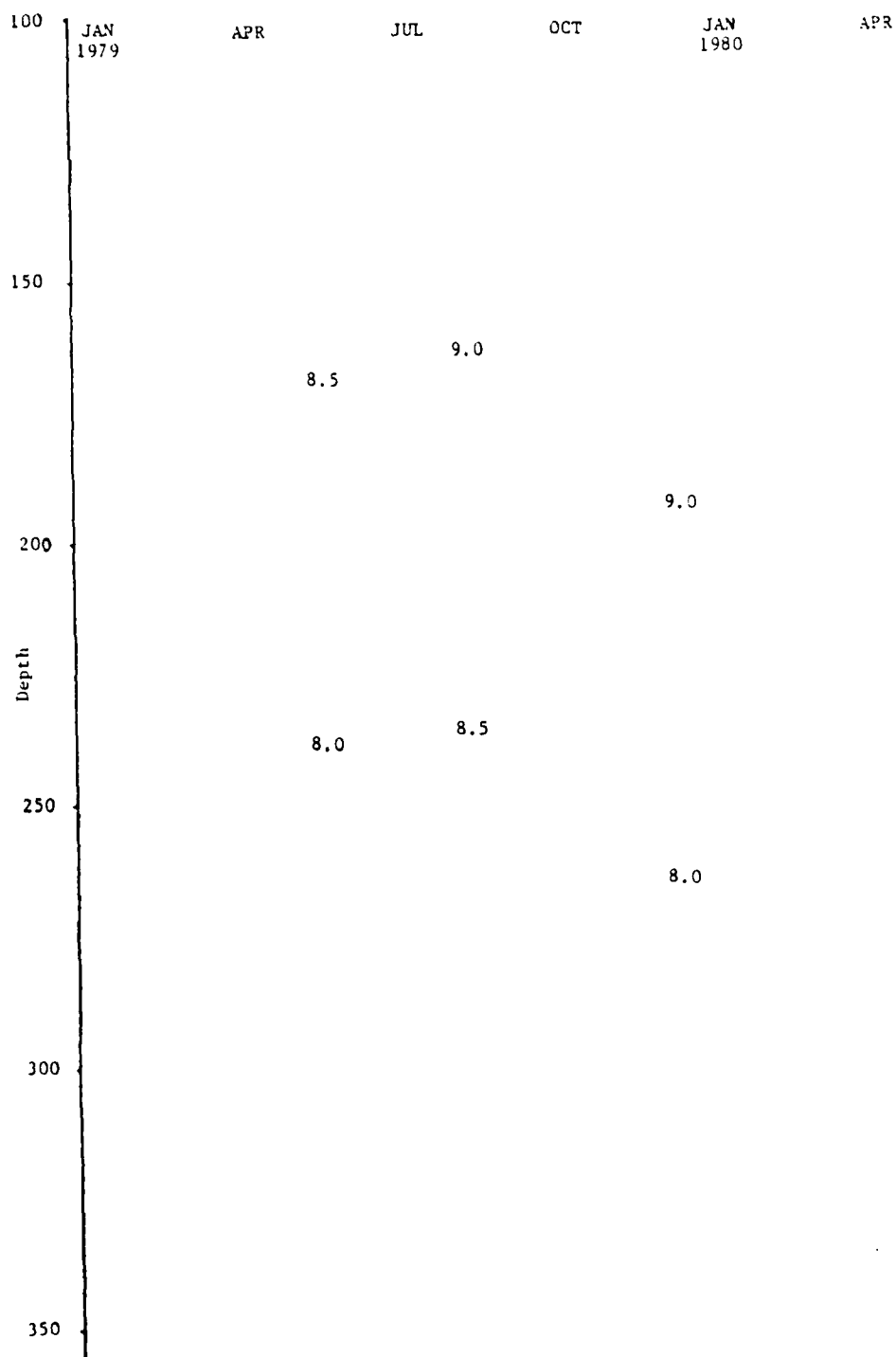


Figure 6. Mean temperatures at Station 2.

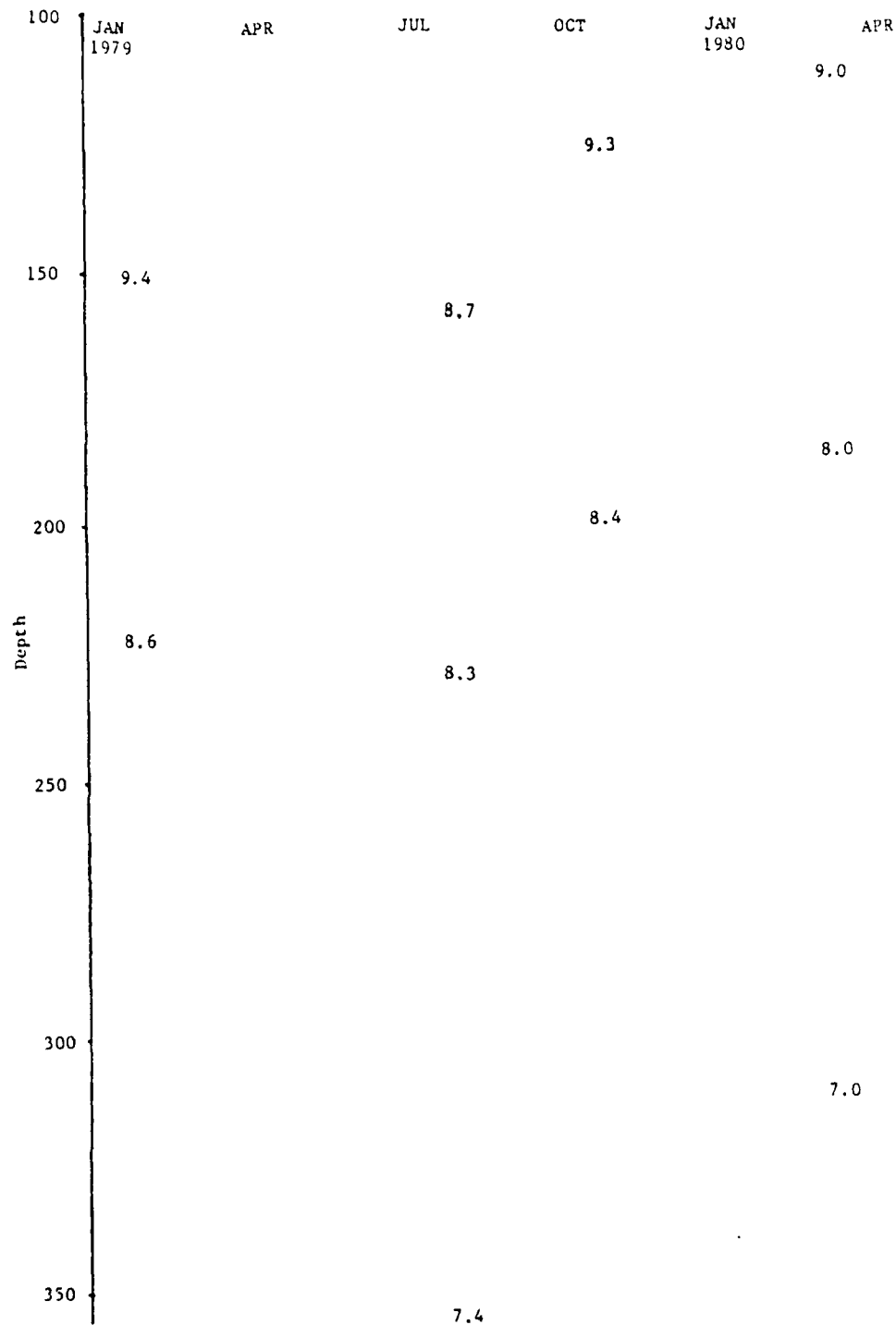


Figure 7. Mean temperatures at Station 7.

APPENDIX A: TIME SERIES PLOTS

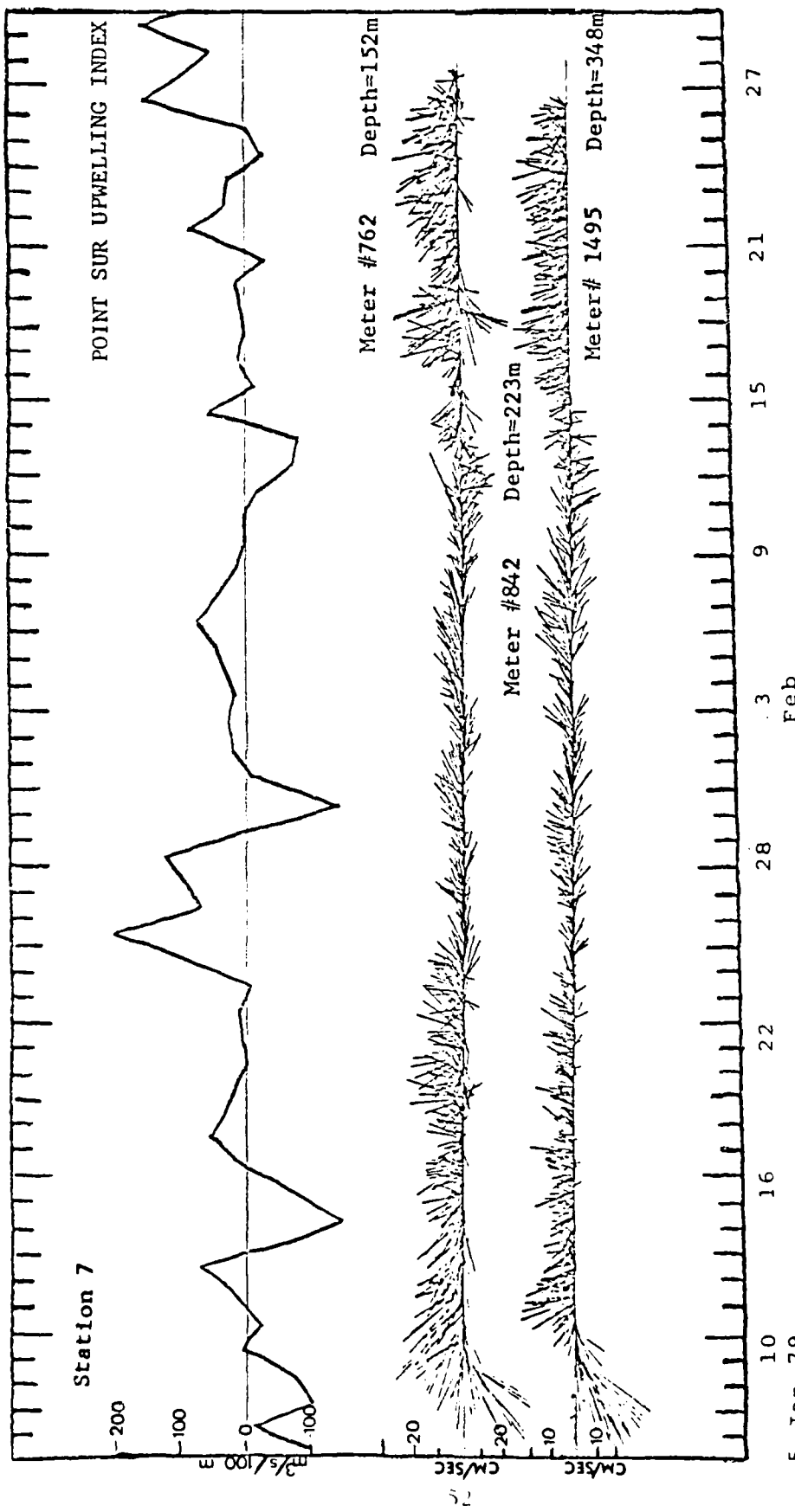


Figure 8. Point Sur Upwelling Index and stickplots of hourly current vectors for the current meters at Station 7 deployed on 5 January 1979.

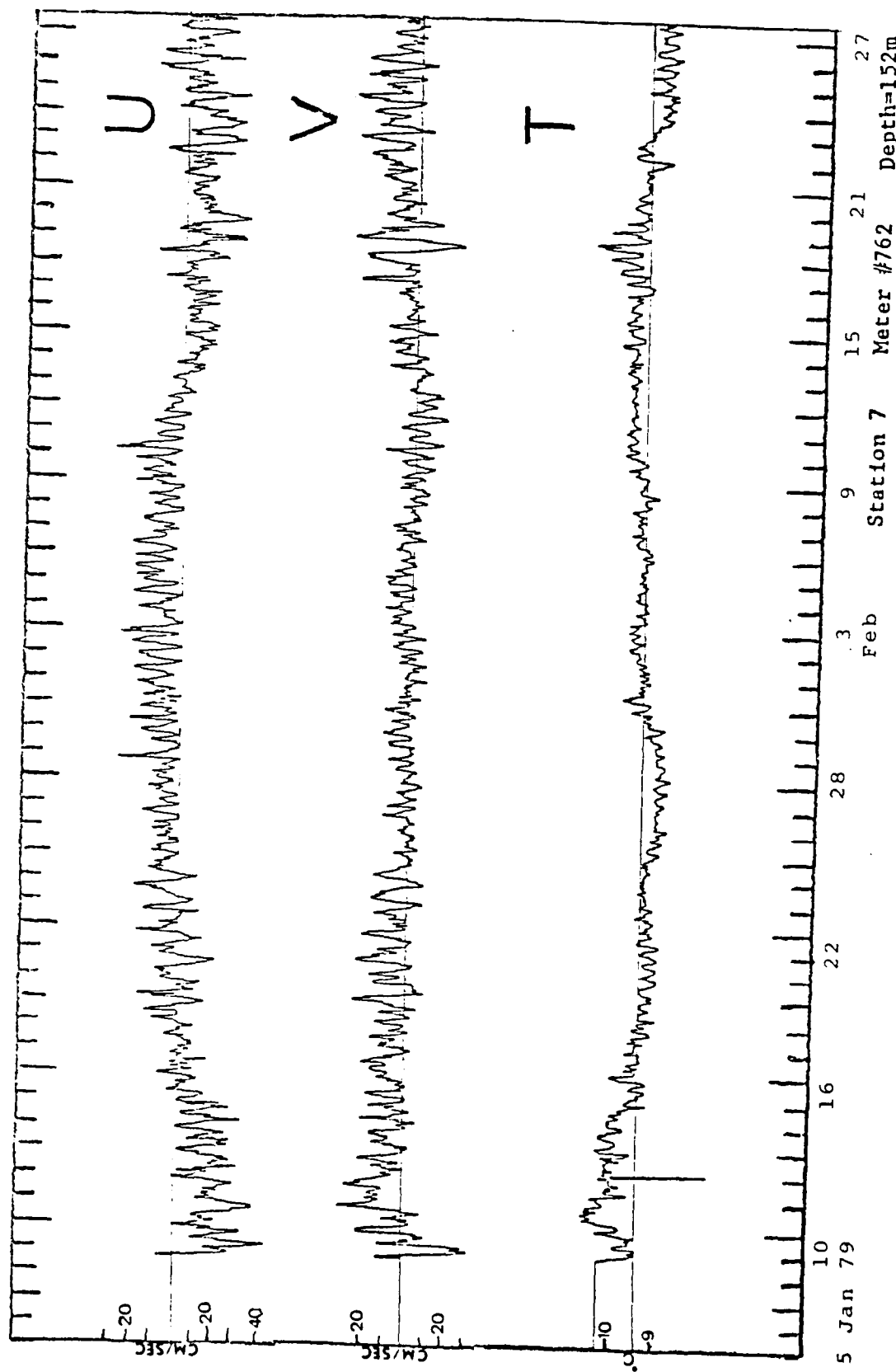


Figure 9. U component, V component, and temperature plots versus time for the current meter at 152 m depth at Station 7 deployed on 5 January 1979.

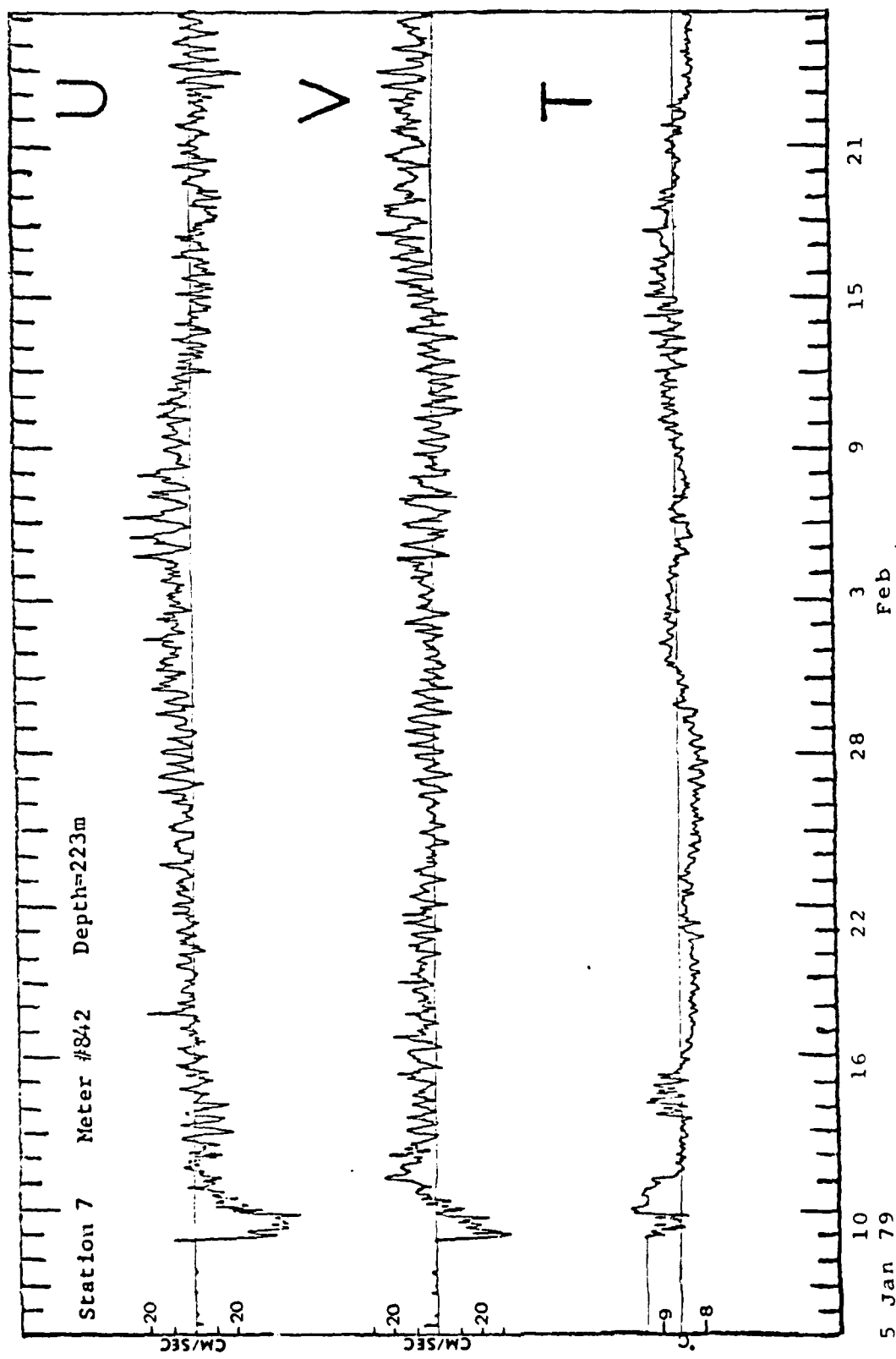


Figure 10. U component, V component, and temperature plots versus time for the current meter at 223 m depth at Station 7 deployed on 23 April 1979.

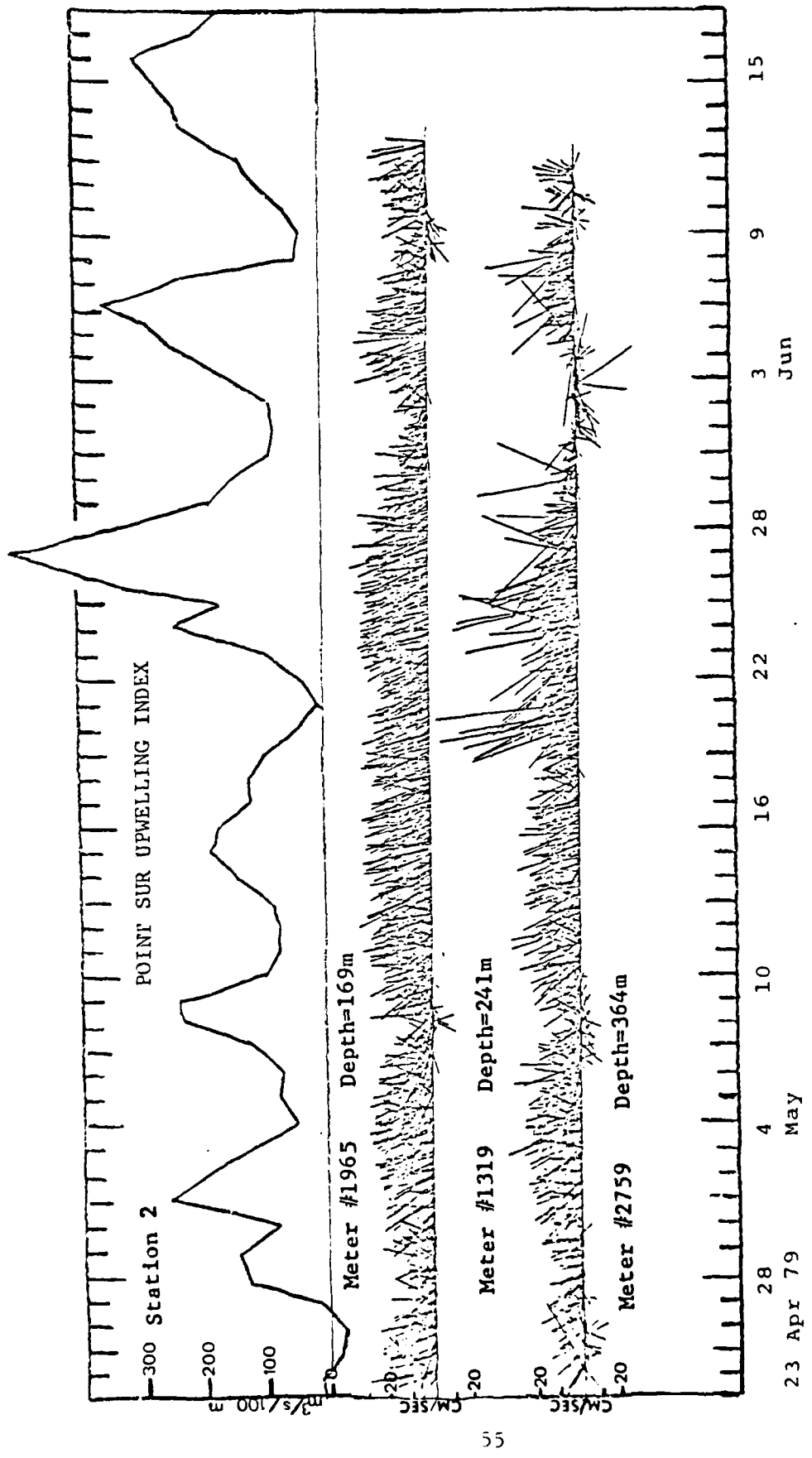


Figure 11. Point Sur Upwelling Index and stickplots of hourly current vectors for the current meters at Station 2 deployed on 23 April 1979.

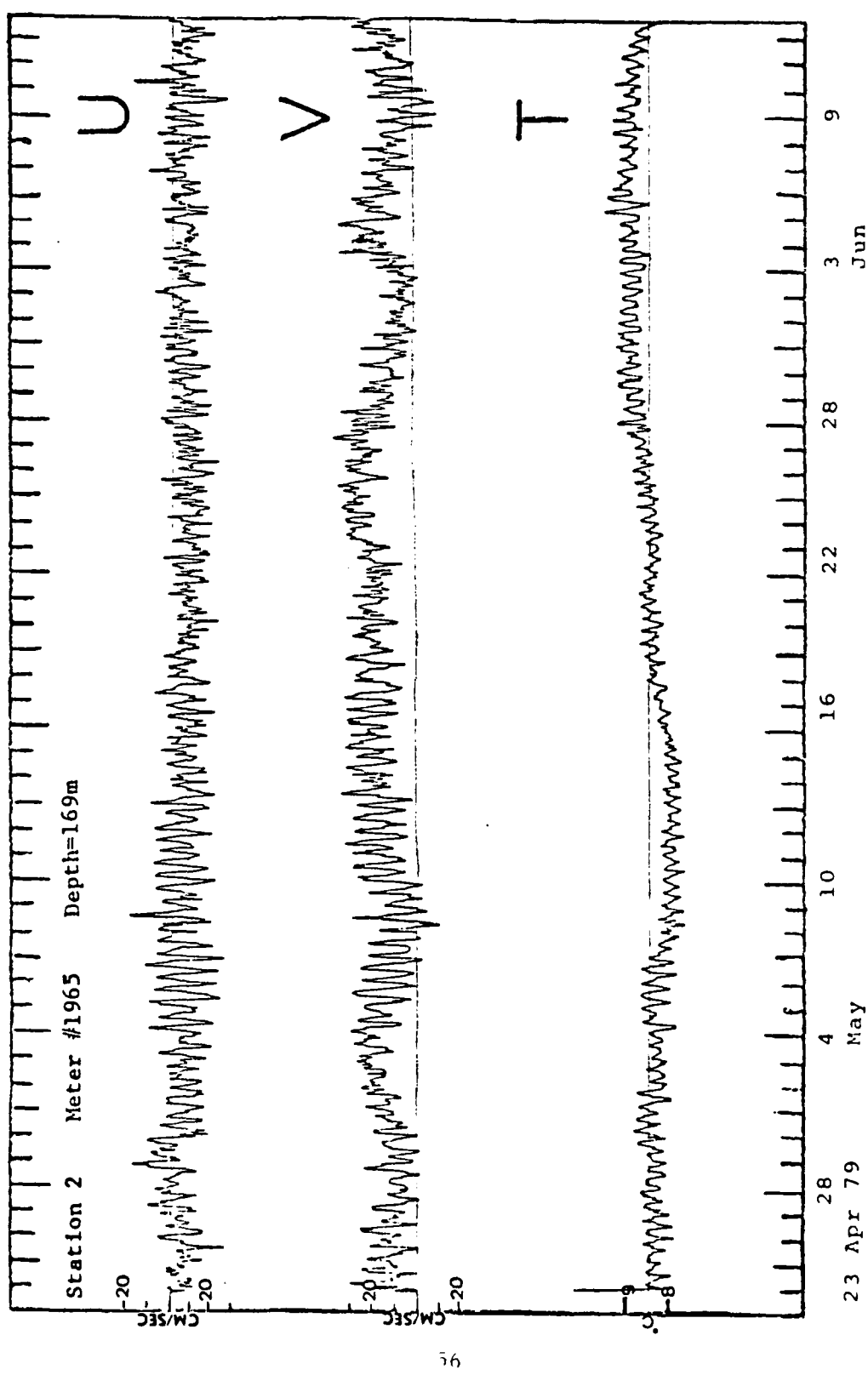


Figure 12. U component, V component, and temperature plots versus time for the current meter at 169 m depth at Station 2 deployed on 23 April 1979.

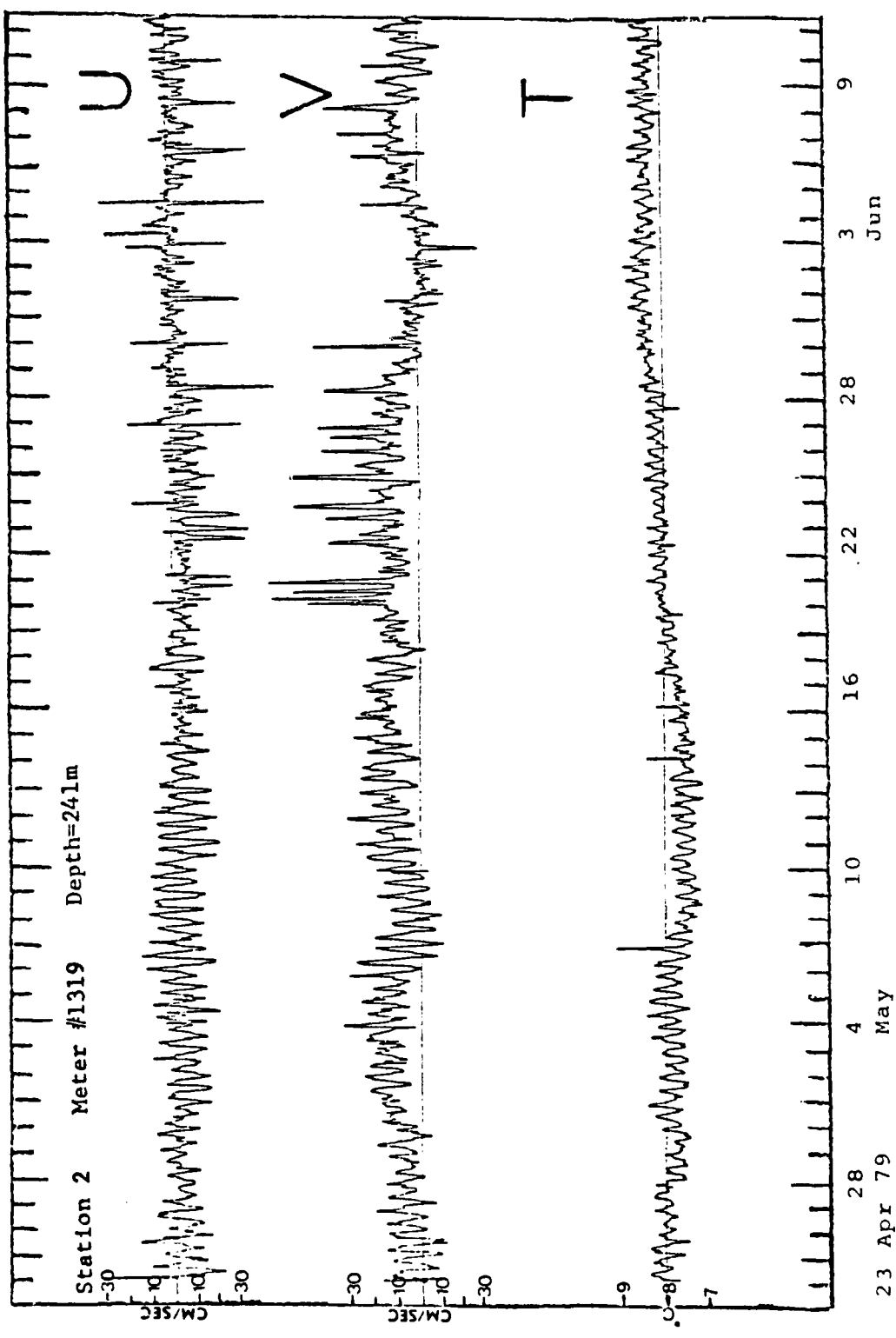


Figure 13. U component, V component, and temperature plots versus time for the current meter at 241 m depth at Station 2 deployed on 23 April 1979.

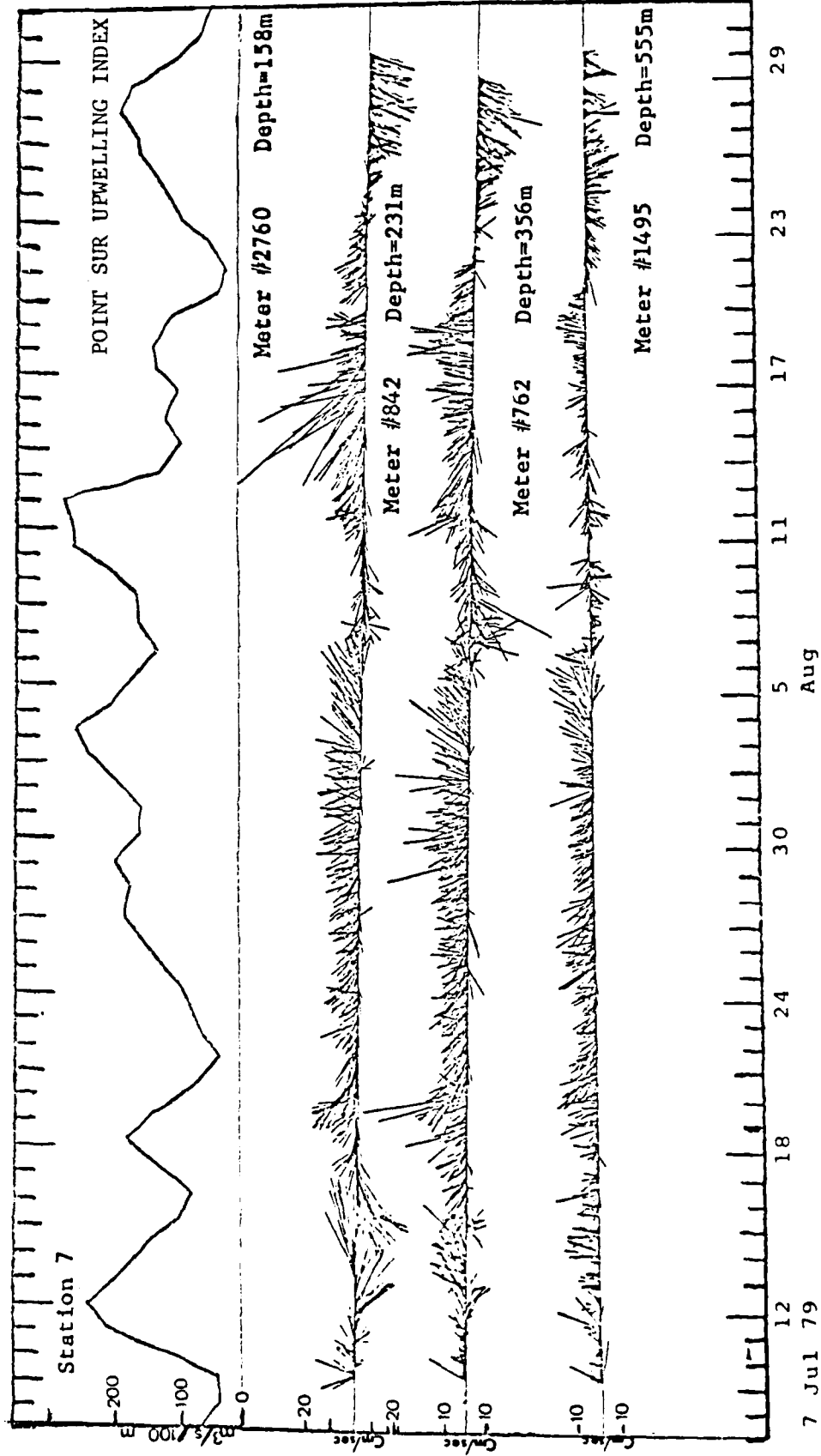


Figure 14. Point Sur Upwelling Index and stickplots of hourly current vectors for the current meters at Station 7 deployed on 7 July 1979.

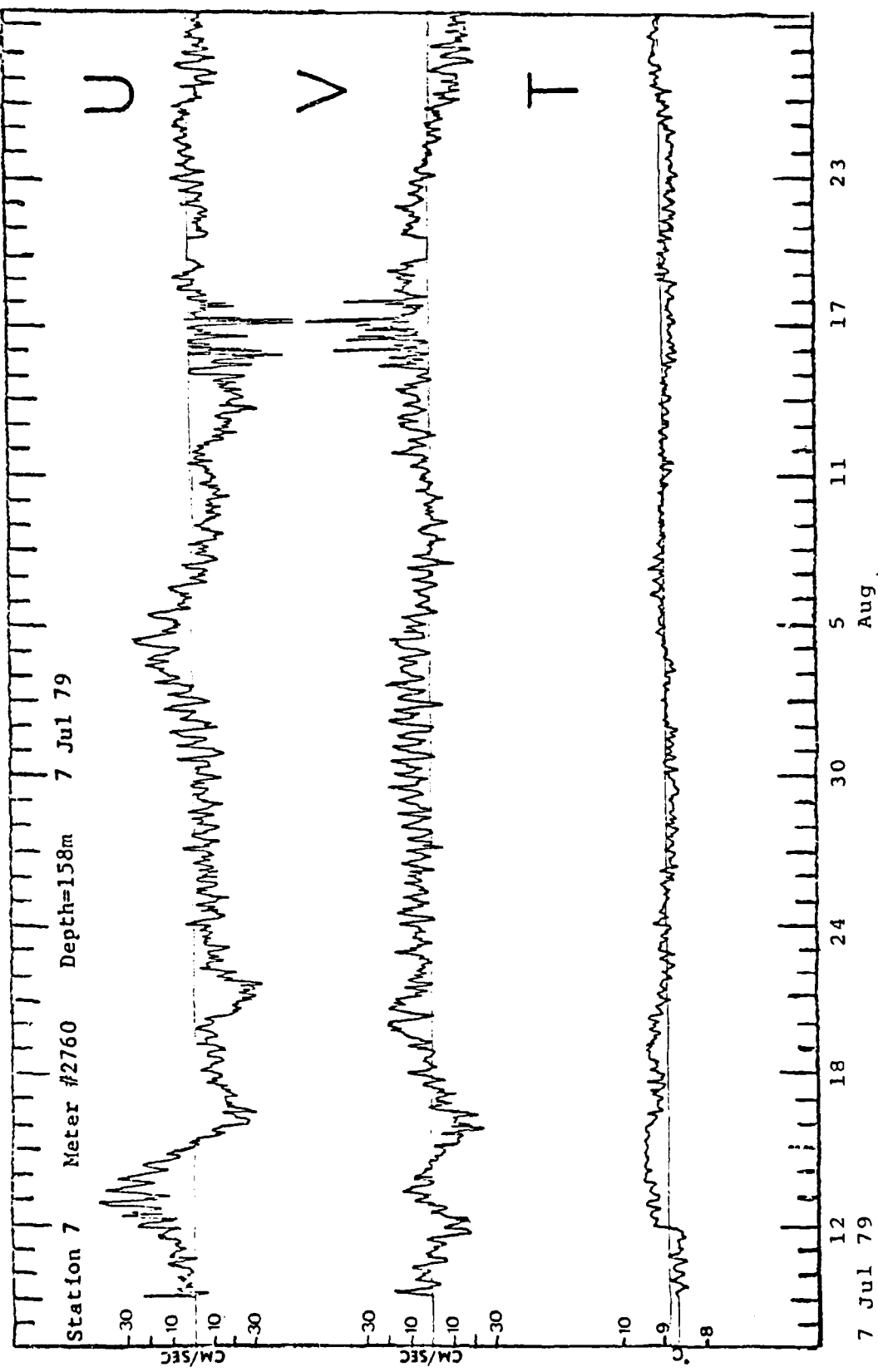


Figure 15. U component, V component, and temperature plots versus time for the current meter at 158 m depth at Station 7 deployed on 7 July 1979.

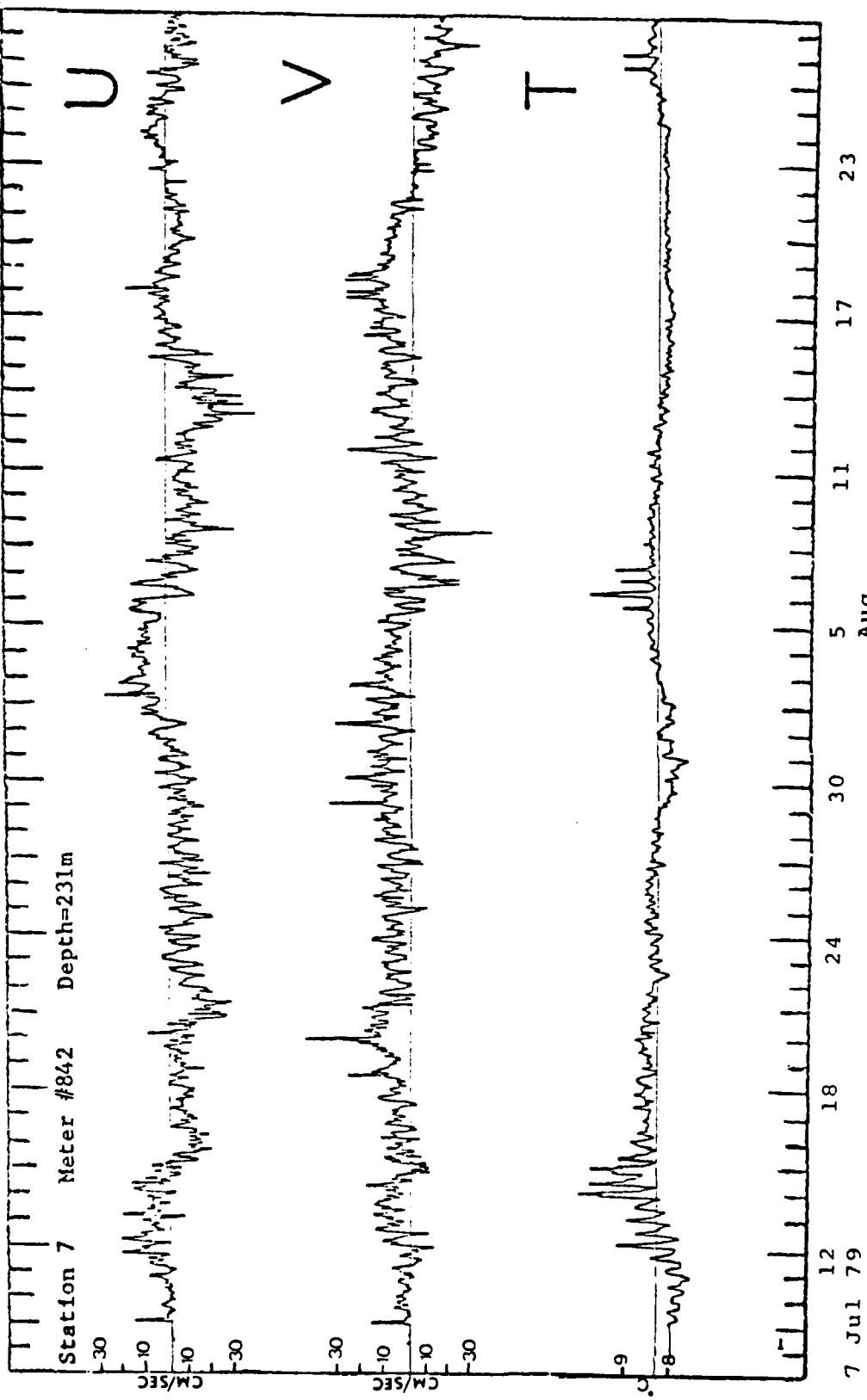


Figure 16. U component, V component, and temperature plots versus time for the current meter at 231 m depth at Station 7 deployed on 7 July 1979.

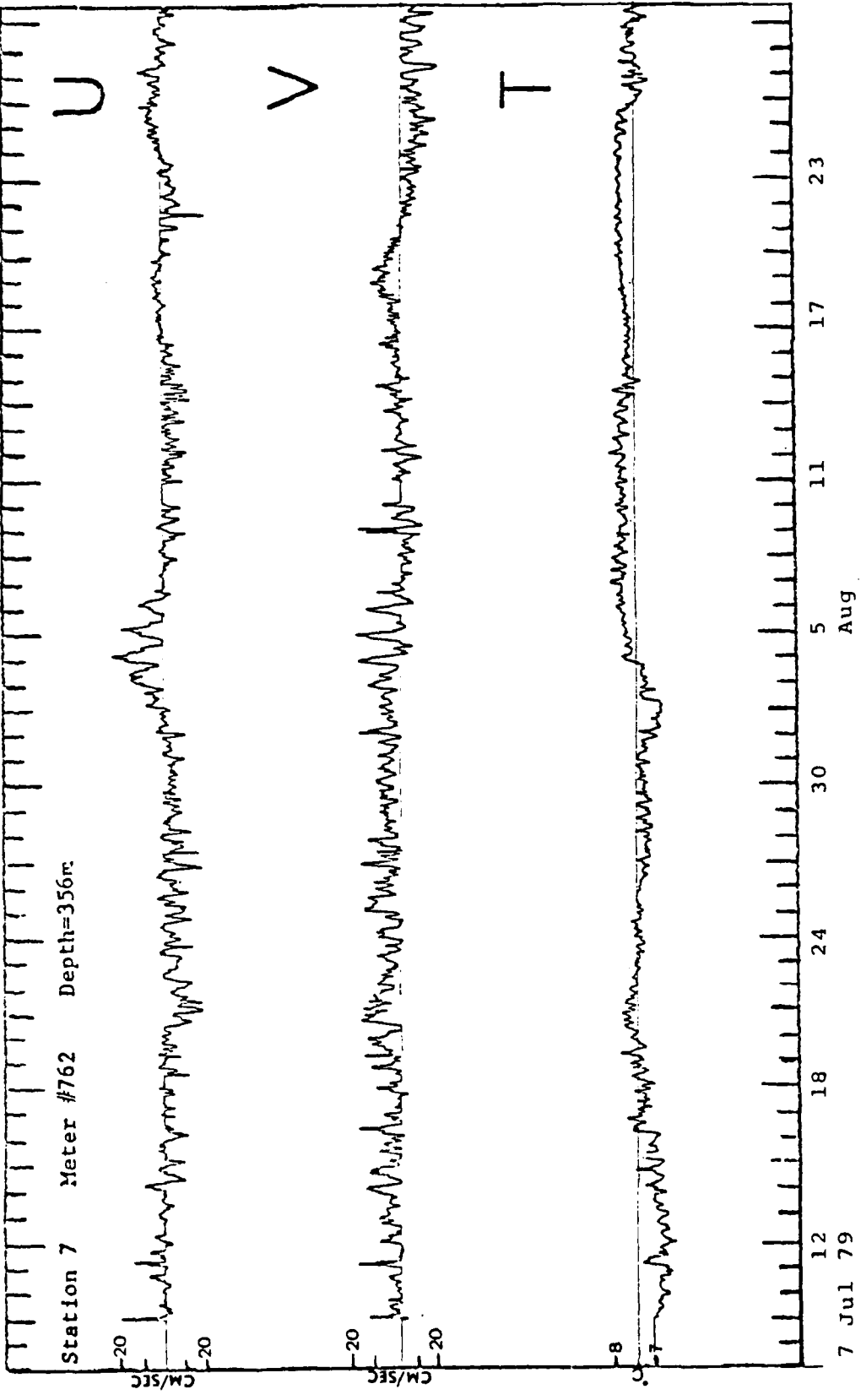


Figure 17. U component, V component, and temperature plots versus time for the current meter at 356 m depth at Station 7 deployed on 7 July 1979.

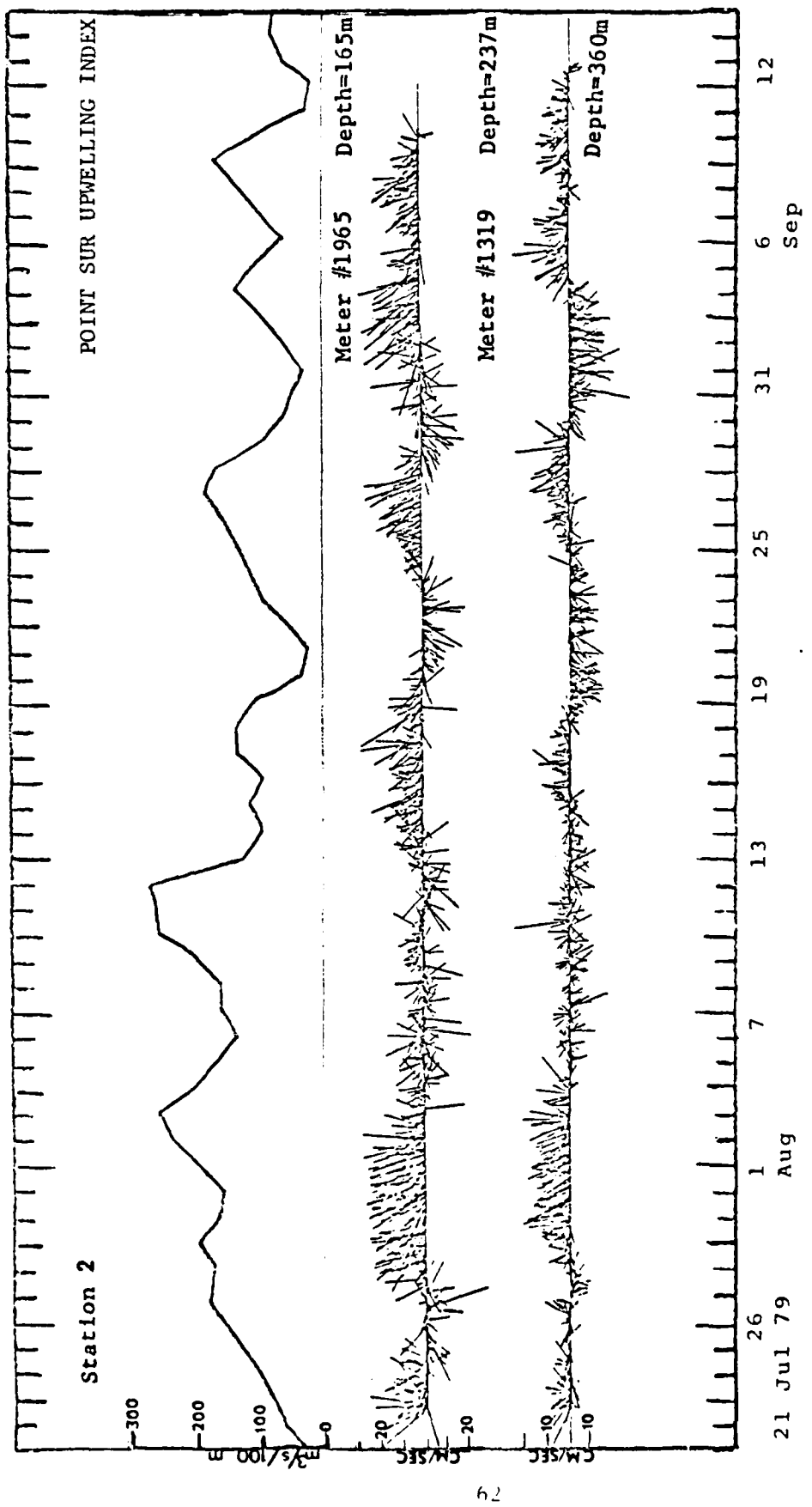


Figure 18. Point Sur Upwelling Index and stickplots of hourly current vectors for the current meters at Station 2 deployed on 21 July 1979.

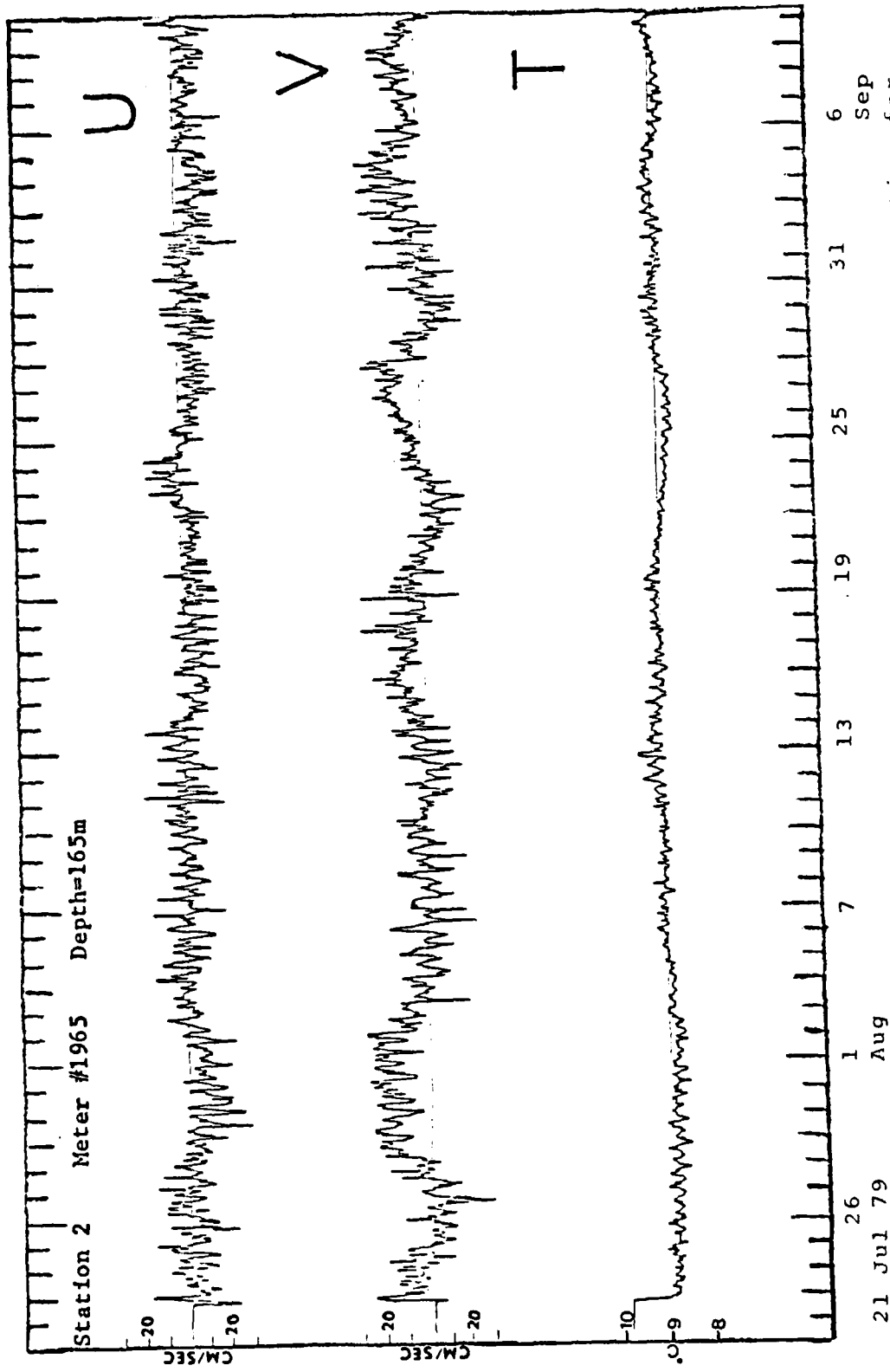


Figure 19. U component, V component, and temperature plots versus time for the current meter at 165 m depth at Station 2 deployed on 21 July 1979.

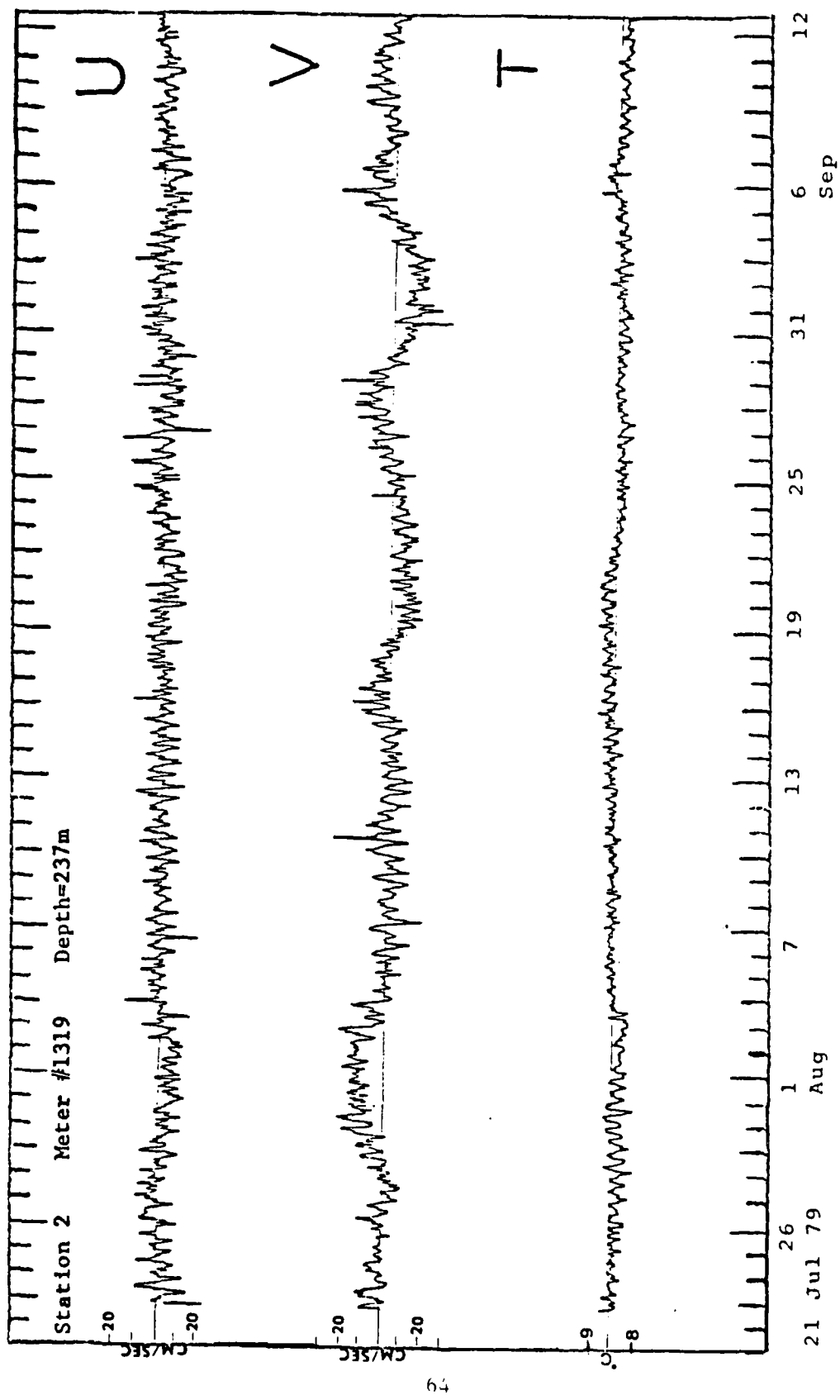


Figure 20. U component, V component, and temperature plots versus time for the current meter at 237 m depth at Station 2 deployed on 21 July 1979.

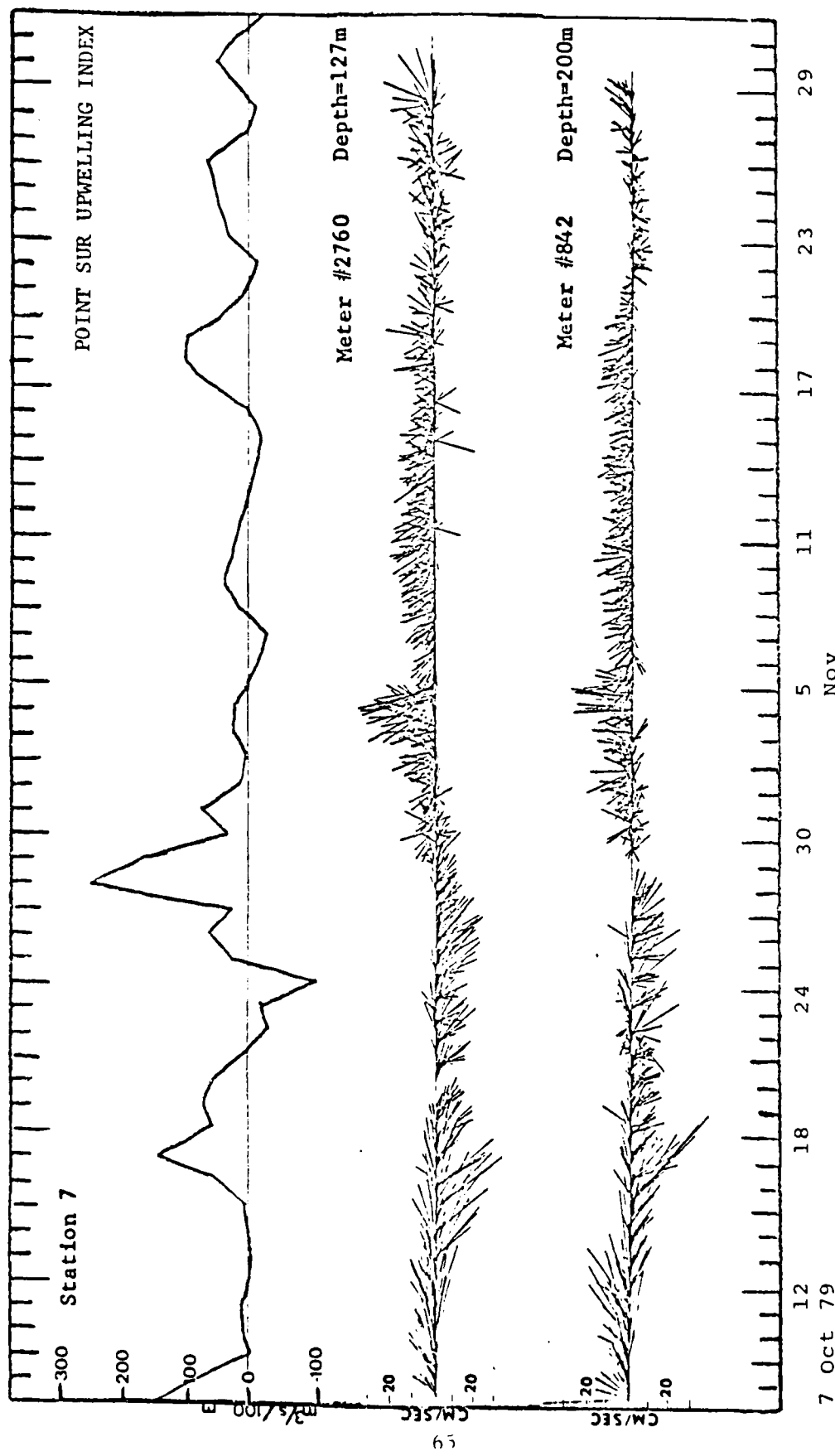


Figure 21. Point Sur Upwelling Index and stickplots of hourly current vectors for the current meters at Station 7 deployed on 7 October 1979.

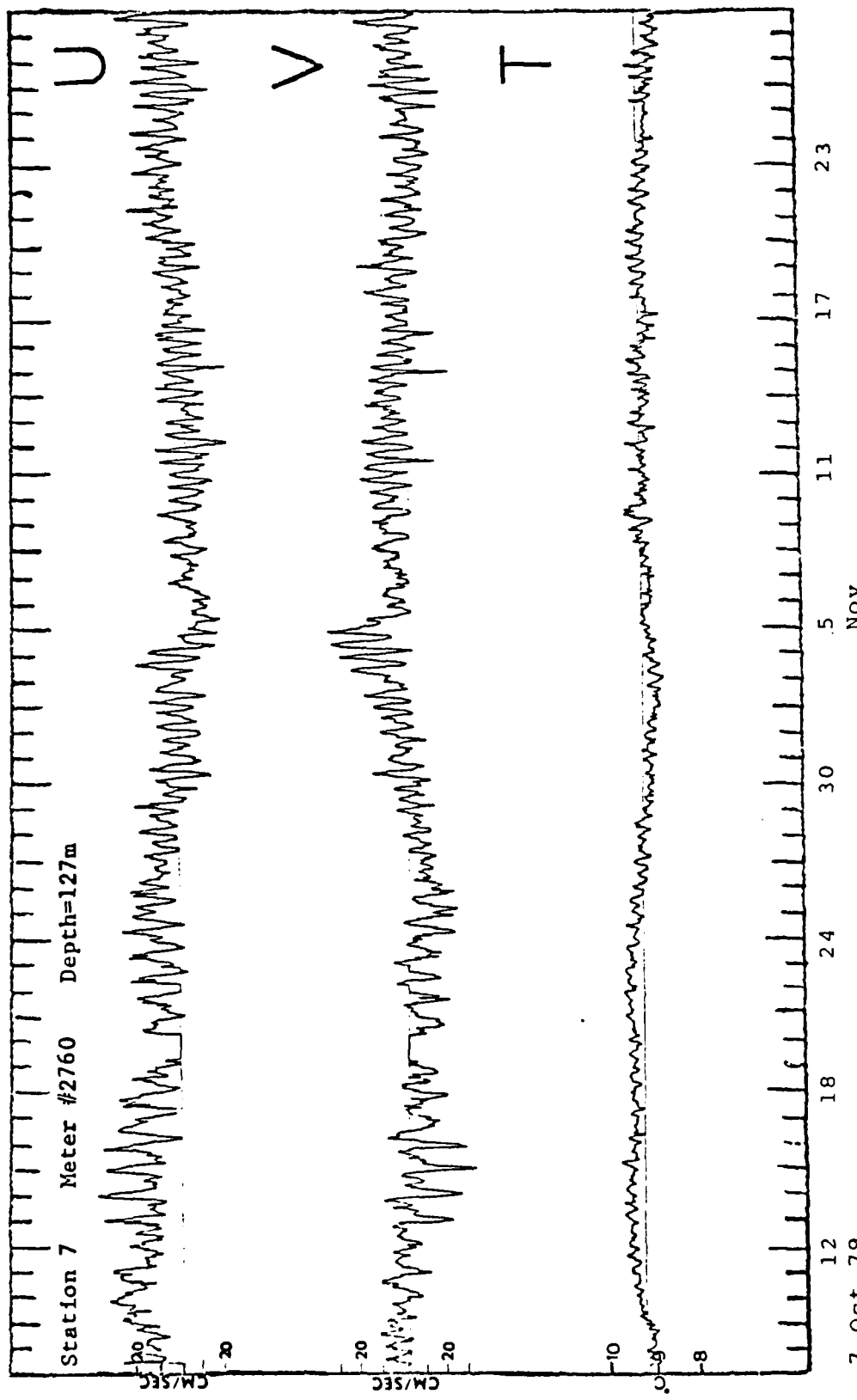


Figure 22. U component, V component, and temperature plots versus time for the current meter at 127 m depth at Station 7 deployed on 7 October 1979.

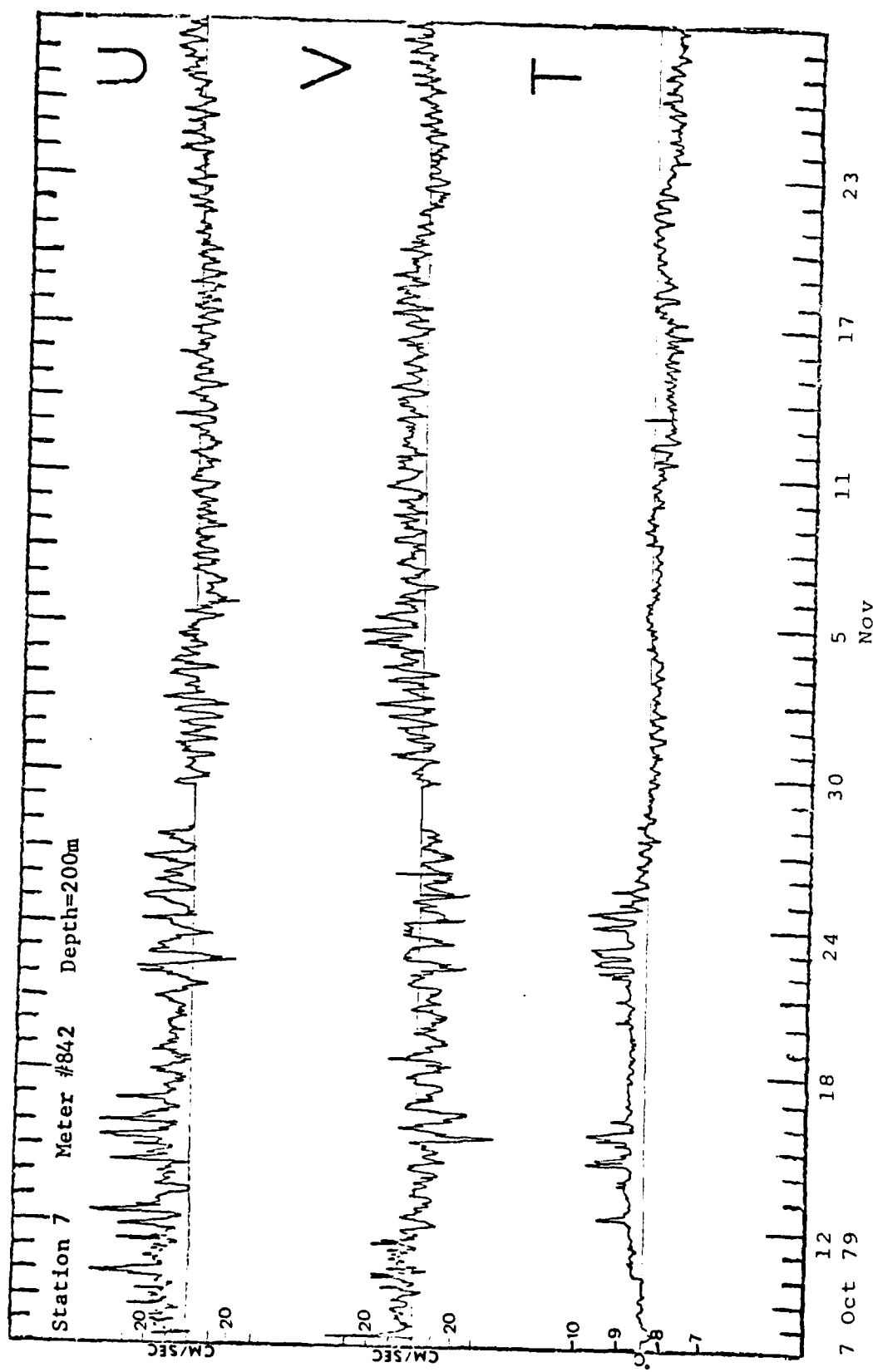


Figure 23. U component, V component, and temperature plots versus time for the current meter at 200 m depth at Station 7 deployed on 7 October 1979.

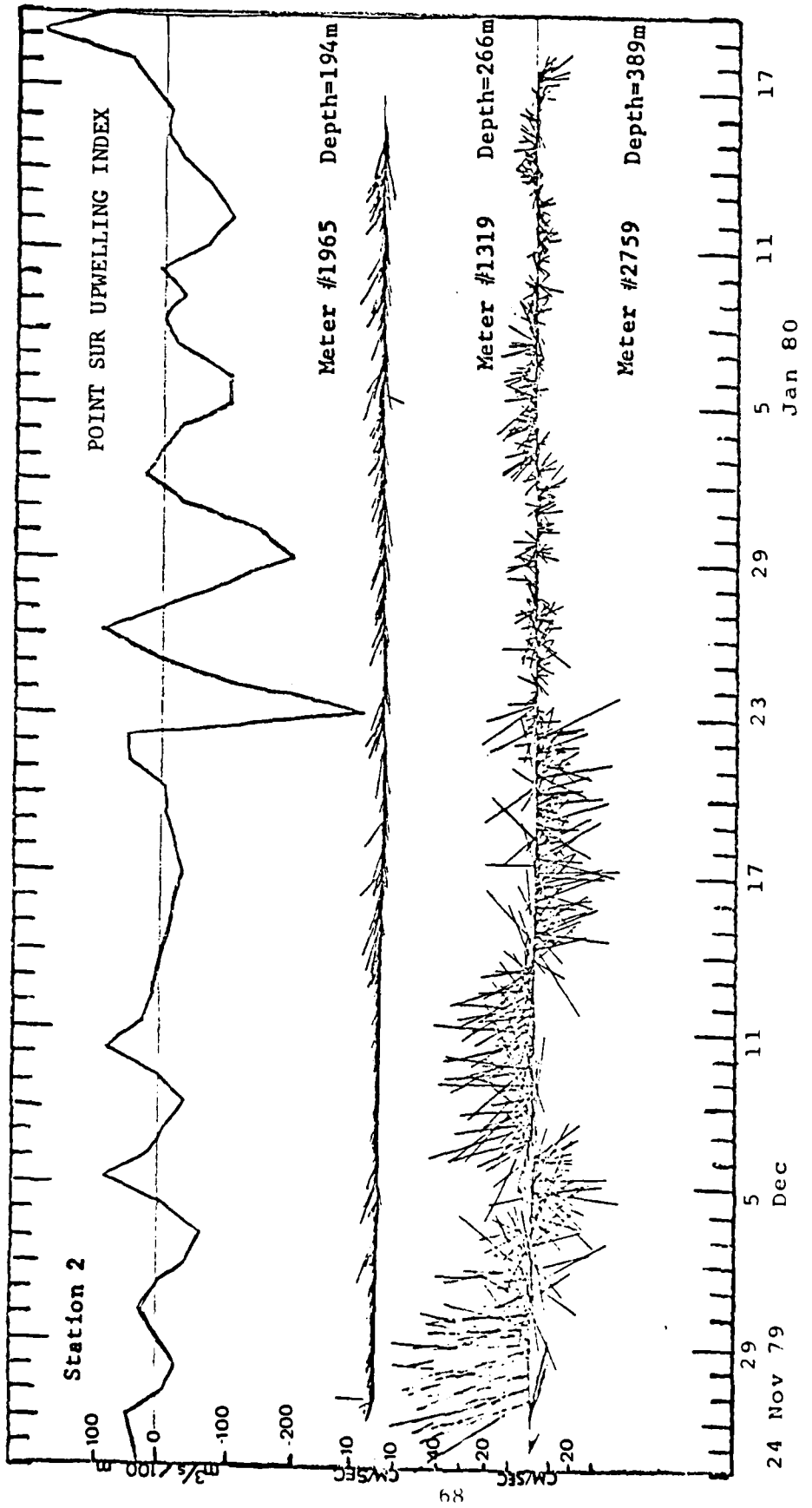


Figure 24. Point Sur Upwelling Index and stickplots of hourly current vectors for the current meters at Station 2 deployed on 24 November 1979.

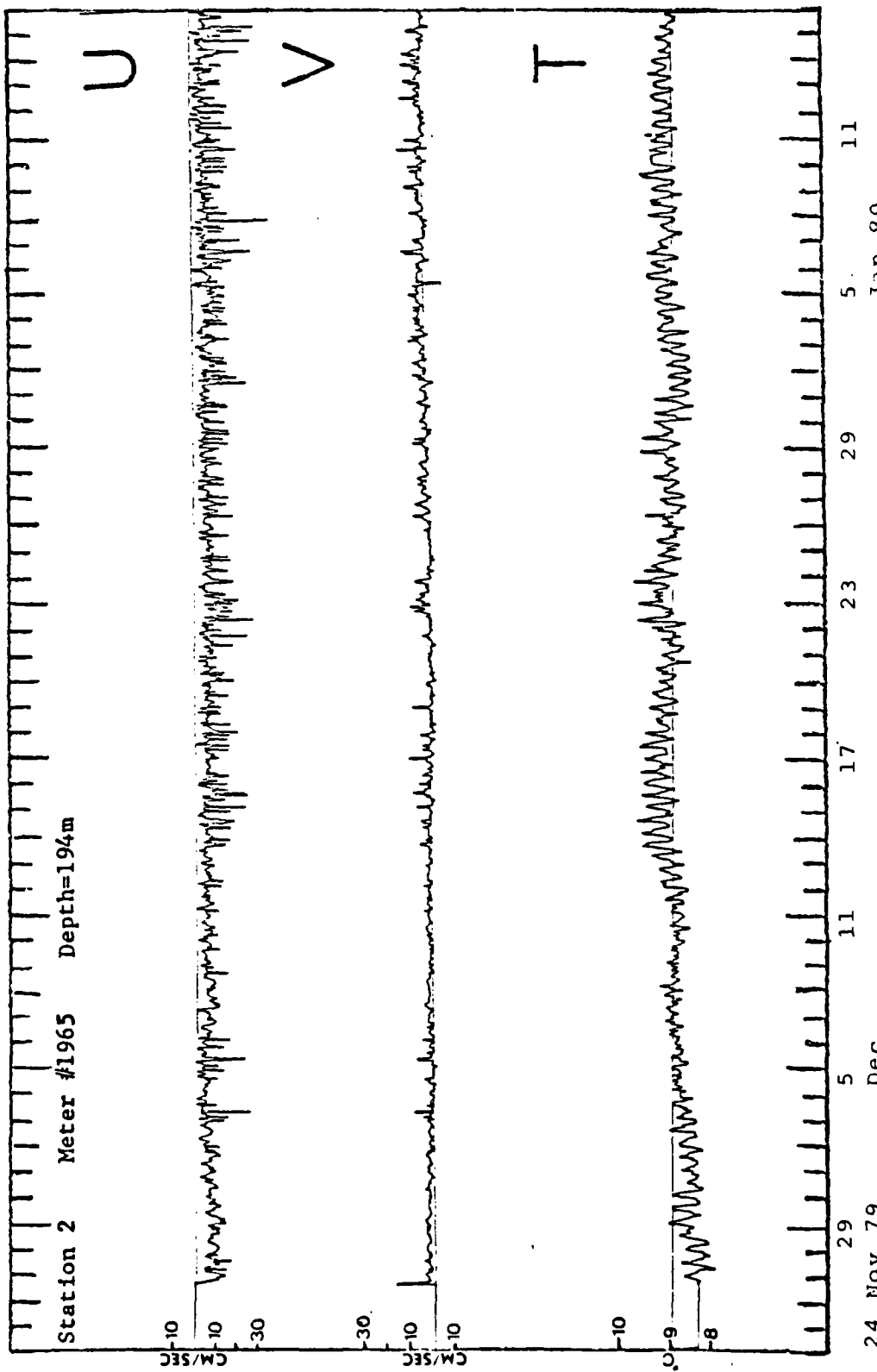


Figure 25. U component, V component, and temperature plots versus time for the current meter at 194 m depth at Station 2 deployed on 24 November 1979.

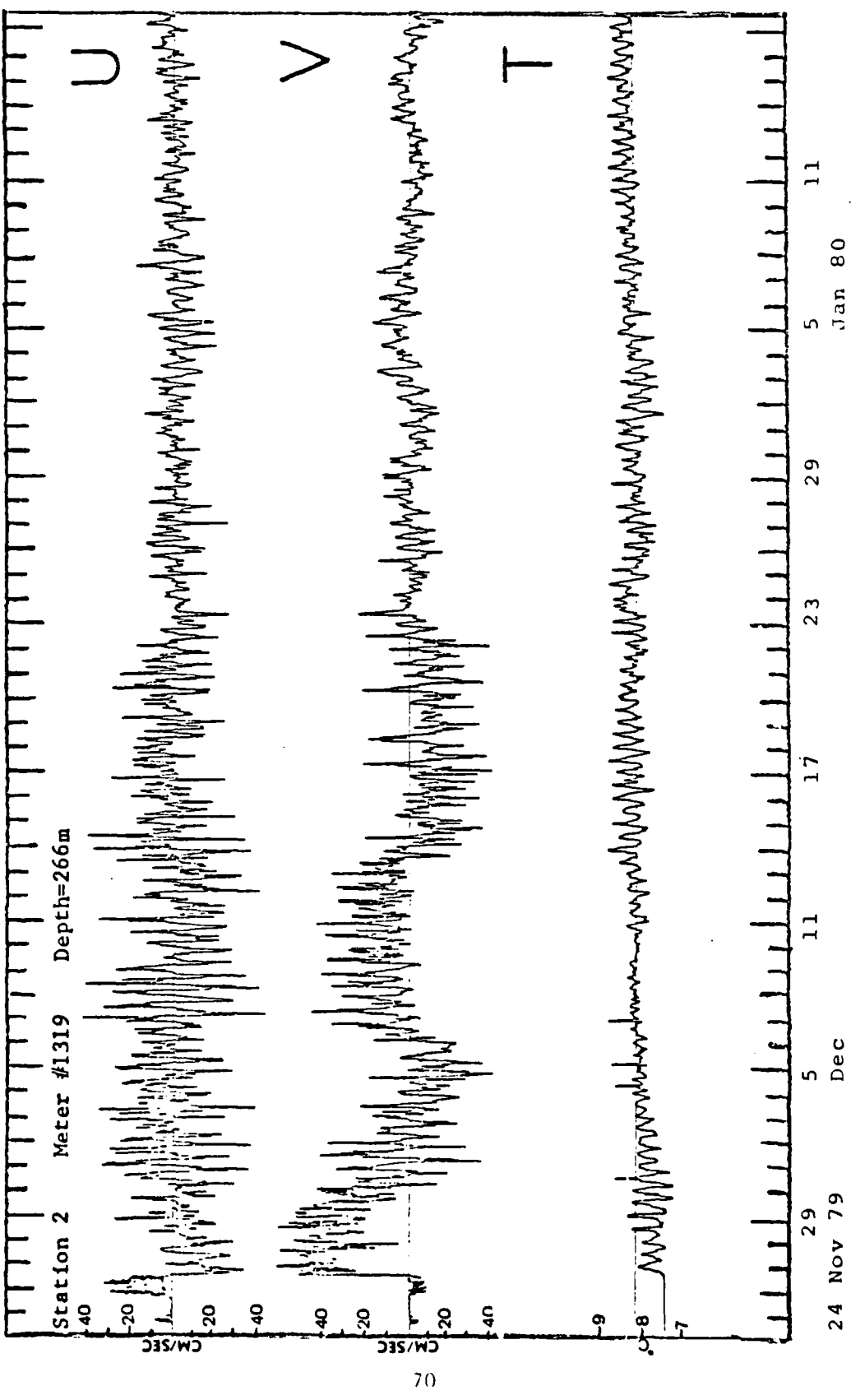


Figure 26. U component, V component, and temperature plots versus time for the current meter at 266 m depth at Station 2 deployed on 24 November 1979.

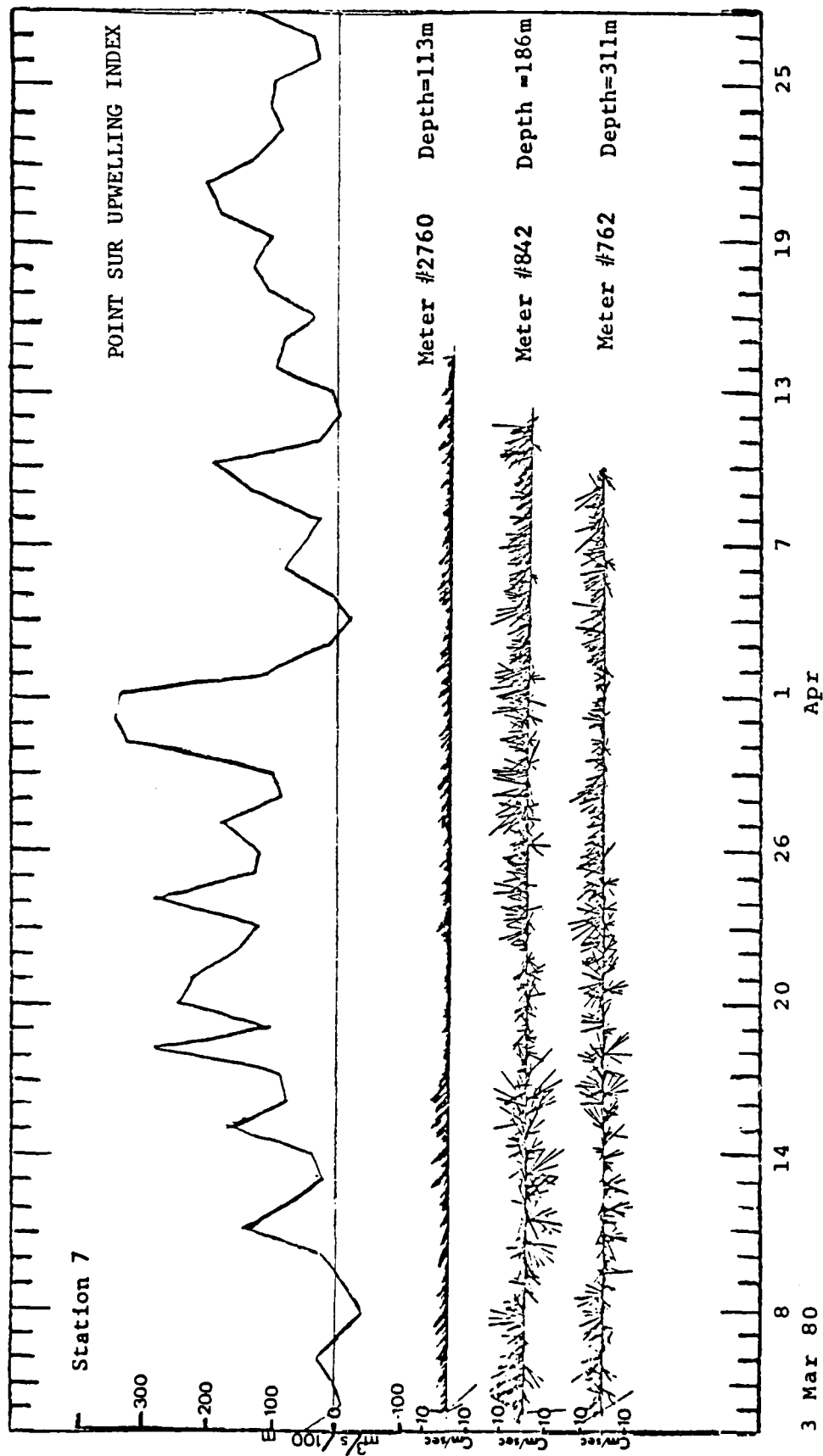


Figure 27. Point Sur Upwelling Index and stickplots of hourly current vectors for the current meters at Station 7 deployed on 3 March 1980.

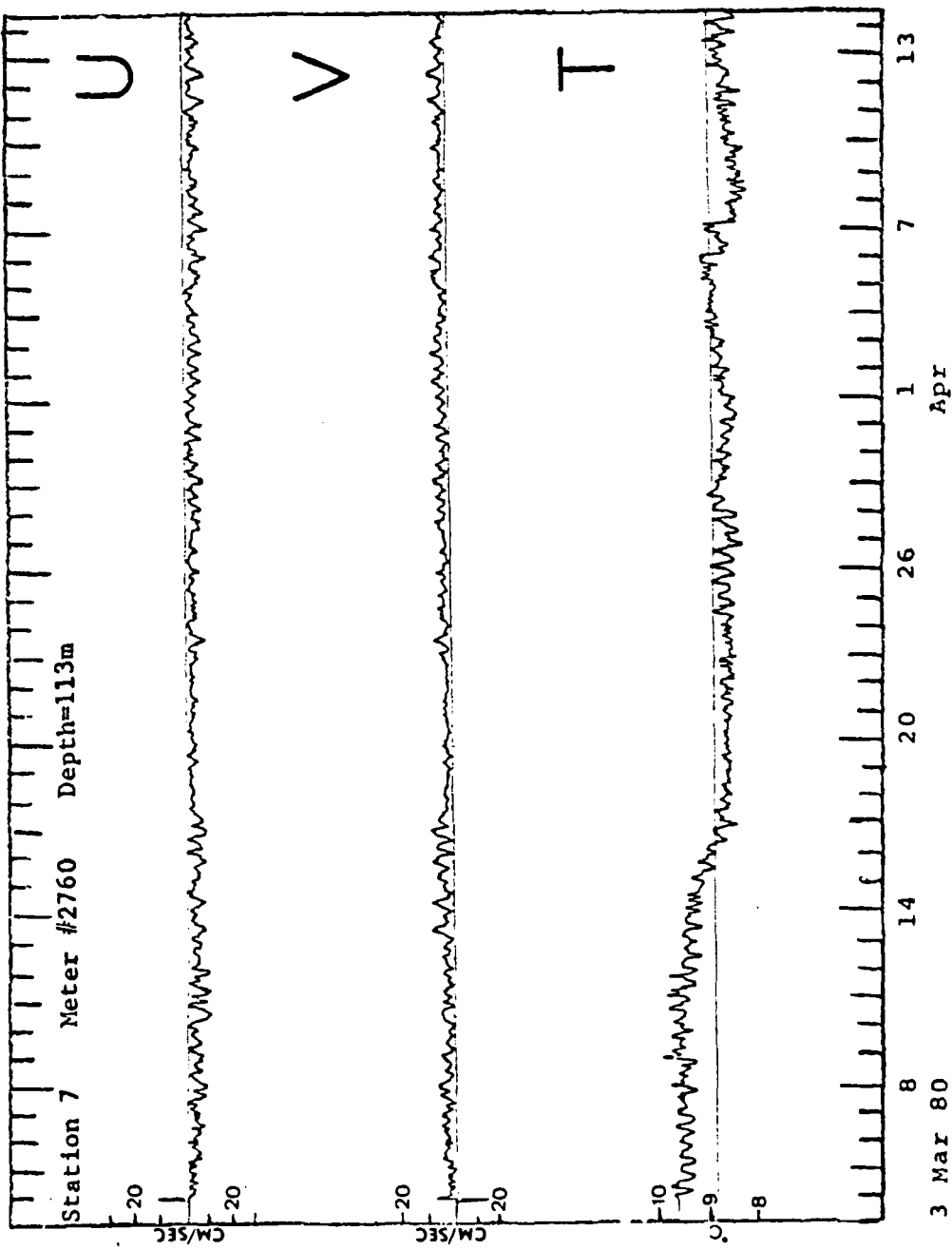


Figure 28. U component, V component, and temperature plots versus time for the current meter at 113 m depth at Station 7 deployed on 3 March 1980.

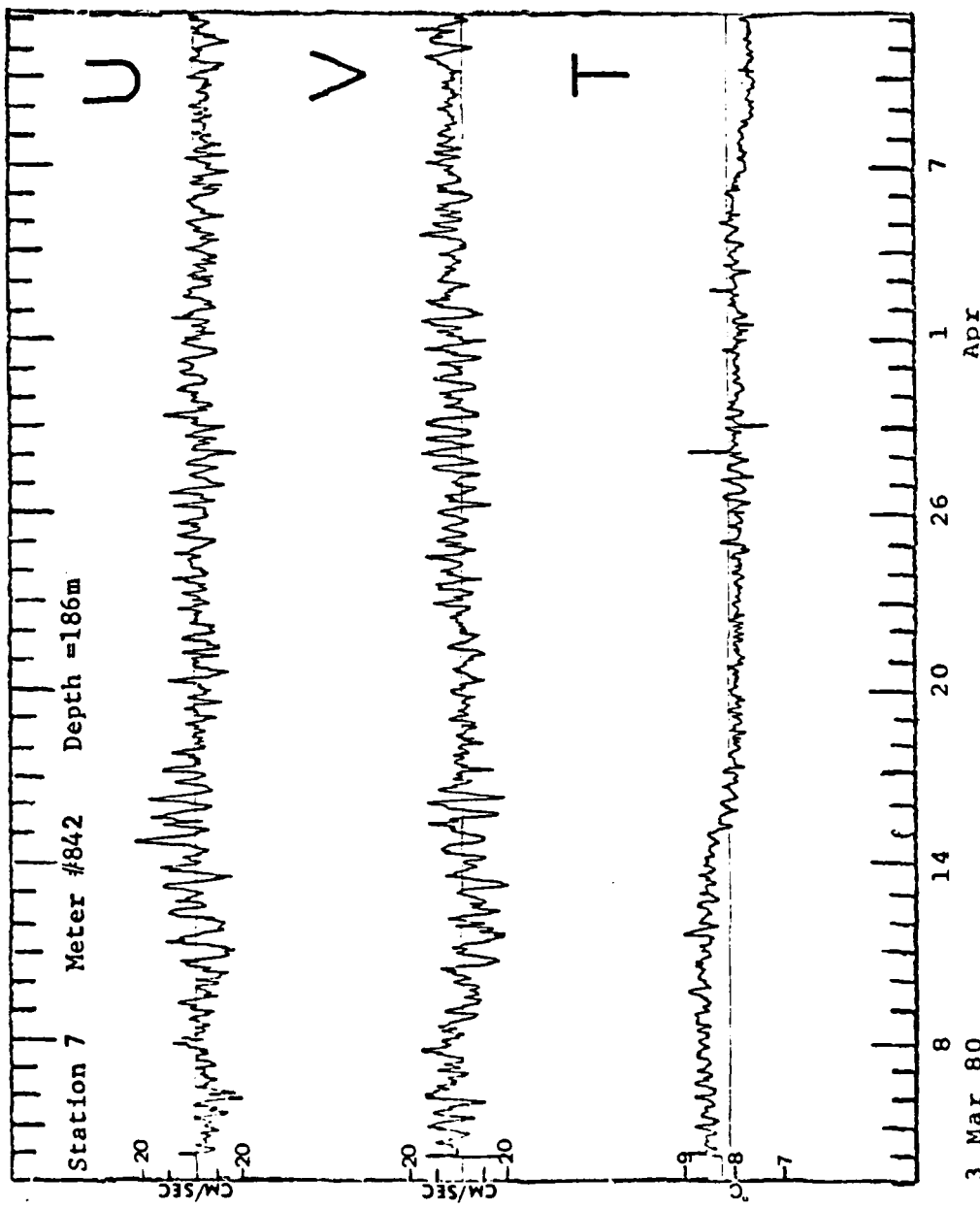


Figure 29. U component, V component, and temperature plots versus time for the current meters at 186 m depth at Station 7 deployed on 3 March 1980.

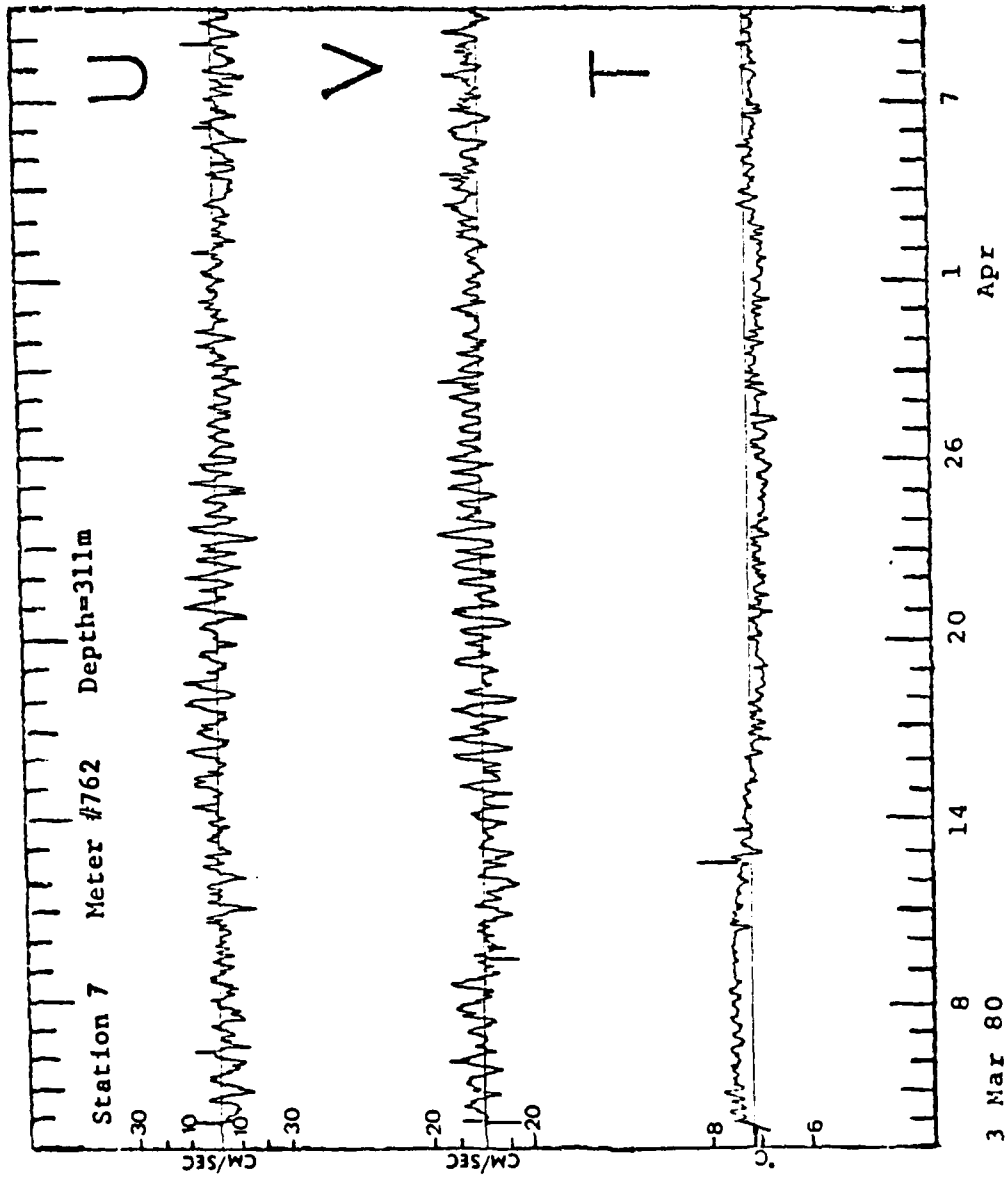


Figure 30. U component, V component, and temperature plots versus time for the current meter at 311 m depth at Station 7 deployed on 5 January 1979.

APPENDIX B: SPECTRUM ANALYSES OF ALONGSHORE FLOW AND
ON/OFFSHORE FLOW

Station 7 Meter #762 Depth=152m 5 Jan 79

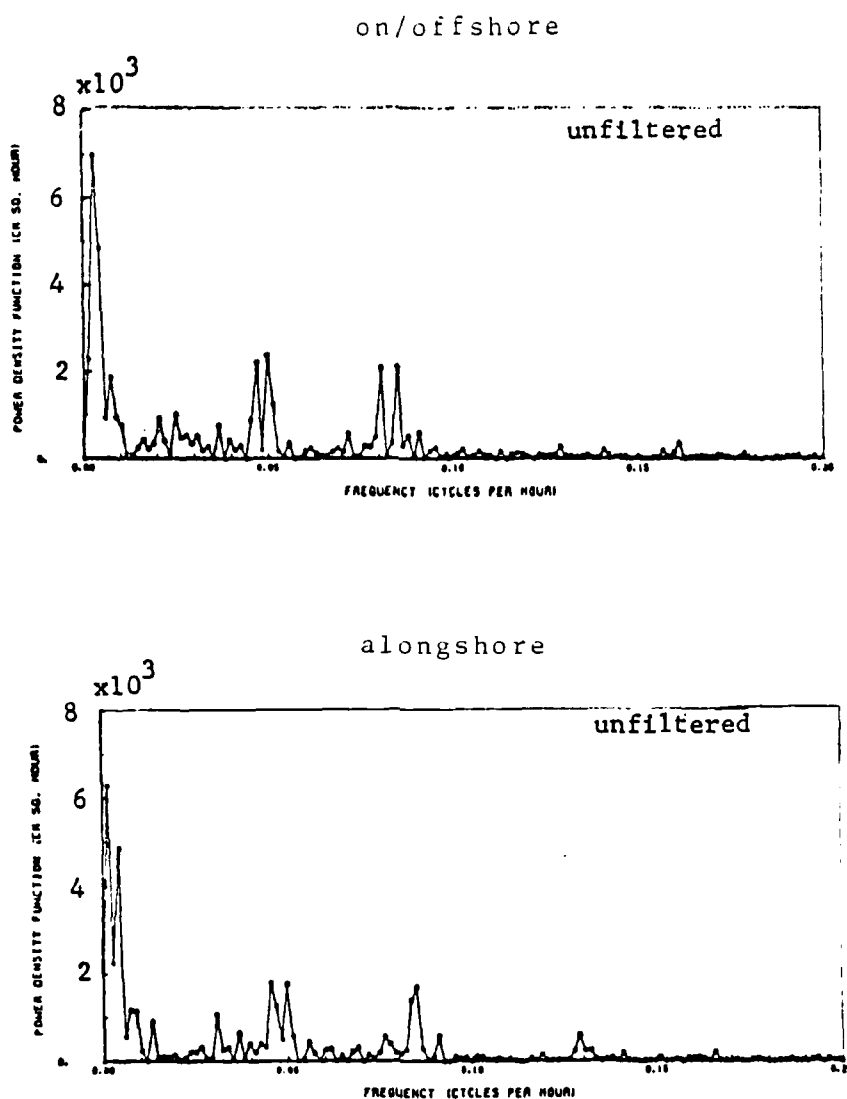


Figure 31. Energy density spectrum of current meter at 152 m depth at Station 7 deployed on 5 January 1979.

Station 7 Meter #842 Depth=223m 5 Jan 79

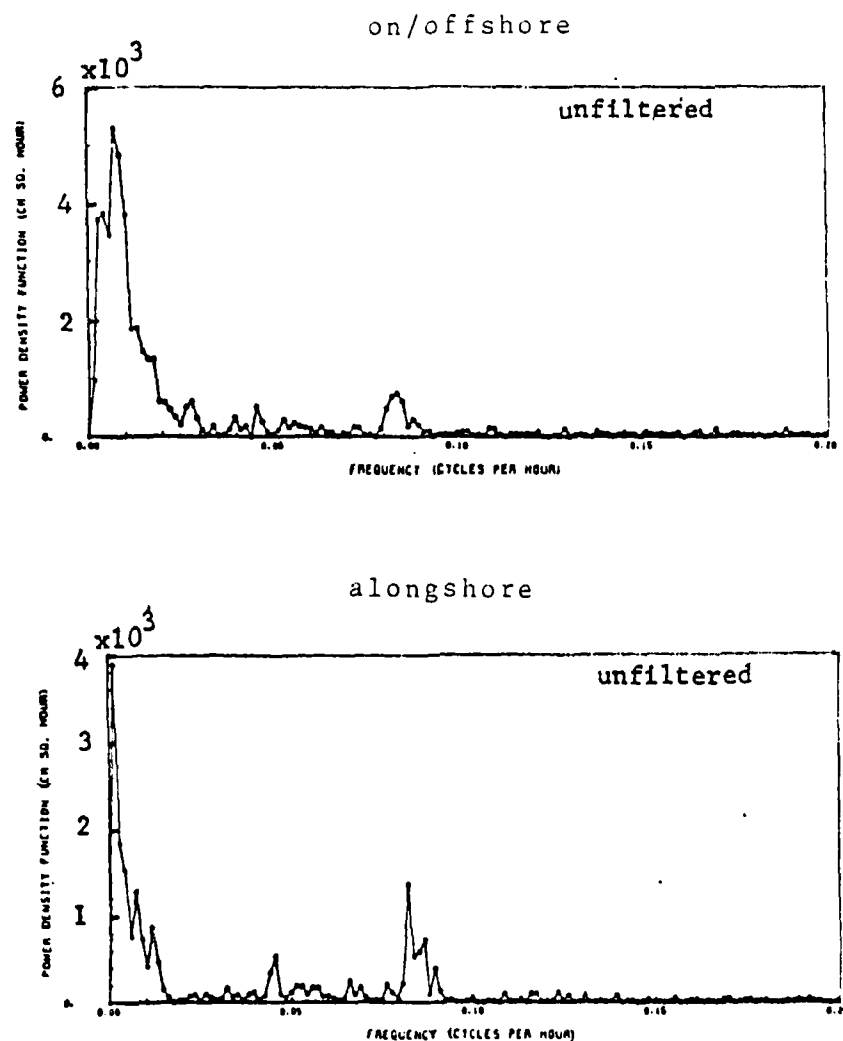


Figure 32. Energy density spectrum of current meter at 223 m depth at Station 7 deployed on 5 January 1979.

Station 2 Meter #1965 Depth=169m 23 Apr 79

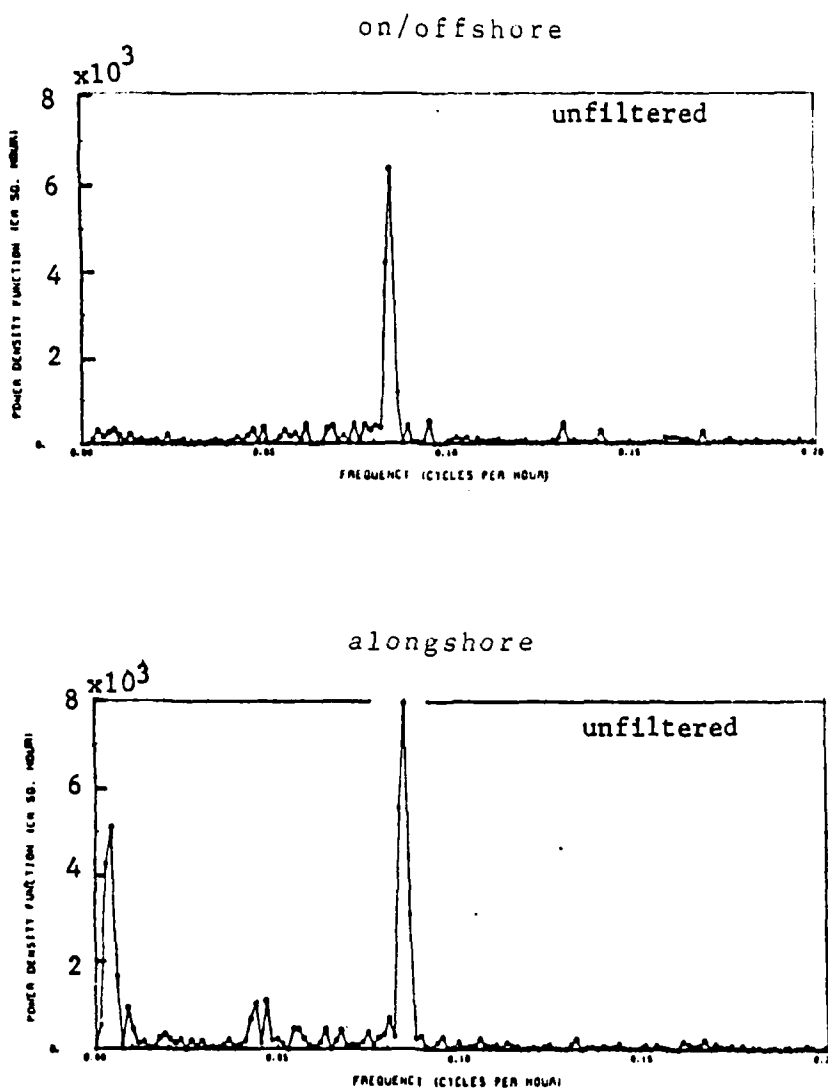


Figure 33. Energy density spectrum of current meter at 169 m depth at Station 2 deployed on 23 April 1979.

Station 2 Meter #1319 Depth=241m 23 Apr 79

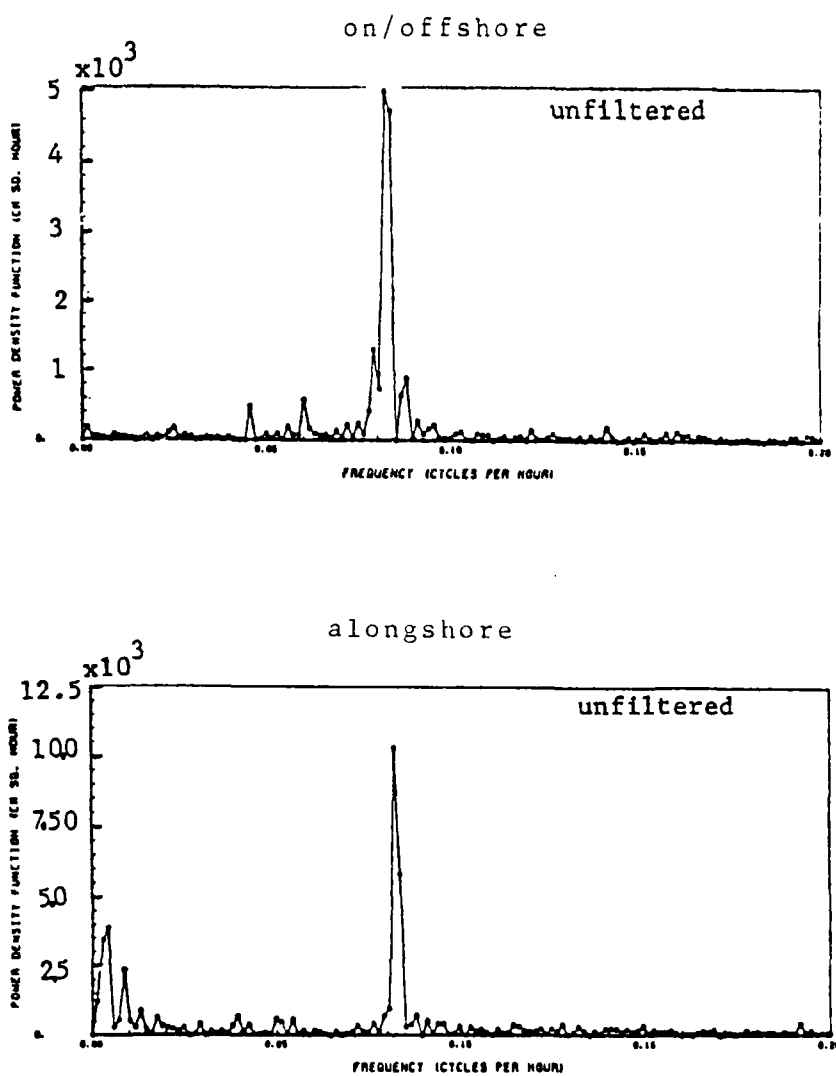


Figure 34. Energy density spectrum of current meter at 241 m depth at Station 2 deployed on 23 April 1979.

Station 7 Meter #2760 Depth=158m 7 Jul 79

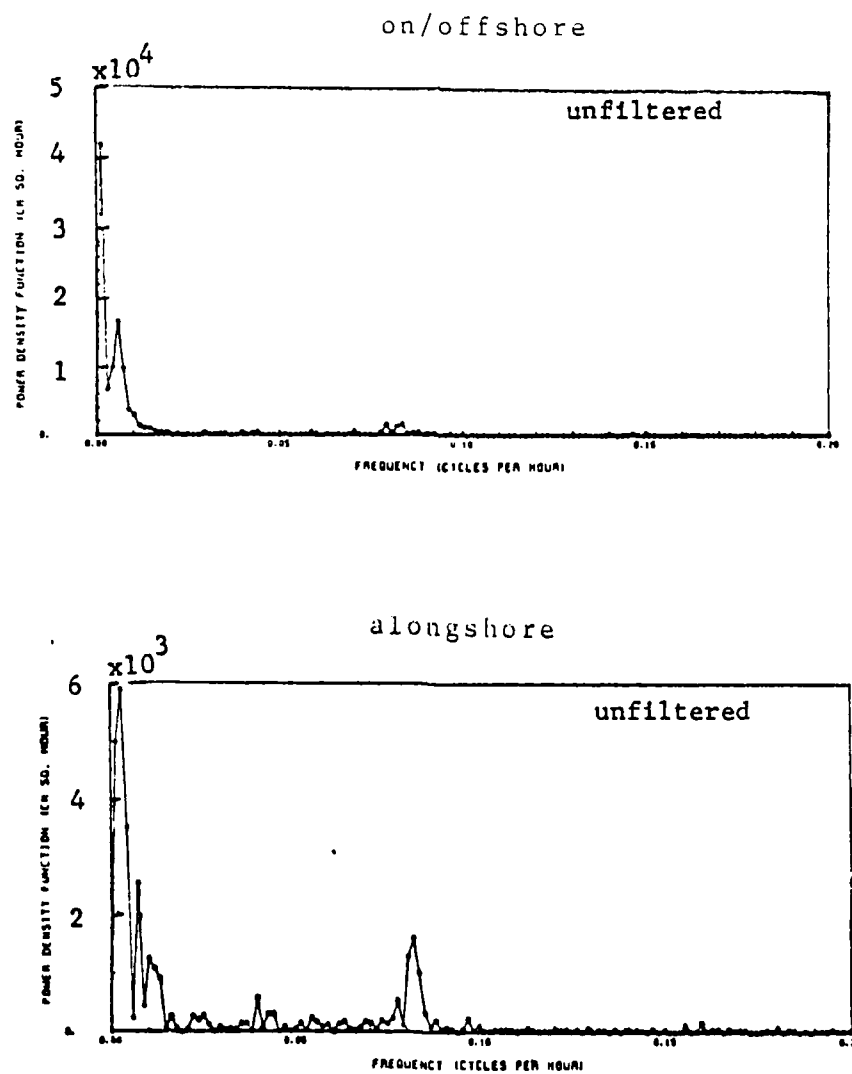


Figure 35. Energy density spectrum of current meter at 158 m depth at Station 7 deployed on 7 July 1979.

Station 7 Meter #842 Depth=231m 7 Jul 79

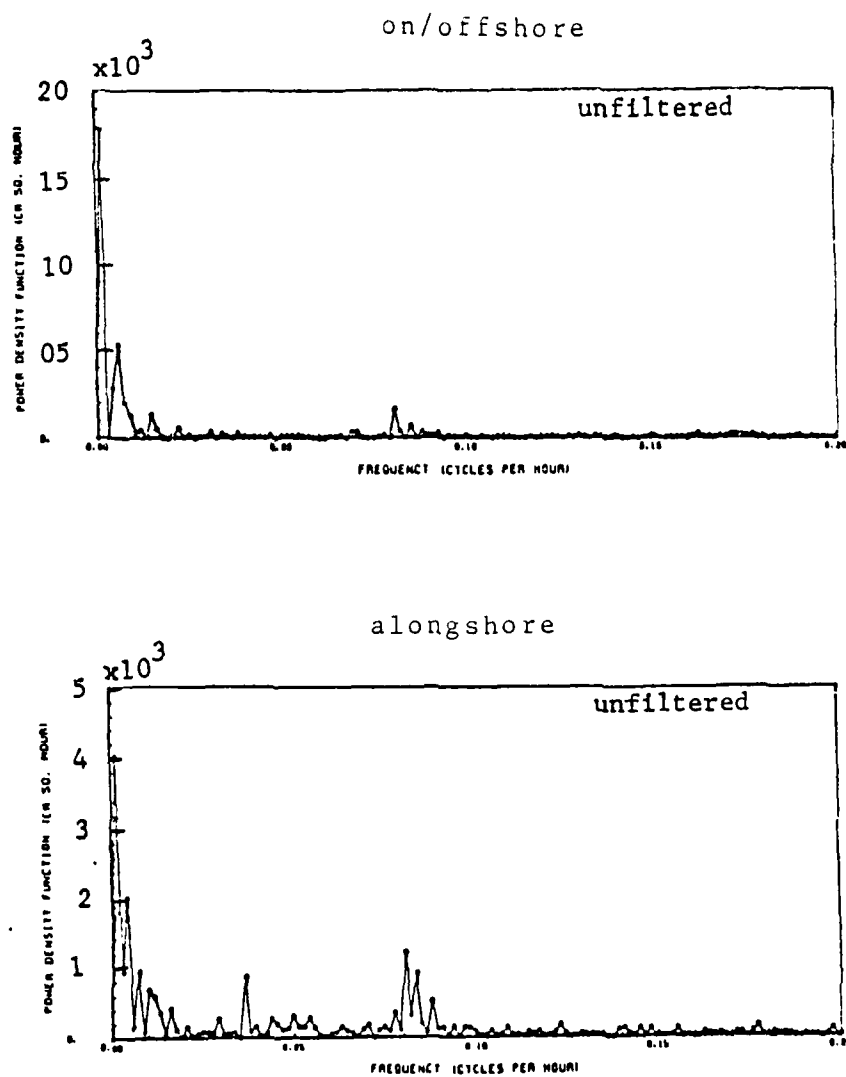


Figure 36. Energy density spectrum of current meter at 231 m depth at Station 7 deployed on 7 July 1979.

Station 7 Meter #762 Depth=356m 7 Jul 79

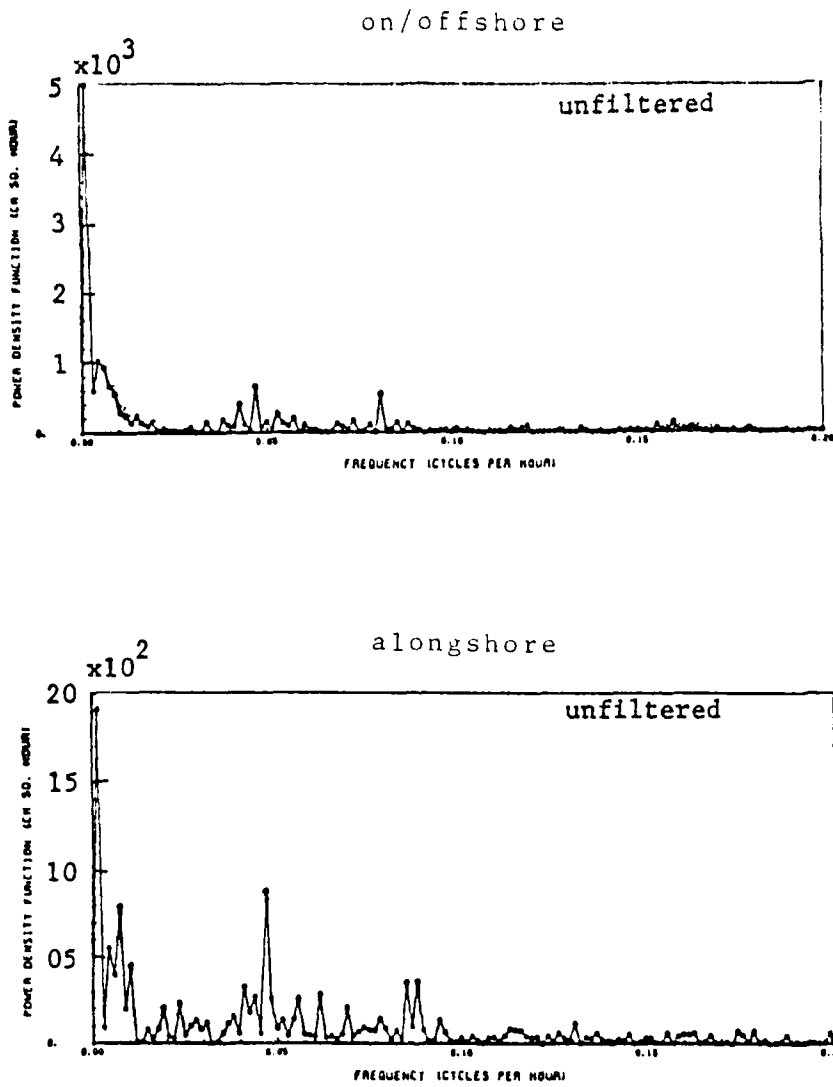


Figure 37. Energy density spectrum of current meter at 356 m depth at Station 7 deployed on 7 July 1979.

Station 2 Meter #1965 Depth=165m 21 Jul 79

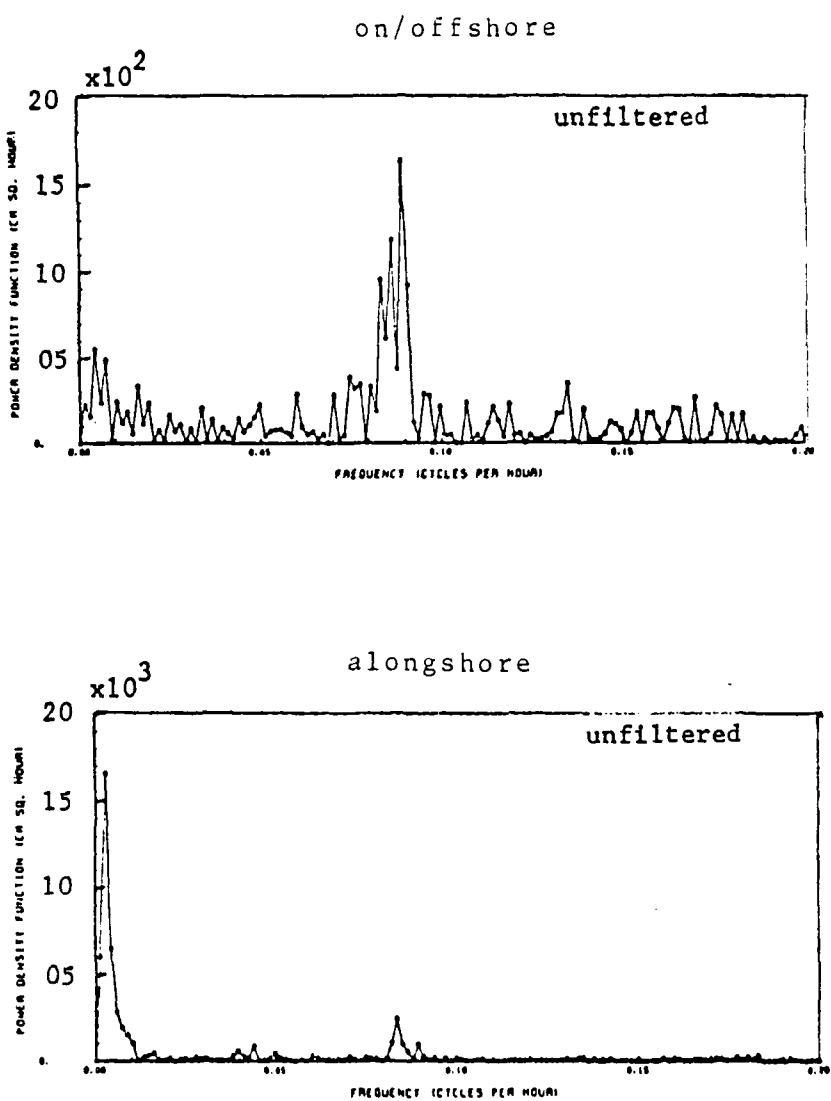


Figure 38. Energy density spectrum of current meter at 165 m depth at Station 2 deployed on 21 July 1979.

Station 2 Meter #1319 Depth=237m 21 Jul 79

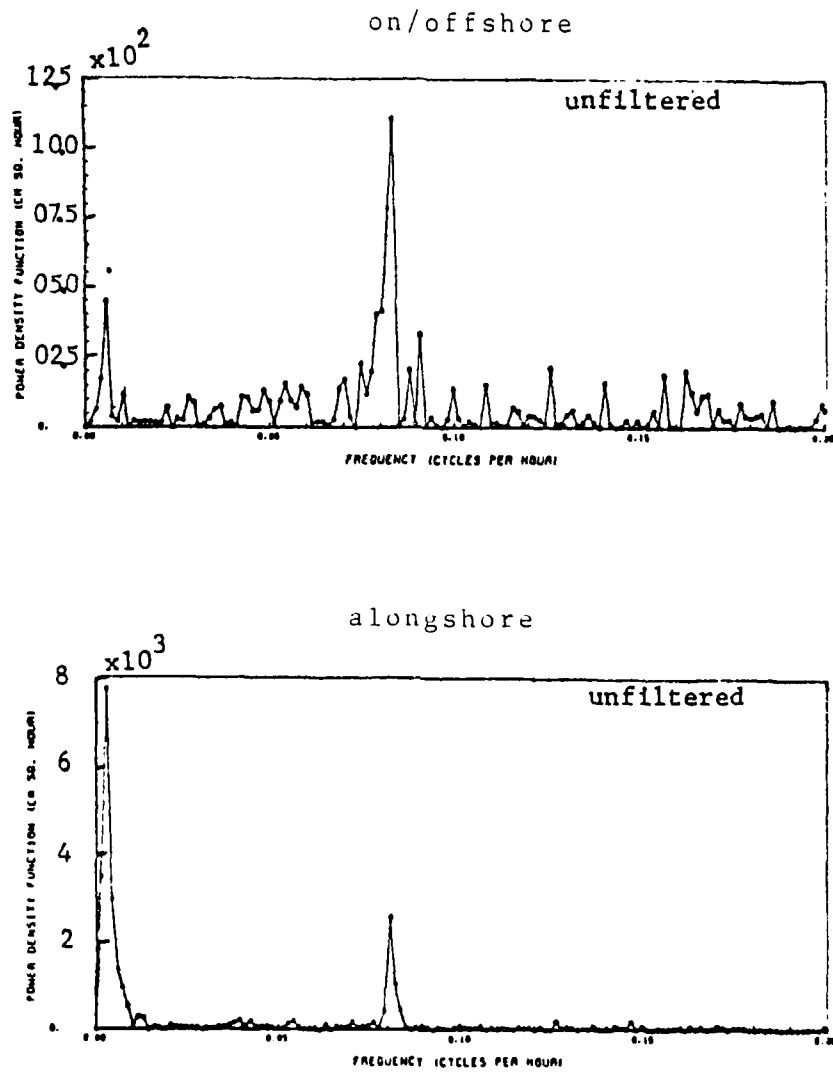


Figure 39. Energy density spectrum of current meter at 237 m depth at Station 2 deployed on 21 July 1979.

Station 7 Meter #2760 Depth=127m 7 Oct 79

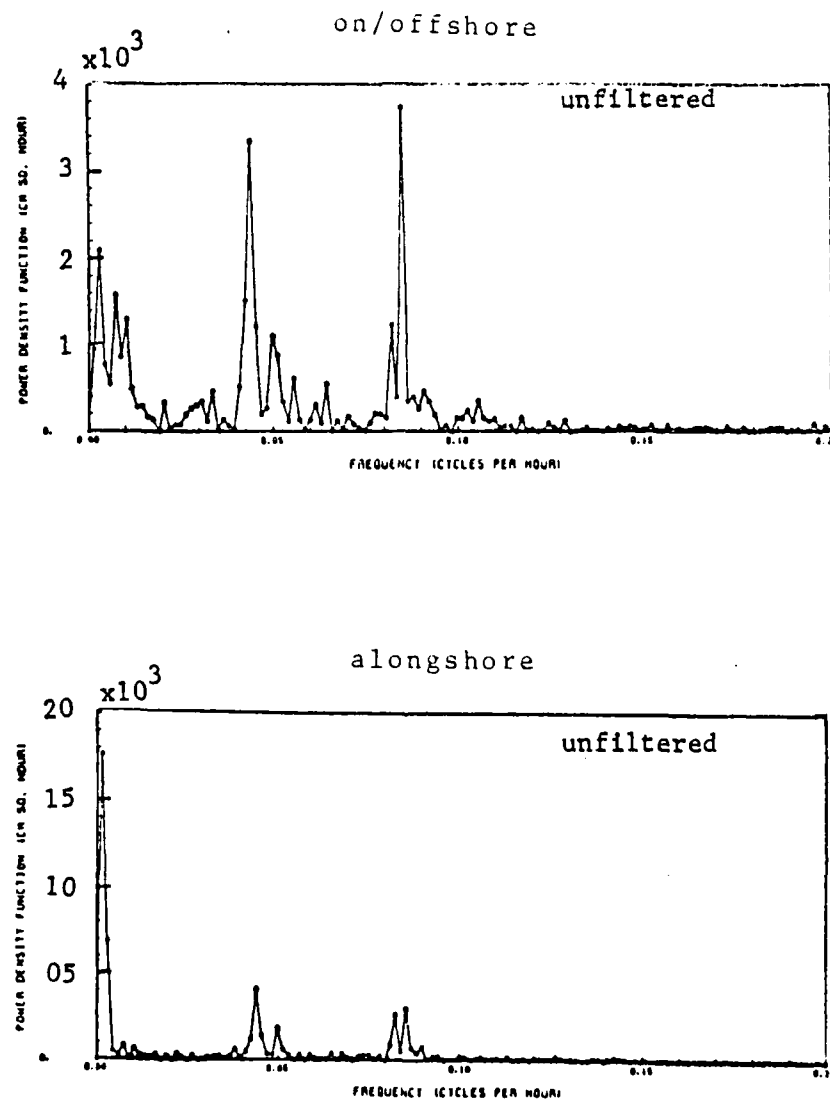


Figure 40. Energy denisty spectrum of current meter at 127 m depth at Station 7 deployed on 7 October 1979.

Station 7 Meter #842 Depth=200m 7 Oct 79

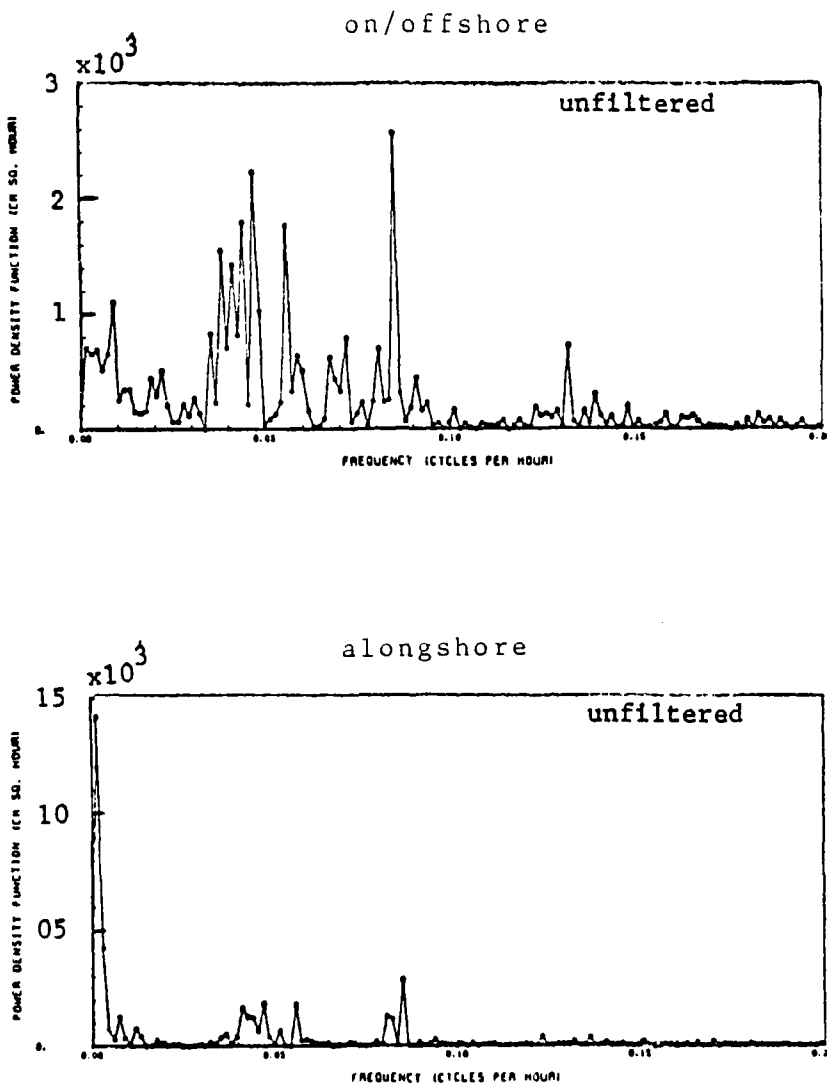


Figure 41. Energy density spectrum of current meter at 200 m depth at Station 7 deployed on 7 October 1979.

Station 2 Meter #1965 Depth=194m 24 Nov 79

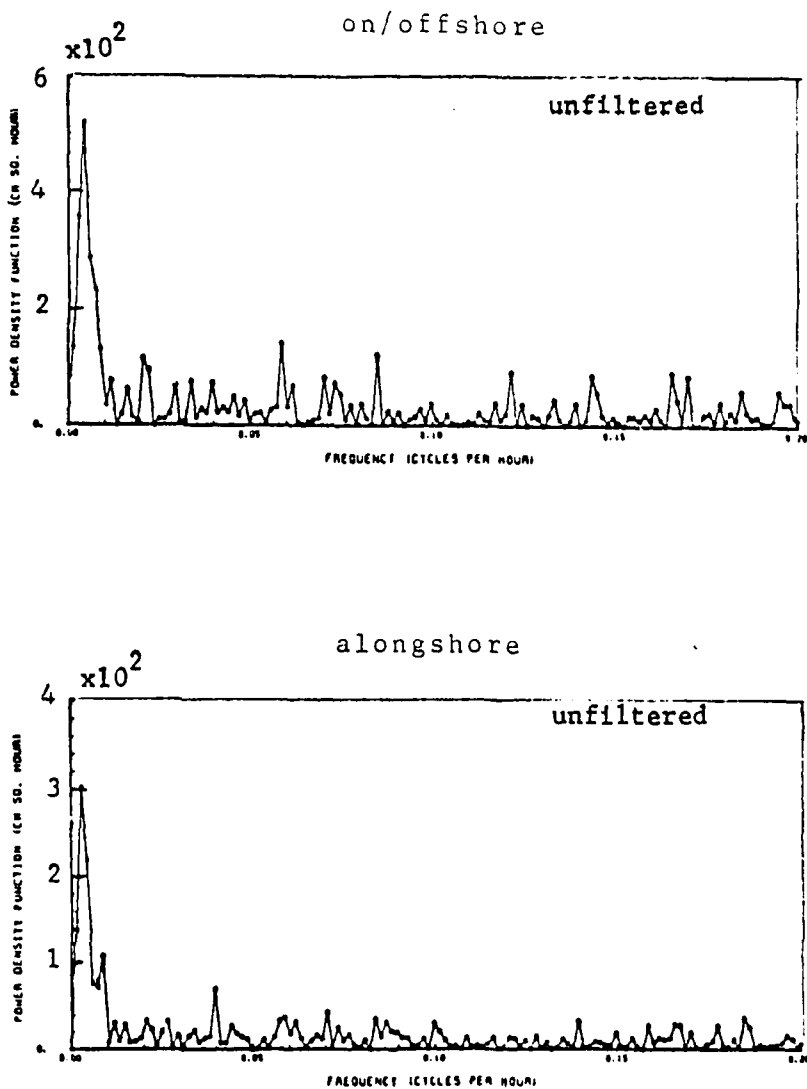


Figure 42. Energy density spectrum of current meter at 194 m depth at Station 2 deployed on 24 November 1979.

Station 2 Meter #1319 Depth=266m 24 Nov 79

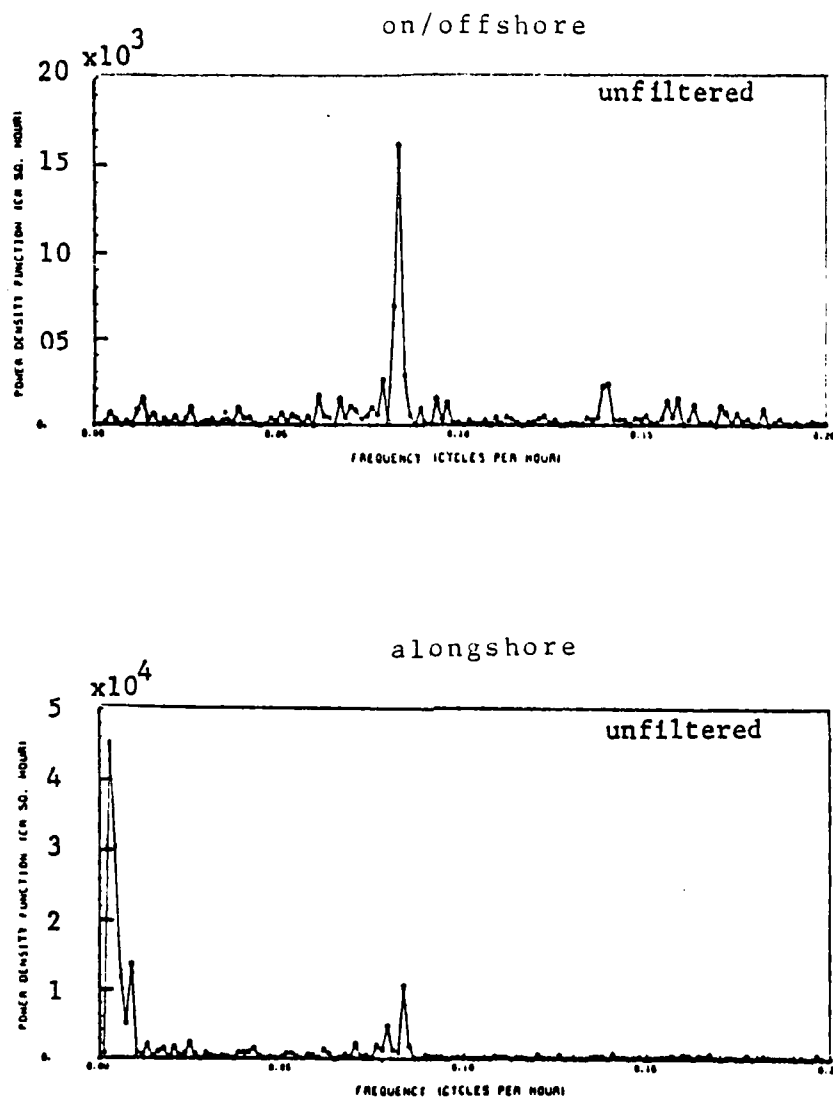
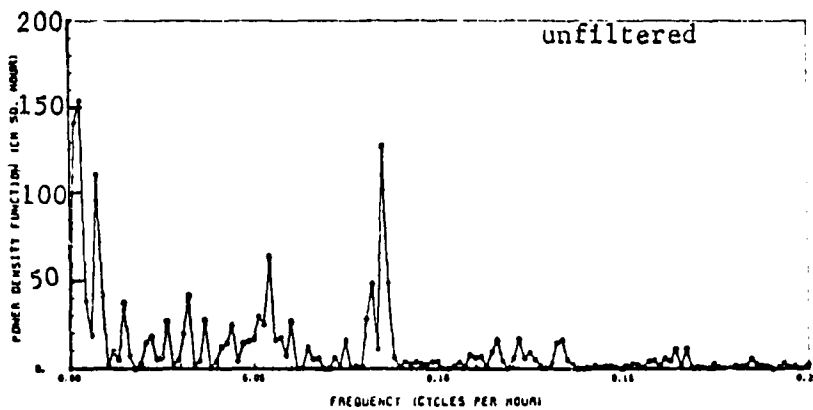


Figure 43. Energy density spectrum of current meter at 266 m depth at Station 2 deployed on 24 November 1979.

Station 7 Meter #2760 Depth=113m 3 Mar 80

on/offshore



alongshore

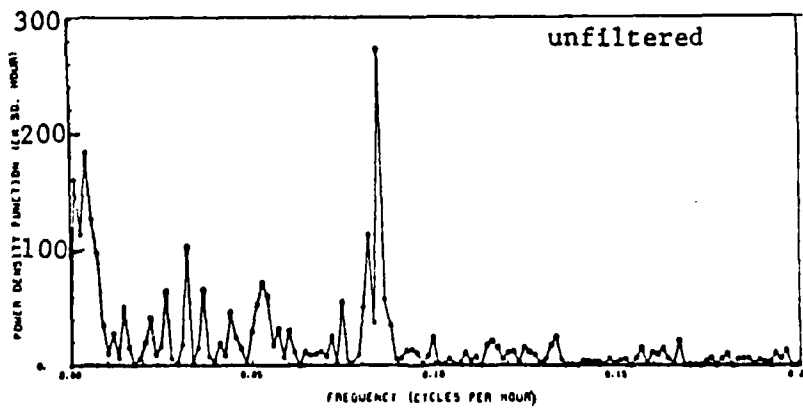


Figure 44. Energy density spectrum of current meter at 113 m depth at Station 7 deployed on 3 March 1980.

Station 7 Meter #842 Depth = 186m 3 Mar 80

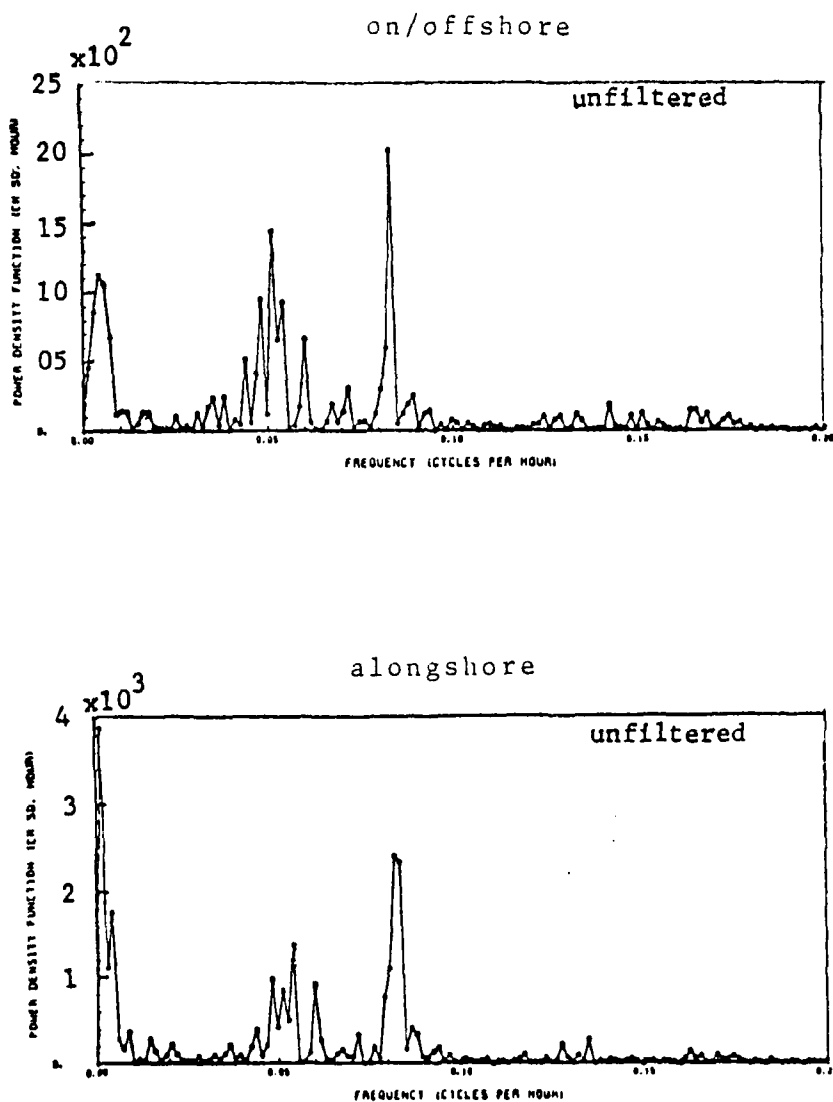


Figure 45. Energy density spectrum of current meter at 186 m depth at Station 7 deployed on 3 March 1980.

Station 7 Meter #762 Depth=311m 3 Mar 80

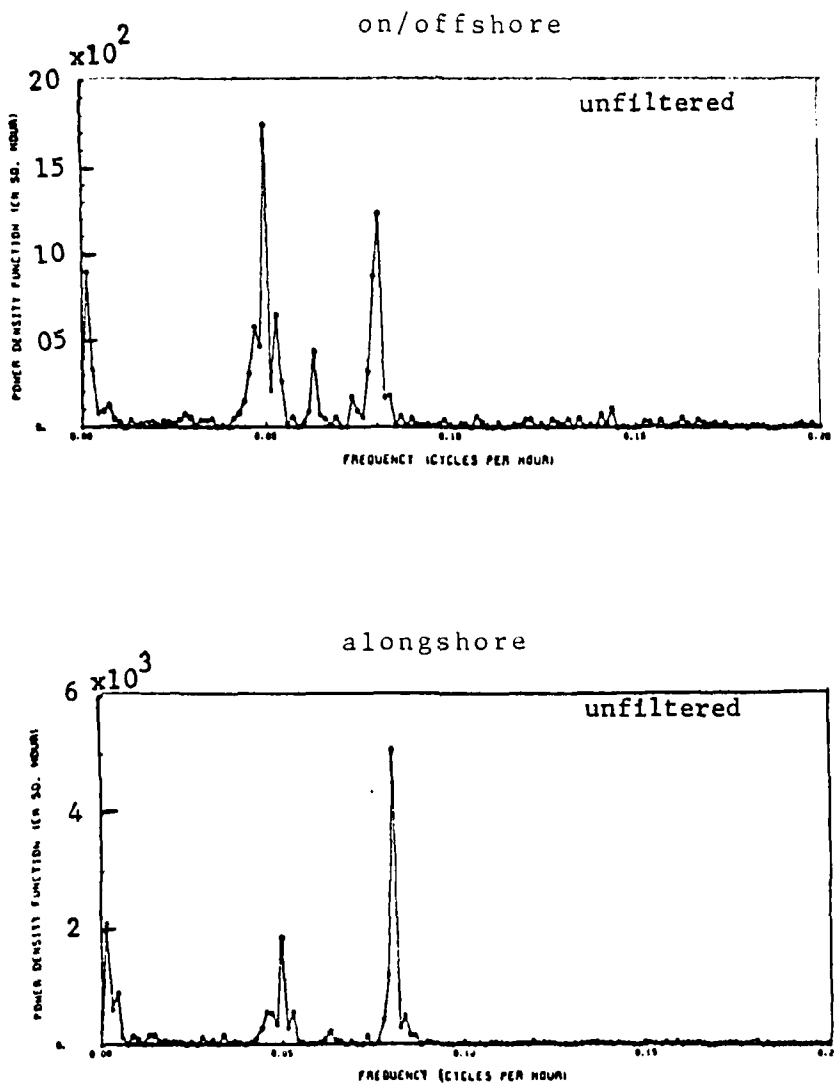


Figure 46. Energy density spectrum of current meter at 311 m depth at Station 7 deployed on 3 March 1980.

APPENDIX C: PROGRESSIVE VECTOR DIAGRAMS

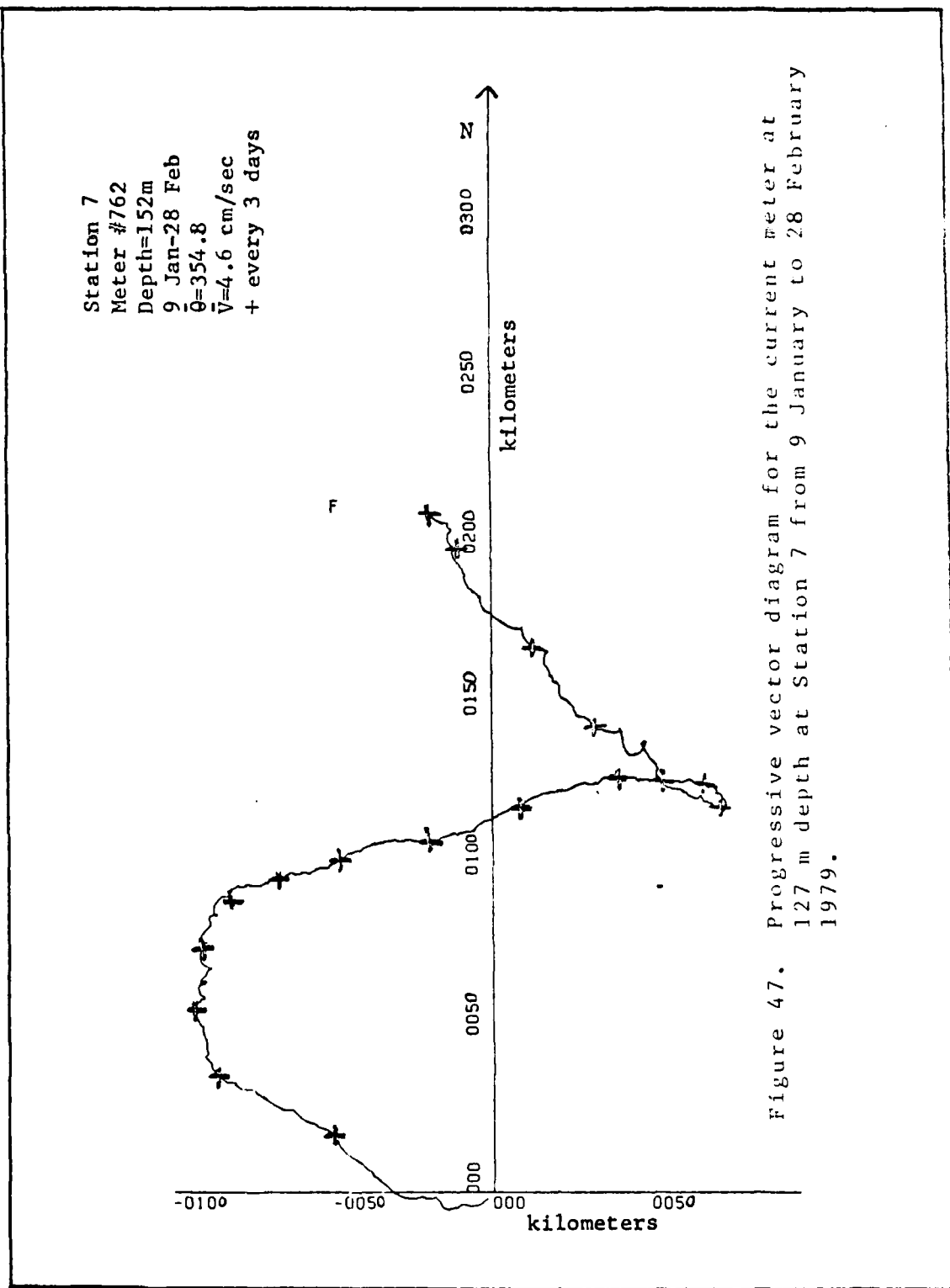


Figure 47. Progressive vector diagram for the current meter at 127 m depth at Station 7 from 9 January to 28 February 1979.

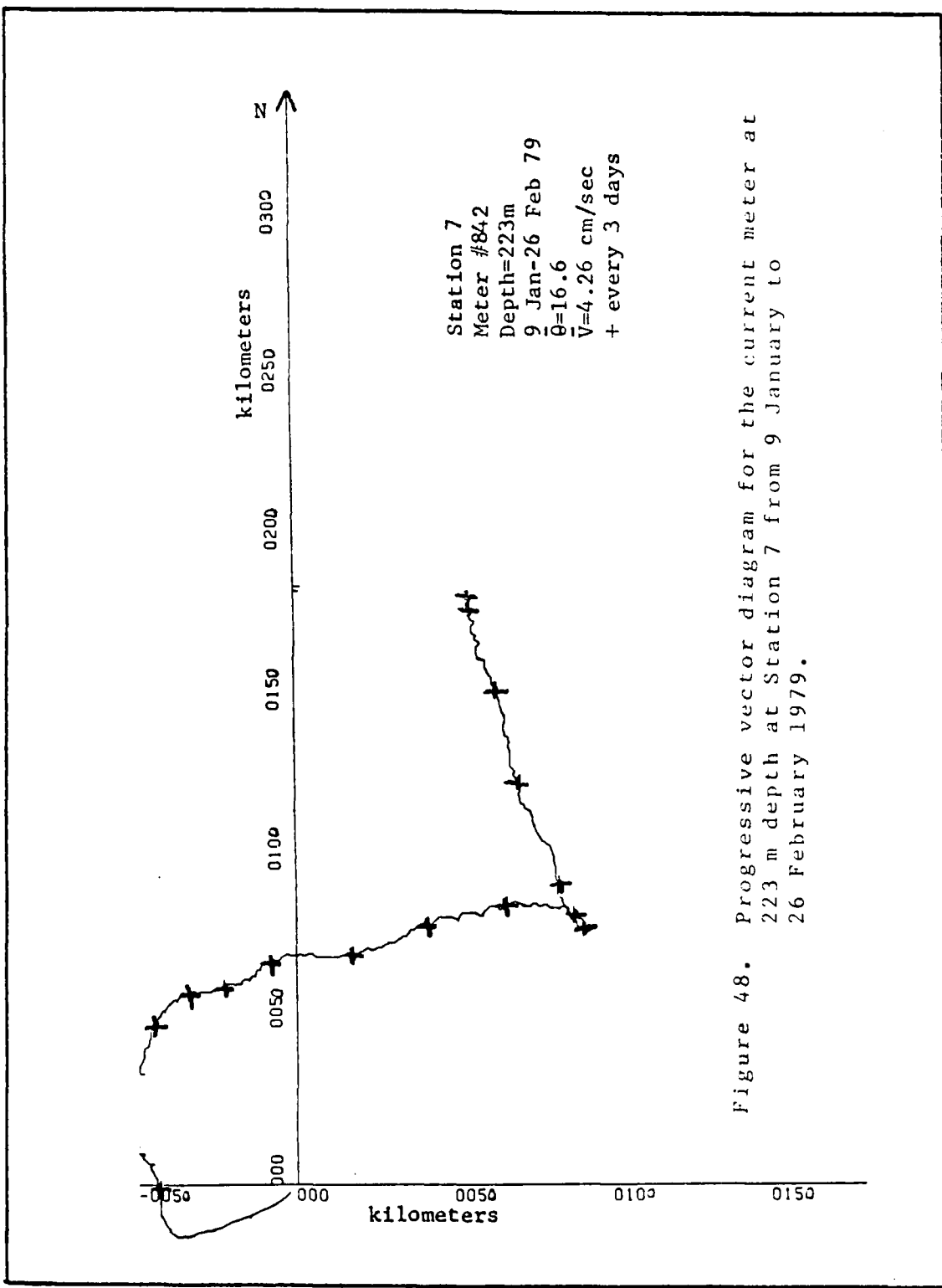


Figure 48. Progressive vector diagram for the current meter at 223 m depth at Station 7 from 9 January to 26 February 1979.

Station 2
Meter #1965
Depth=169m
24 Apr-13 June 79
 $\theta=341.2$
 $\bar{V}=16.01$ cm/sec
+ every 3 days

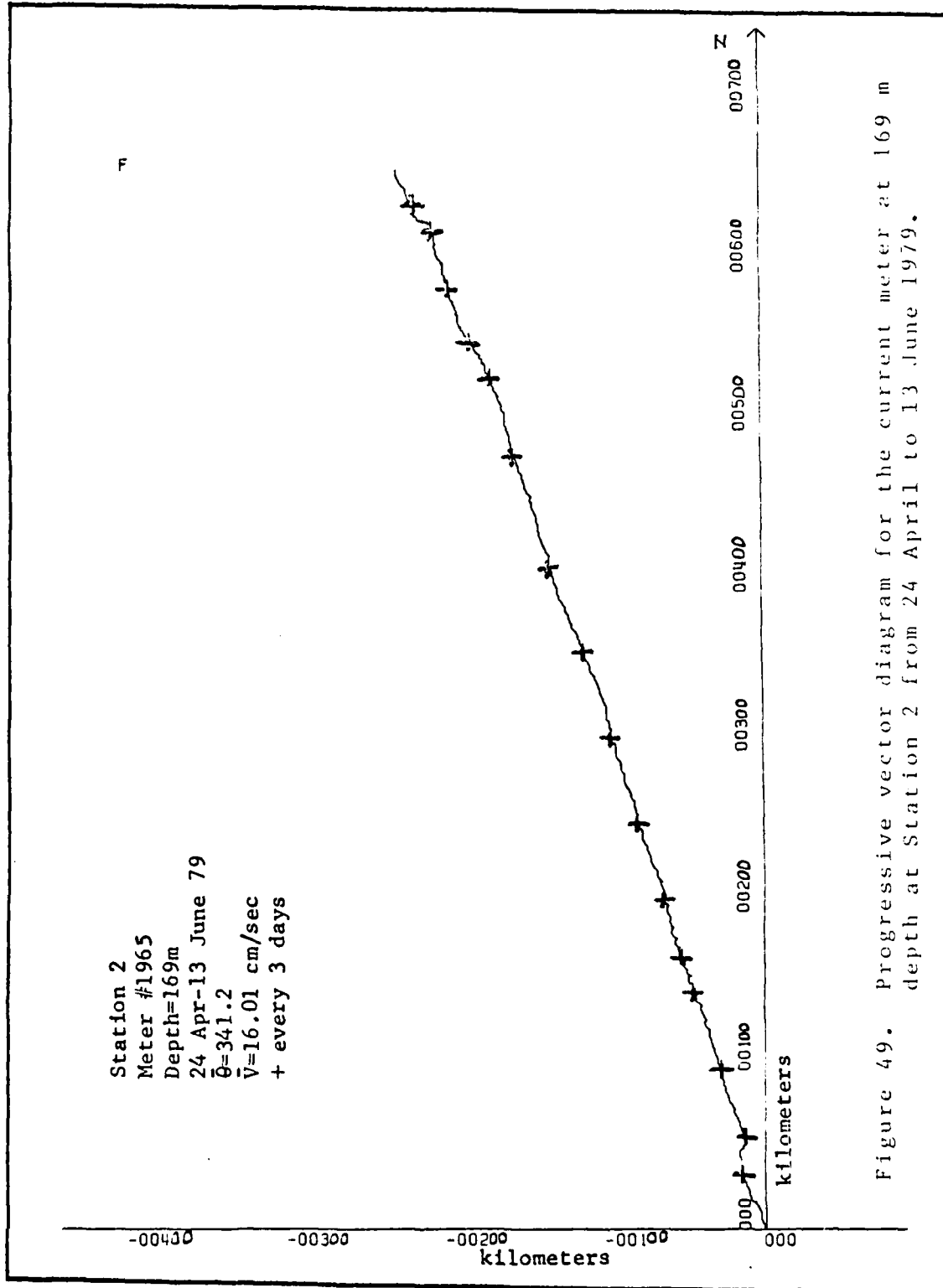


Figure 49. Progressive vector diagram for the current meter at 169 m depth at Station 2 from 24 April to 13 June 1979.

Station 2
Meter #1319
Depth=241m
24 Apr-12 June 79
 $\bar{\theta}=340.4$
 $\bar{v}=11.11$ cm/sec
+ every 3 days

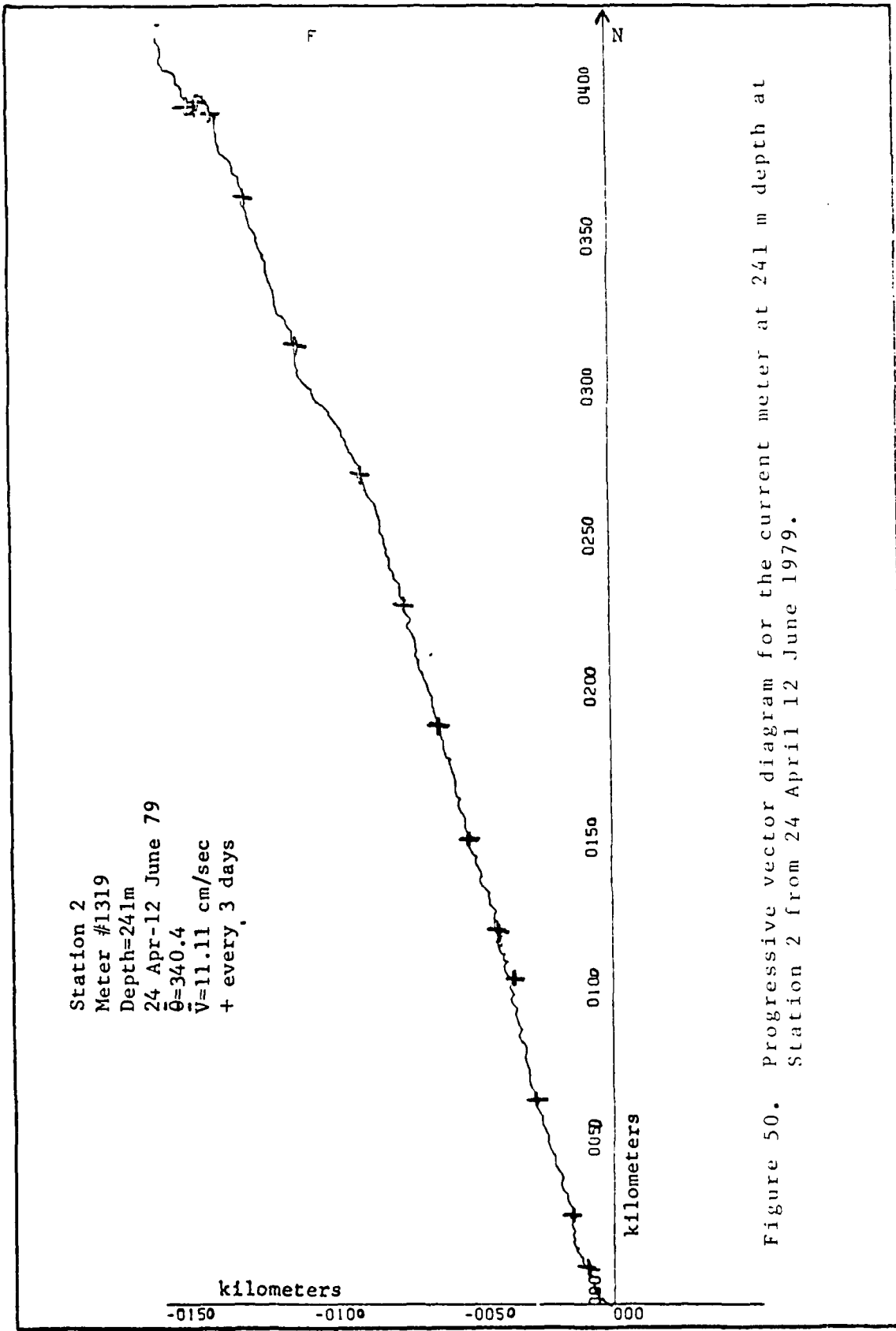


Figure 50. Progressive vector diagram for the current meter at 241 m depth at Station 2 from 24 April 12 June 1979.

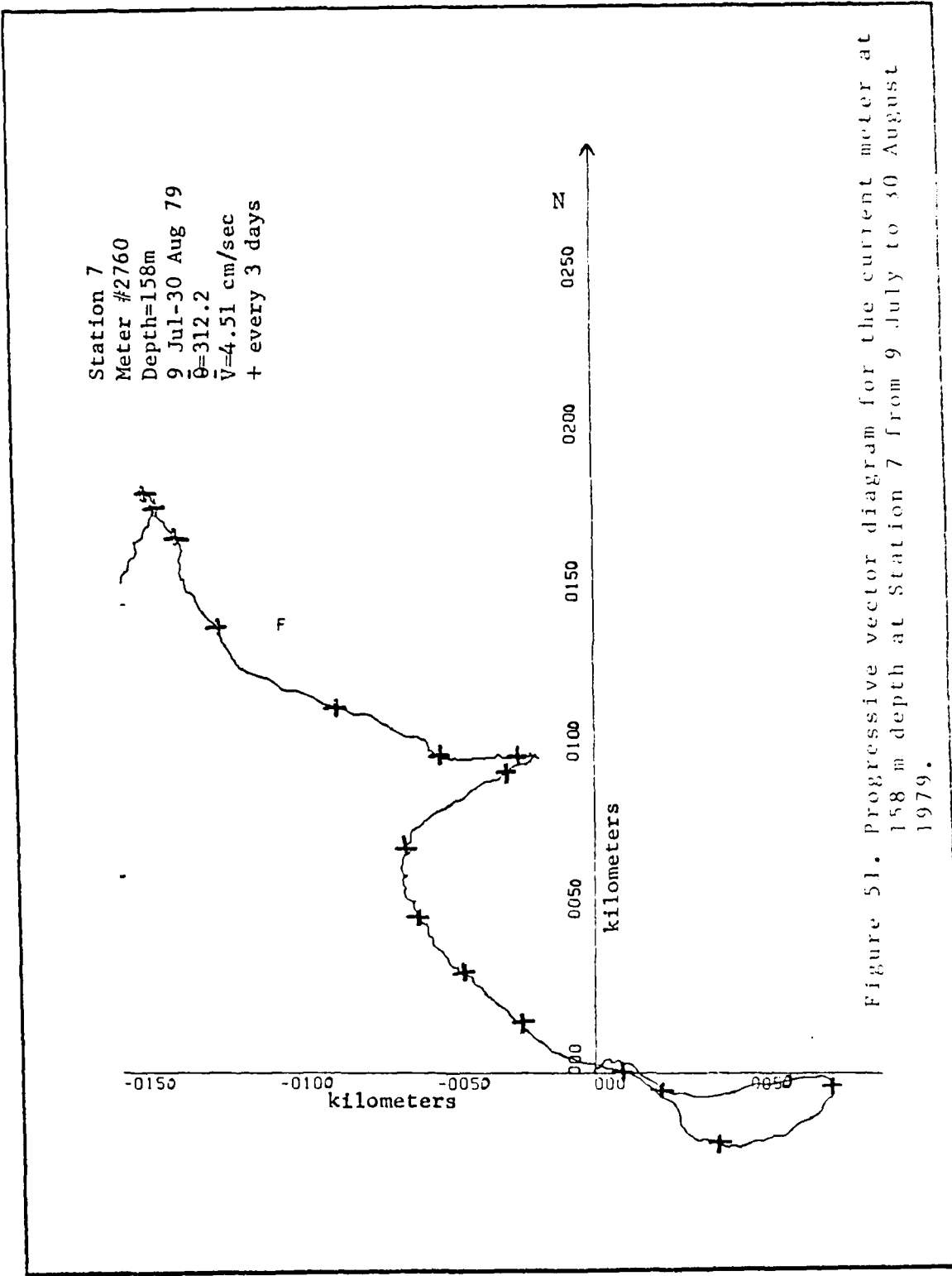


Figure 51. Progressive vector diagram for the current meter at 158 m depth at Station 7 from 9 July to 30 August 1979.

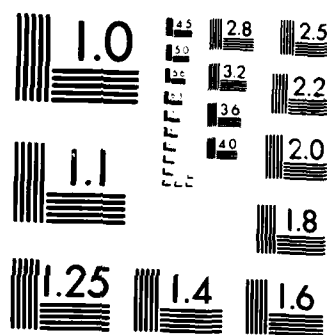
AD-A150 781 OBSERVATIONS OF THE CALIFORNIA COUNTERCURRENT(U) NAVAL 2/2
POSTGRADUATE SCHOOL MONTEREY CA R L HARROD JUN 84

UNCLASSIFIED

F/G 8/3

MI

END



MICROCOPY RESOLUTION TEST CHART
NATIONAL BUREAU OF STANDARDS 1963 A

Station 7
Meter #842
Depth=231m
9 Jul-29 Aug 79
 $\bar{\theta}=330.6$
 $\bar{V}=5.84$ cm/sec
+ every 3 days

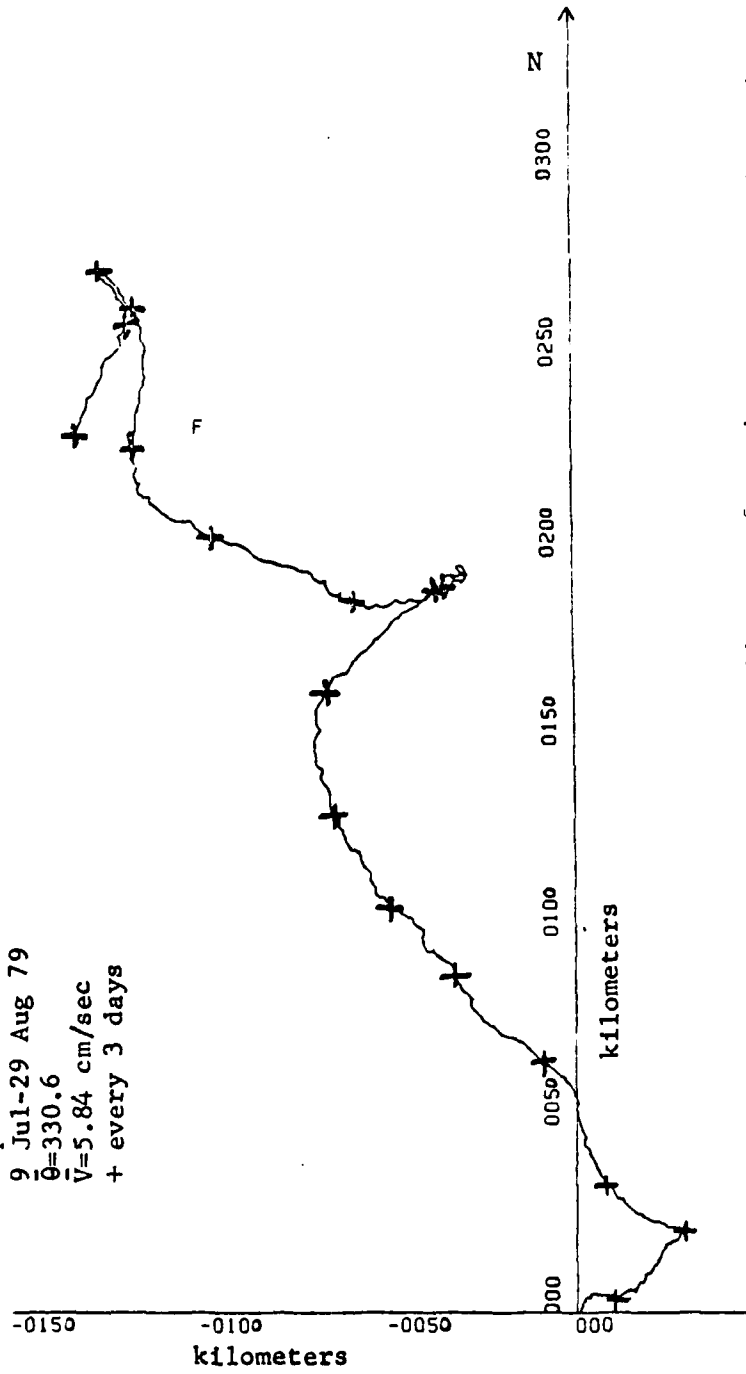


Figure 52. Progressive vector diagram for the current meter at 231 m depth at Station 7 from 9 July to 29 August 1979.

Station 7
Meter #362
Depth=356m
9 Jul-30 Aug 79
 $\bar{d}=338.6$
 $\bar{v}=2.77$ cm/sec
+ every 3 days

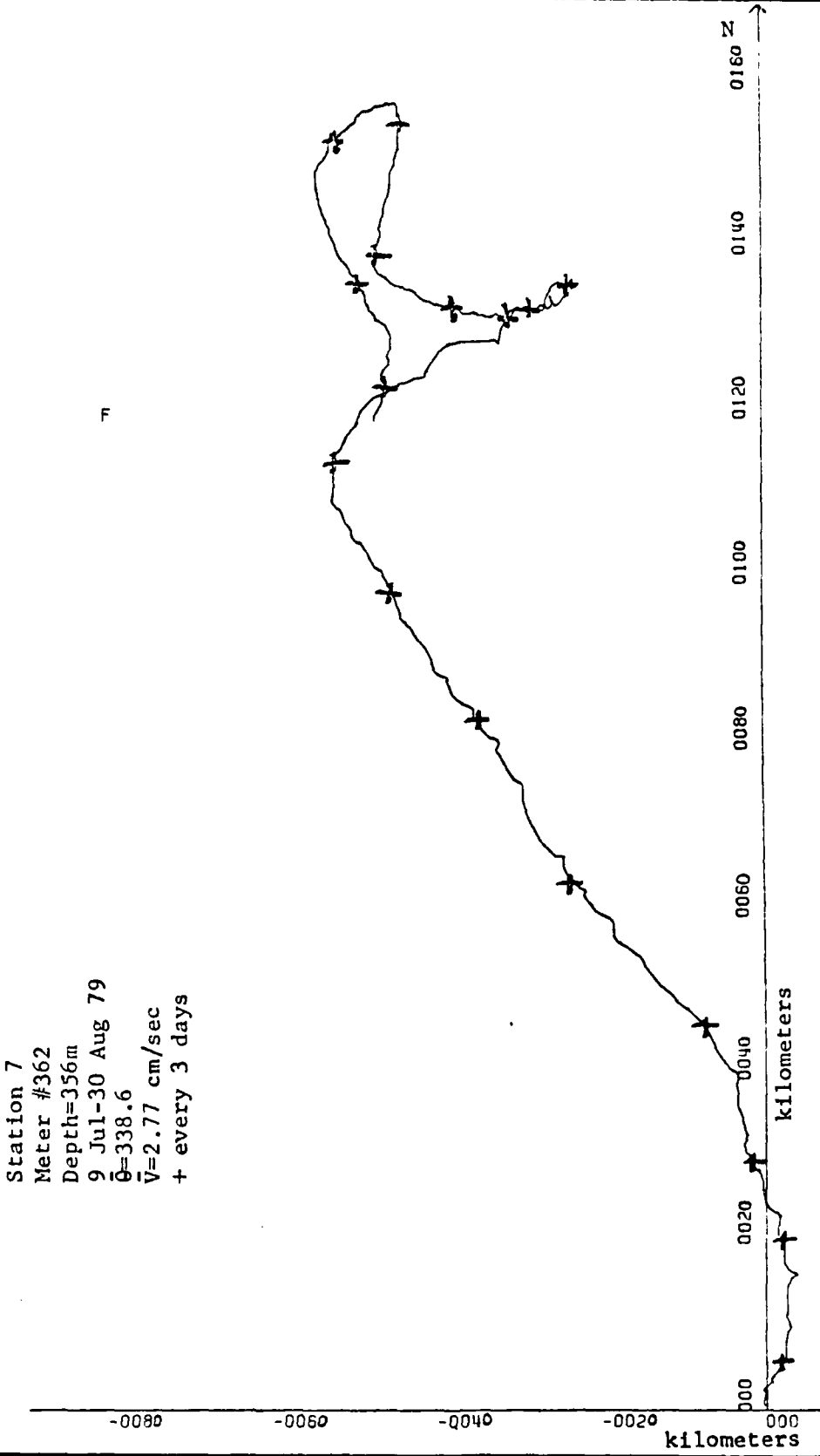


Figure 53. Progressive vector diagram for the current meter at 356 m depth at Station 7 from 9 July to 30 August 1979.

Station 2
 Meter #1965
 Depth=165 m
 23 Jul-11 Sep 79
 $\bar{Q}=325.1$
 $\bar{V}=6.13 \text{ cm/sec}$
 + every 3 days

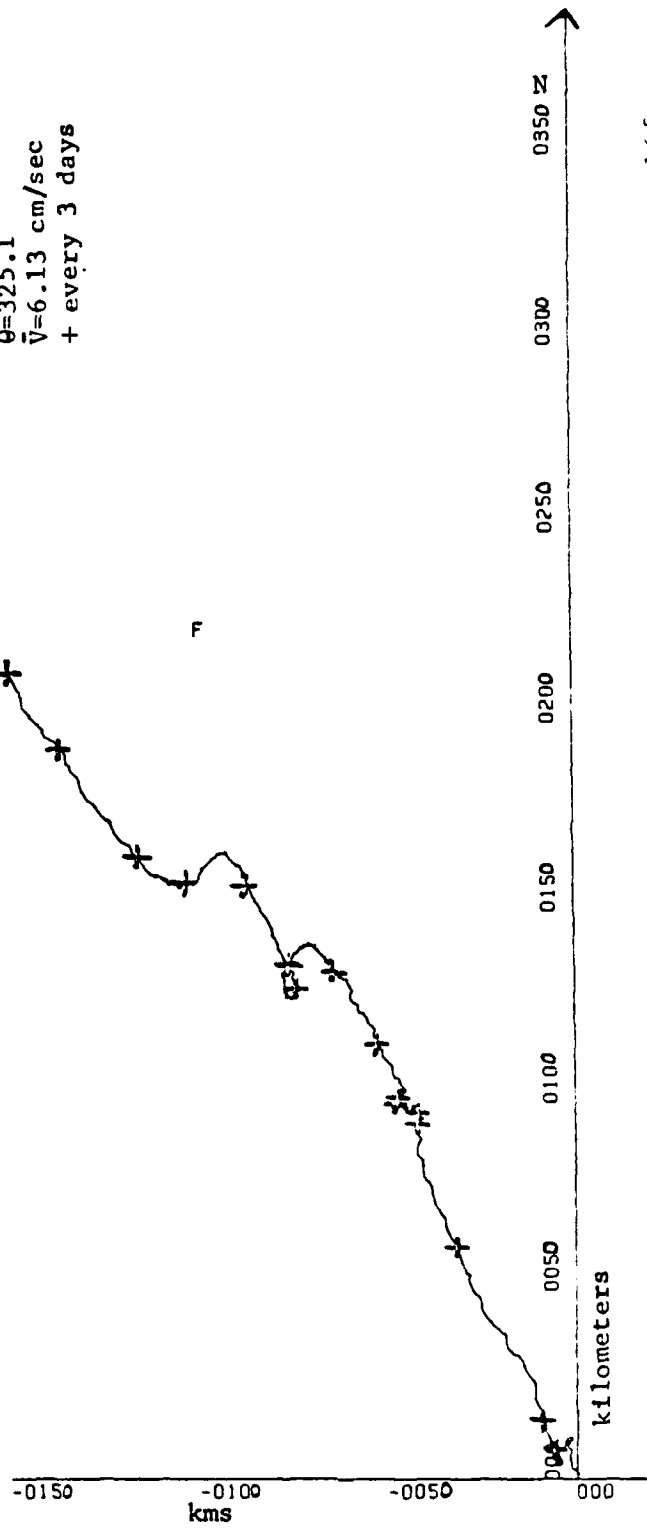


Figure 54. Progressive vector diagram for the current meter at 165 m depth at Station 2 from 23 July to 11 September 1979.

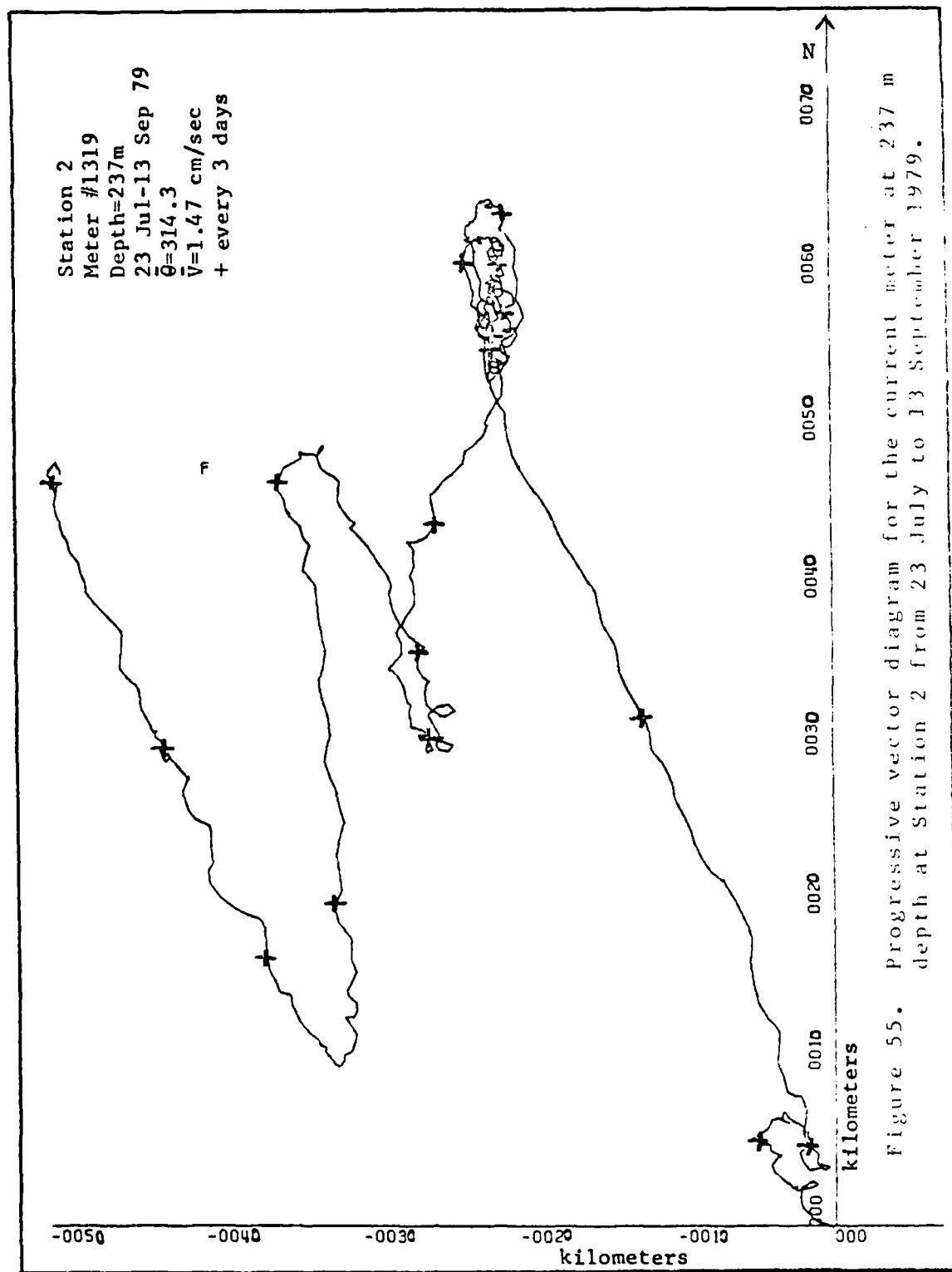


Figure 55. Progressive vector diagram for the current meter at 237 m depth at Station 2 from 23 July to 13 September 1979.

Station 7
Meter #2760
Depth=127m
9 Oct-29 Nov 79
 $\theta=68.1$
 $V=5.05$ cm/sec
+ every 3 days

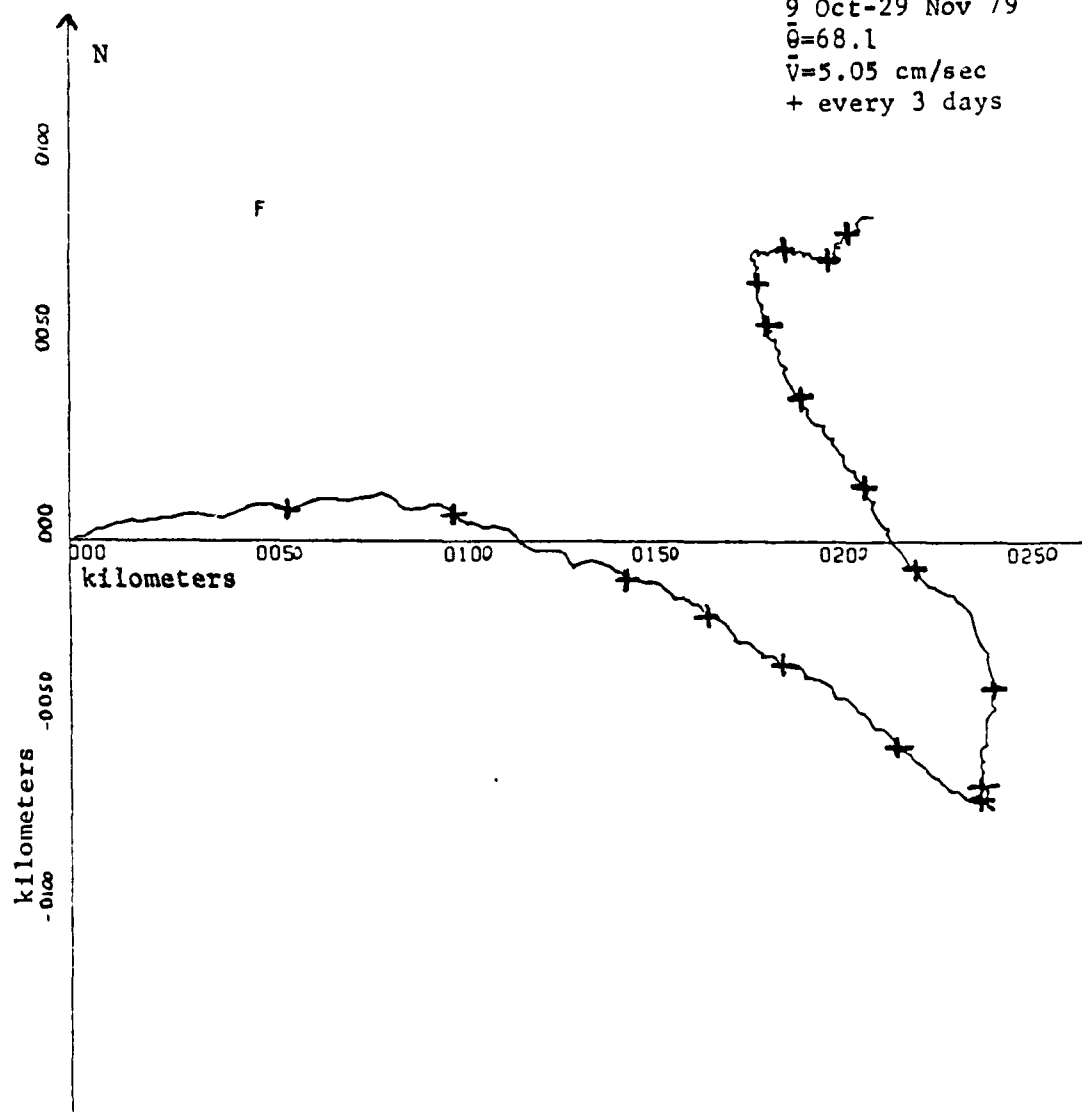


Figure 56. Progressive vector diagram for the current meter at 127 m depth at Station 7 from 9 October to 29 November 1979.

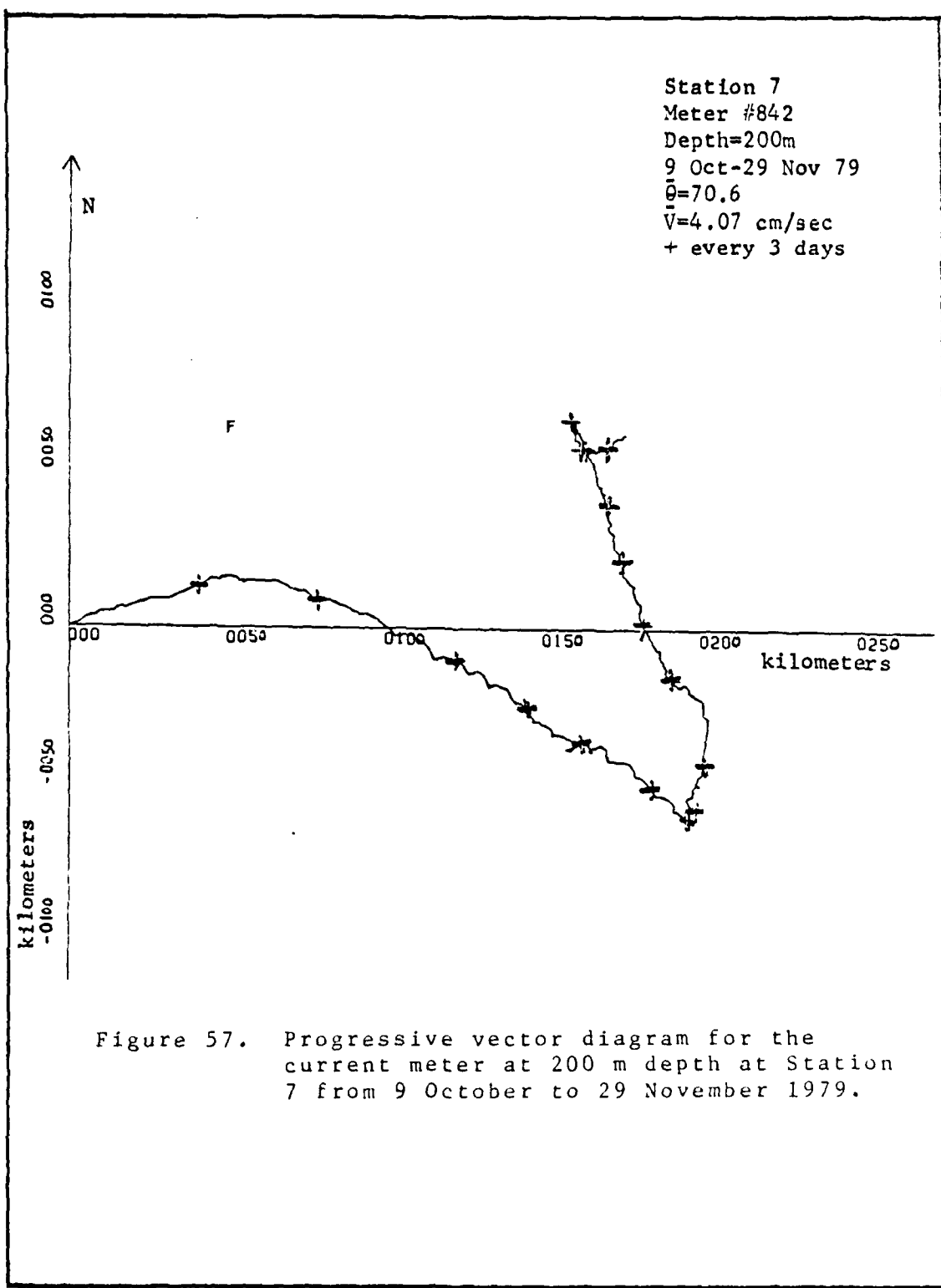


Figure 57. Progressive vector diagram for the current meter at 200 m depth at Station 7 from 9 October to 29 November 1979.

Station 2
Meter #1965
Depth=194m
27 Nov 79-16 Jan 80
 $\theta=279.8$
 $V=6.24$ cm/sec
+ every 3 days

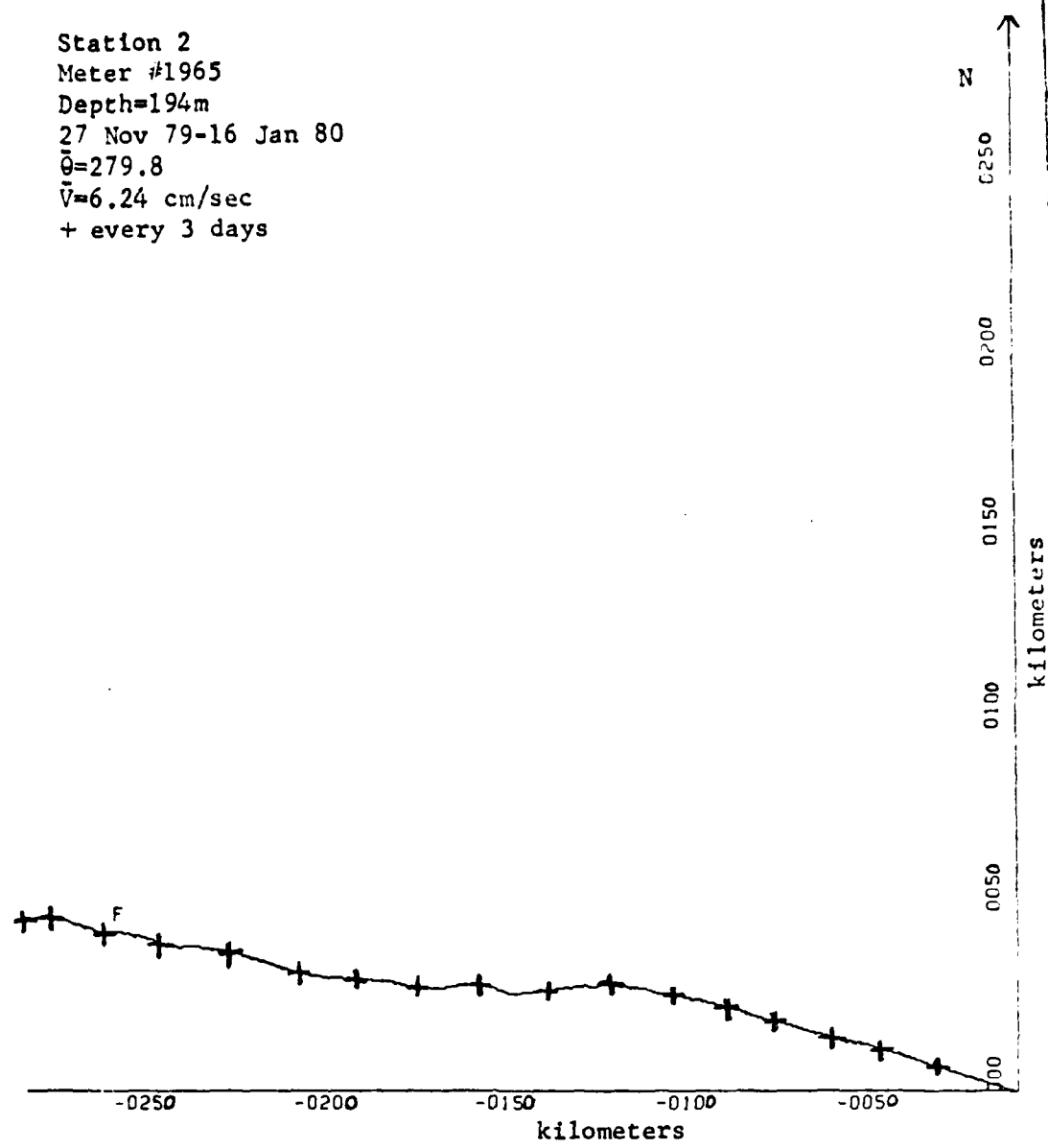


Figure 58. Progressive vector diagram for the current meter at 169 m depth at Station 2 from 27 November 1979 to 16 January 1980.

Station 2
Meter #1319
Depth=266m
27 Nov 79-18 Jan 80
 $\theta=3.1$
 $\bar{v}=2.66$ cm/sec
+ every 3 days

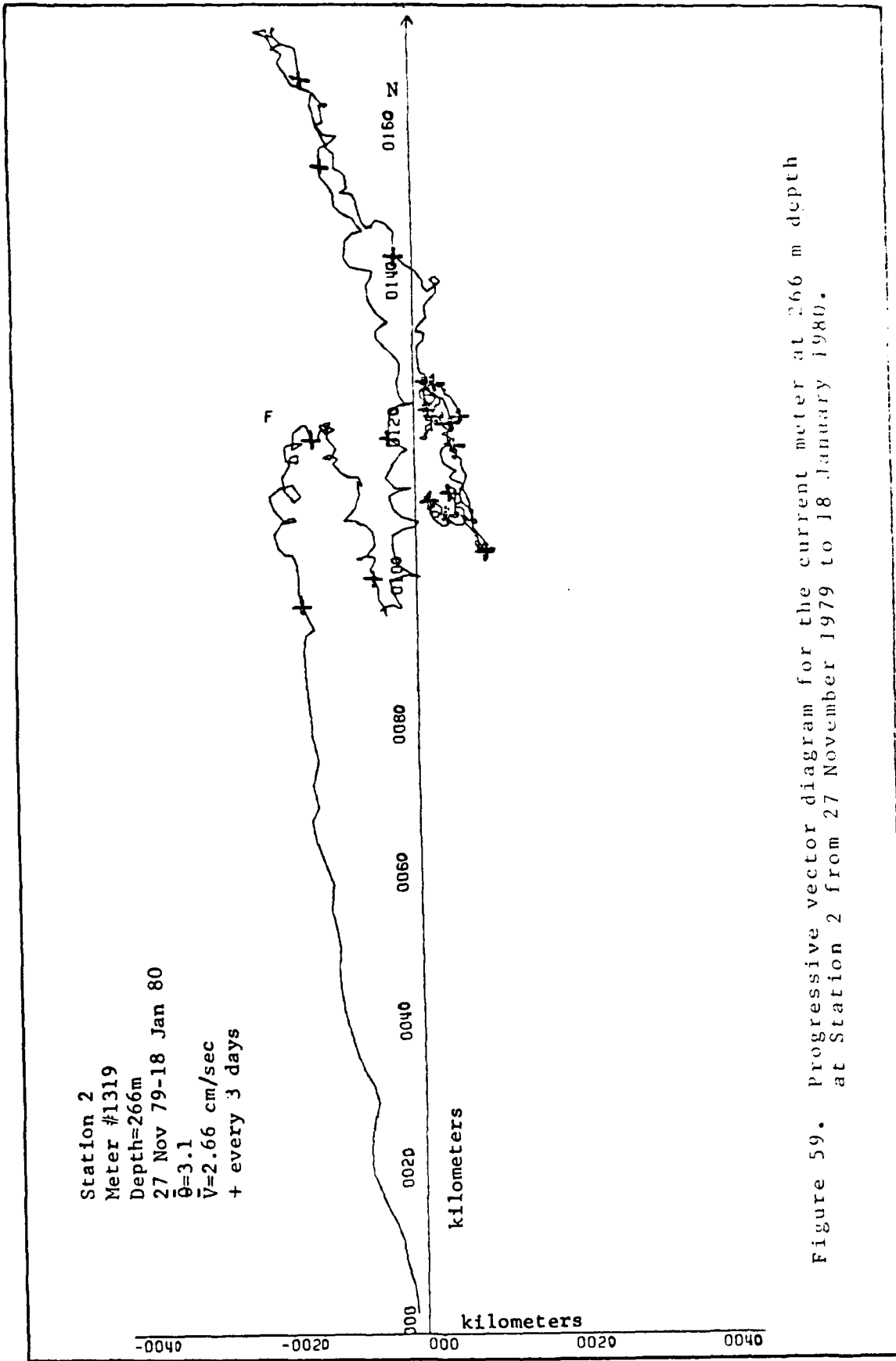


Figure 59. Progressive vector diagram for the current meter at 266 m depth at Station 2 from 27 November 1979 to 18 January 1980.

Station 7
Meter #2760
Depth=113m
4 Mar-15 Apr 80
 $\bar{\theta}=310.5$
 $\bar{V}=4.41 \text{ cm/sec}$
+ every 3 days

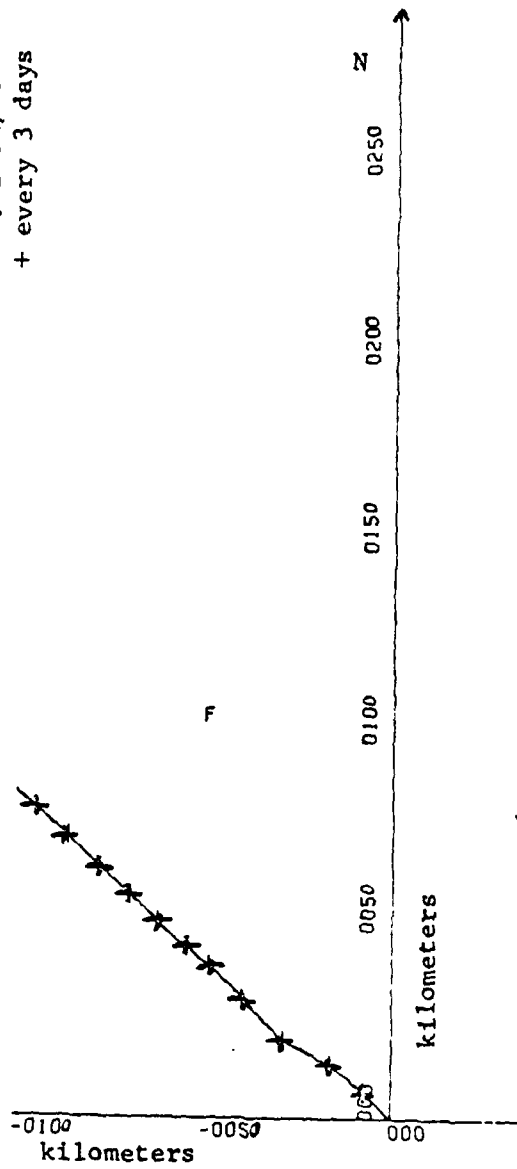


Figure 60. Progressive vector diagram for the current meter at 113 m depth at Station 7 from 4 March to 15 April 1980.

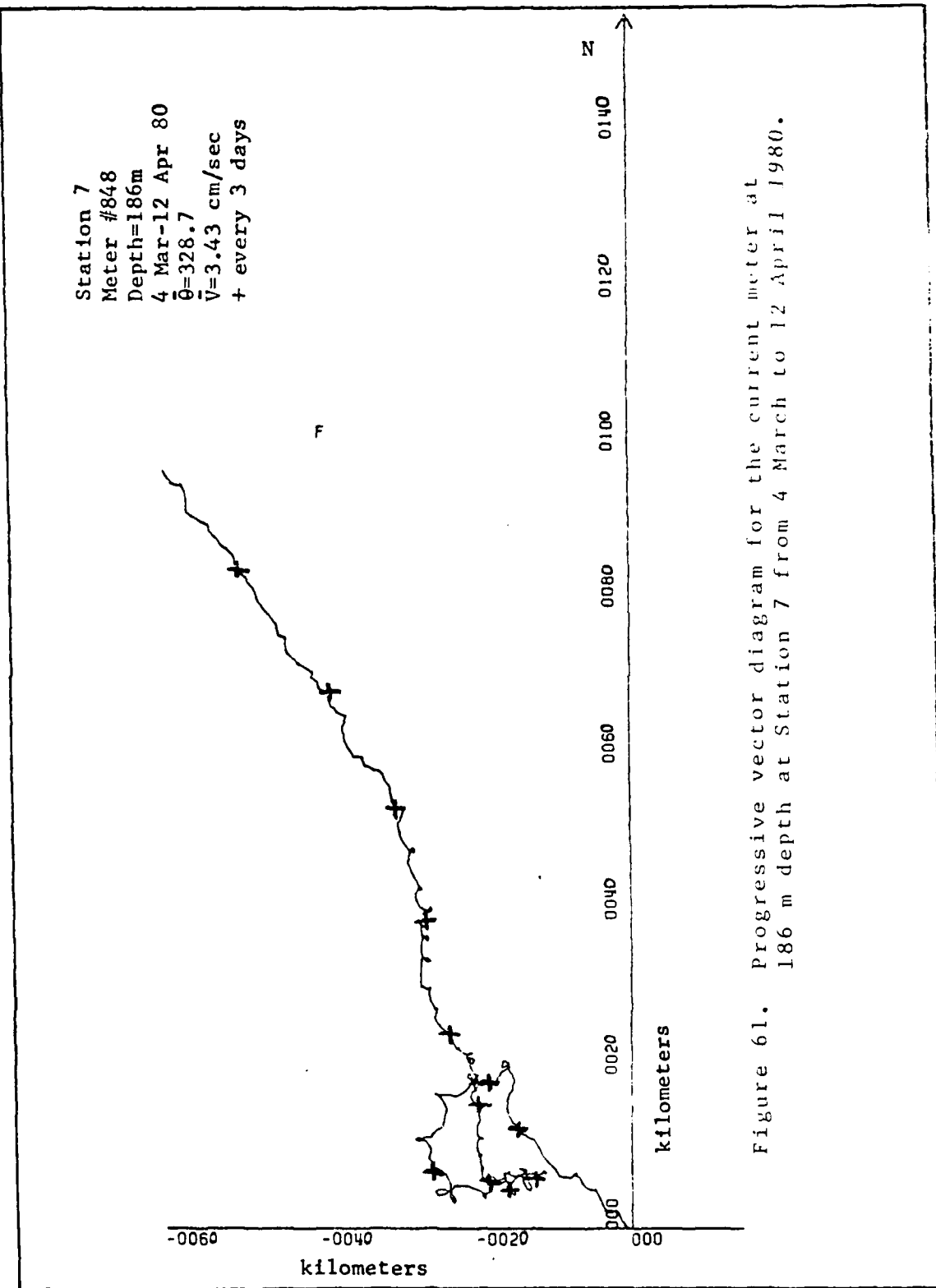


Figure 61. Progressive vector diagram for the current meter at 186 m depth at Station 7 from 4 March to 12 April 1980.

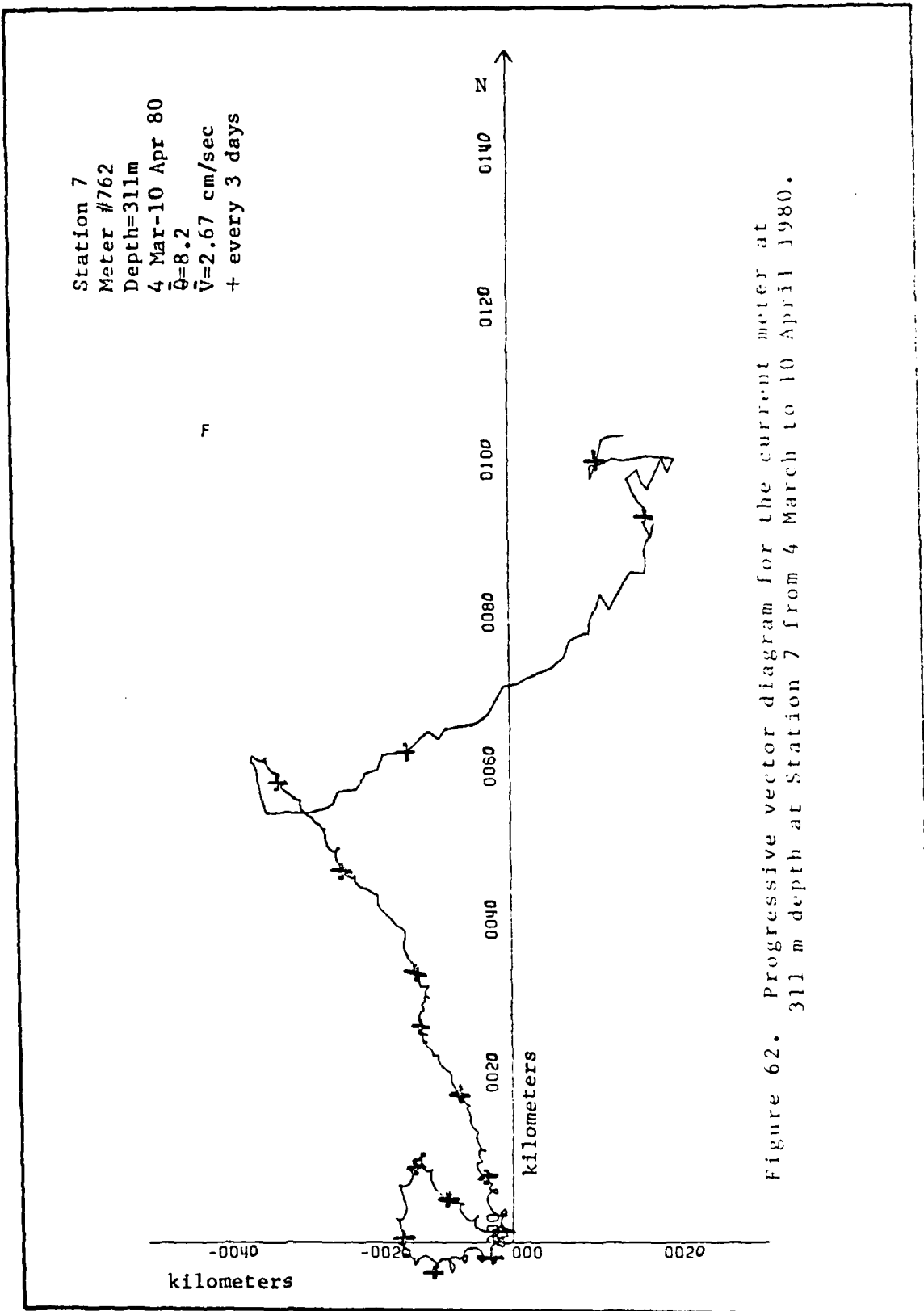


Figure 62. Progressive vector diagram for the current meter at 311 m depth at Station 7 from 4 March to 10 April 1980.

APPENDIX D: COMPUTER PROGRAM LISTINGS

```

C THIS IS A PROGRAM FOR AIMS FILE AND CURRENT METER DATA INPUT
C FROM A CENTERED SOURCE FILE RECORD ENVIRONMENTAL;
C
C BITS: 256 FOR FILE RECORD ENVIRONMENTAL;
C 512 FOR INPUT FILE RECORD ENVIRONMENTAL;
C 512 FOR OUTPUT FILE RECORD ENVIRONMENTAL;
C 512 FOR FIELD OF 512 VARYING STATIC;
C 1536 FOR FIELD OF 512 BASED ON,
C 256 FOR FIELD OF 1,
C 3456 FOR FIELD OF 5;
C 128 FOR RECORDS STATIC;
C 512 FOR RECORDS ACCOUNT;
C 512 FOR INPUT FILE RECORD ENVIRONMENTAL;
C
C OPEN FILE (INPUT) INPUT;
C OPEN FILE (OUTPUT) OUTPUT;
C P = ADDRESS(FIELD);
C KULI, KCOUNTER = 0;
C KK=0;
C
C L=0;
C IF KK=255 THEN GETC THEEND;
C KK=KK+1;
C READ KK FIELD (INPUT) INTO (FIELD);
C KK = LENGTH(FIELD);
C DO J=1 TO KK;
C IF J=1 THEN DO;
C IF SYNC(J,FIELD)= '1'E THEN DO;
C L=J;
C IF SYNC(J,FIELD)= '1'E THEN SJ;
C IF SYNC(J,FIELD)= '1'E THEN CJ;
C SJ=XX;
C CJ=XX;
C END;
C I=I+1;
C IF I< L THEN UC;
C IF I=1 THEN FL1$KIP(1);
C J= ADDRESS(FIELD(J));
C CALL STORE(I,J,1);
C END;
C J=J+1;
C KK;
C UC; /* UC = 1 IC K */;
C SJ UC;
C THEEND;

```

```

PUT EDIT (55, *BLOCKS READ WRITTEN)
      SKIP(1) F(6), A, FILE, A);
SYSTEM: FILE(5) EDIT(16) STAT(I);
DCL OUTFILE FILE(16) BASED( );
DCL CFILENAM CHAR STATIC;
DCL P2INFILE EDIT(16) BASED(P);
DCL =ALC(OUTFILE(1)) I'CCCCC'@;
SUBSTR(JOUTFILE(I),1,6) = 'CCCCC'@;
DO I=1 TO 5;
SUBSTR(CUTFILE(I),II+1,1)=SUBSTR(INFILEC,II+3,1);
SUBSTR(CUTFILE(I),II+5,1)=SUBSTR(INFILEC,II+11);
END;
PUT EDIT(SUM(I))(X(4),F(6));
IF I = 5 THEN DO;
KOUTFILE = KOUTFILE + 1;
PRINT FILE(KOUTFILE) FILE(KOUTFILE);
END; /* FILE IF I = 5 */
END; /* SYSTEM */
/* PROGRAM */

```

```

C THIS POLICY APPLIES CALIBRATION PAYMENT TO EACH INDIVIDUAL CURRENT METER'S
C SPOT RATE ACCORDING TO EACH INDIVIDUAL CURRENT METER'S
C INTEGRATE? #2 AR(55555)
C REAL XXX(E) /6*(55555)
C Y=7
C I1=1
C I2=2
C IR=1
C
C READ IN FILE DATA.
C
C 22 READ(I1,I2)END=90)(AR(I1),I=I1,I2)
C 23 FCRD(I1,I2)
C I1=I2+1
C I2=I2+5
C G5 TC 22
C
C LOCATE REF NUMBER IN THE REGION?
C USE A WINDOW OF APPROXIMATELY 20, IN CASE SYNCBIF STUPPS.
C
C 90 IF((I1+(N-1)).LE.970.AND.AR(N).GE.54) GC TC 5
C
C      G5 TC 5
C      IF(REF>WINDCW, DATA CONSIDERED FAULTY. ZERO OUT ALL
C      VALUES)
C      IF((AR(N).GE.571.AND.AR(N).LE.53)) GC TC 1C
C
C      CALLIBRATION PARAMETERS AREPLIED. FORMULAS ARE FROM ANDERSON
C      OPERATING MANUAL. SALINITY AND PRESSURE SENSORS ARE ACTUATED.
C      T=2.12524*(02277*AR(Y+1)-(134*(N+1)*(-5)*(M+1)*2)+1
C      S=0.51251*(1C.*(-(8))+(AR(4+1)*4))
C      P=1.512512*AR(M+4)
C      TF=(2*(N+5)*EQR(0.5)/168*AR(Y+5))GO TC 5
C
C      Y=1C
C      G5 TC 5
C
C 150 REF=EX(S)
C      R21T(I1,I2,150) IR,REF,T,S,P,S,V
C      R21T(I1,I2,150) CALIBRATED DATA VALUES (10 MINUTE) TO MASS STOCKAGE.
C      R21T(I1,I2,150) IR,REF,T,S,P,S,V
C      R21T(I1,I2,150) IR,REF,T,S,P,S,V
C      R21T(I1,I2,150) IR,REF,T,S,P,S,V
C
C 550 REF=EX(S)
C      R21T(I1,I2,550) IR,REF,T,S,P,S,V

```

```
10      WRITE (6,150) IR,XXX
        WRITE (1) IR,XXX
        IR=IR+1
        IF (N*(I+1).SC)00) GC TO 16C
        N=N+6
        GOTO 1
      ENDFILE 1
      STOP
      END
```

100

THIS PROGRAM USES TEN MINUTE CALIBRATED DATA VALUES AS INPUT.
 MISSING RECORDS ARE FILLED IN BY A BINOMIAL FILTER IS USED TO
 CREATE FAIRLY EQUAL VALUES. PLOTS ARE PRODUCED CURRENT DIRECTION
 & SPEED AT TIME OF PLOT. CURRENT TIME, V CURRENT, TIME, AND
 EXPERIMENT NUMBER ARE USED TO SPECIFY THE PLOT. REF(1000),
 TIME(1000), V(1000), EXP(1000), SP(1000), AR(6), REF(1000),
 LU(1000), H(1000), T(1000), FORT(1000), TEXT(1000), THETA(1000),
 LC FORMAT (ix,1), 2F1C.2
 J=0

```

C      READ DATA FROM MASS STORAGE
C
  20  READ(L,END=25) 11,AR
      1R(I)=L1
      1R(I)=AR(1)
      TEV(I)=1R(2)
      SALS=AR(3)
      PKES=2R(4)
      CIR(I)=AR(5)
      SP(I)=AR(6)
      GU(I)=FC(2)
      25  CCNT=L1
      NPIS=L1
  11
C      CREATE ARTIFICIAL VALUES FOR MISSING RECORDS. (THIS SUBROUTINE
C      LEAVES THE DIFFERENCE NUMBER ZERO FOR READY IDENTIFICATION
C      ARTIFICIAL VALUES.)
  25
MPTS=NPIS-2
  26  IF(I>7) THEN
      WHERE I>7: CURRENT SEEDS GREATER THAN 100 CM/SEC ARE NOT ACCEPTED
      HERE BUT SUBSTITUTED WITH INTERPOLATED VALUES.
      IF(P(I)<100) GC(1) = 6
      IF(CRF(I)<1) NE(J)=GC(1)
      CALL FILE2(I,SPC,CR,FCUT,JRCUT)
      SP(I)=FCUT
      CR(I)=JRCUT
      ELSE
        GC(1)=I
        IF(GC(1)>100) FAULTY DATA IS SEARCHING FOR THE RECORD FOR AN
        ACCEPTABLE VALUE.
        IF(TEV(I).GE.5.0.AND.TEV(I).LE.12.0) GC(1)=7
        J=1
        IF(TEV(J+1).GE.5.0.AND.TEV(J+1).LE.12.0) GC(1)=10
        J=J+1
        GC(1)=I
        TEV(I)=TEV(I-1)+TEV(J+1))/2
  3

```

7 CALL LINE
 C CREATE A REPRESENTATIVE FAULTY CURRENT VALUE EACH TIME 10 MINUTE
 RECCES.

```

NPTS=INPIS/6
CALL READ(NPTS,NP156,SPD,JIR,RSPE,U,V,T,TRU,THETA,TEM,
1 RJUR,HOUR,HOURL,RGE)
STOP
END

```

C CREATE DATA PLOTS.

```

NPTS=NPTS+2
APTS2=AFTS**2
CALL SUEFL(NPTS,NFTS2,IF,RSPE,HOURU,FCURV,FCURV,FCURF)
STOP
END

```

C SUEFL LINE FILLER (I,SPC,CIR,SPCOUT,CIROUT)

C SUEFL LINE FILLER CREATES SPEED AND DIRECTION VALUES FOR THE CURRENT
 METER READING. THIS IS DONE TO PROVIDE REASONABLE APPROXIMATIONS
 FOR THE OCCASIONAL RECORD INSTRUMENT (METER)
 MALFUNCTION. THE AVERAGING READING AVOIDS TRICKPUPATING FAULTY
 DATA.

C INVERTS CIR(I), SPC(I)

```

3 IF(SPC(I+1).LE.1.5C.)GC 1C 3
  J=J+1
  SP=RSPE(I-1)+SPC(I-1)/2*(I+1)/2*(I+1)*CIR(I+1)*27C.) GC TO 10
  IF(DIR(I-1).LE.90.. AND.CIR(I-1).LE.90.) GC TO 10
  IF(DIR(I-1).GT.270.. AND.CIR(I-1).LE.90.) GC TO 15
  IF(DIR(I-1)-DIR(I+1).GT.135.) GC TO 15
  IF(DIR(I-1)-DIR(I+1).LT.-135.) GC TO 15
  DIR(I)=DIR(I-1)+DIR(I+1))/2.
  GC TO 20
  IF(DIFF=(CIR(I-1)-CIR(I+1))/2.*DIR(I+1)+18C.
  IF(DIFF<0.15C.) DIFF=0.15C.
  IF(DIFF>0.36C.) DIFF=0.36C.
  IF(DIFF>0.25C.) DIFF=(CIR(I-1)+CIR(I+1))/2.+18C.
  15 GC TO 20
  2C CONTINUE
  FIL
  SUEFL LINE RMEEAN(NPTS,NFTS2,SPC,DIR,RSPE,U,V,T,TRU,THETA,

```

1 TILY, RÜLT, HÜRT, HÜRT

SUCCESSIVE MEAN CREAMS CREATE HOURLY CURRENT VALUES AND TEMPERATURE VALUES FROM A 9-POINT WEIGHTED NOMINAL FILTER.

LIMEN; ICH SPE(NP TS), CIR(NP TS), HESPO(NP TS), CURU(NP TS),
HCLKT(NP TS), U(NP TS), V(NP TS), T(NP TS), FRU(NP TS),
TFITA(NP TS), TEF(NP TS)

CHAPTER 16 MAGNETIC DIRECTIONS.

```

VARE=L2*D1/VAR
TRU(1)=CIR(1)+VAR
IF (TRU(1)*CE*360.) TRU(1)=TRU(1)-360.
CONEVERTIC RADIAN S
THETAL=CIRU(1)*(CL7452)
U(1)=SF((1)*SIN(THETA(1)))
V(1)=SF((1)*COS(THETA(1)))
WRITE 15,WINL TE U & V CONVERNTS TG NA
351= (2250) U(1),V(1)
253= (2250) U(1),V(1)
254= (2250) U(1),V(1)

```

卷之三

U₁ = J + 1
 U₂ = 1 * J + 1
 U₃ = 2 * J + 1
 U₄ = 5 * J + 1
 U₅ = 7 * J + 1
 U₆ = 16 * J + 1
 U₇ = 28 * J + 1
 U₈ = 38 * J + 1
 U₉ = 81 * J + 1
 F₁ = U₁ + U₂ + U₃ + U₄ + U₅ + U₆ + U₇ + U₈ + U₉
 F₂ = U₁ + 2 * U₂ + 2 * U₃ + 2 * U₄ + 2 * U₅ + 2 * U₆ + 2 * U₇ + 2 * U₈ + 2 * U₉
 V₁ = 1
 V₂ = 8 * J + 1
 V₃ = 25 * J + 1
 V₄ = 52 * J + 1
 V₅ = 75 * J + 1
 V₆ = 112 * J + 1
 V₇ = 231 * J + 1
 V₈ = 448 * J + 1
 V₉ = 891 * J + 1
 F₃ = V₁ + V₂ + V₃ + V₄ + V₅ + V₆ + V₇ + V₈ + V₉

```

HOURV(2)= (V1+V2+V3+V4+V5+V6+V7+V3+V9)/
1   (2+1+2.*3.+2.*28.+2.*56.+70.)
T1=1.*ITEM(1)
T2=3.*ITEM(1+1)
T3=2.*ITEM(1+2)
T4=5.*ITEM(1+3)
T5=7.*ITEM(1+4)
T6=5.*ITEM(1+5)
T7=2.*ITEM(1+6)
T8=3.*ITEM(1+7)
T9=1.*ITEM(1+8)
HOURV(2)=(T1+T2+T3+T4+T5+T6+T7+T8+T9)/
1   (2+1+2.*6+2.*2+2.*56.+70.)
HRSPC(J)=SQR((HOURV(J))**2*(HCRV(J))**2)
IF (HOURV(J).LE.5.5) GOTO 20
IF (HOURV(J).GE.10.0) GOTO 20
K=K+1
HT=HOURV(J)+HCT
CONTINUE
SUBROUTINE STKPLOT(NPTS,NP152,IR,HRSPU,HCLRL,HCURV,HGURV,RHCT)
      SUBROUTINE STKPLOT(NPTS,NP152,IR,HRSPU,HCLRL,HCURV,HGURV,RHCT)
      RHCT=(HCT/K)**2.0)-14.
      ARTEFF(IX,FE.2)
      RETURN
END
SUBROUTINE STKPLOT(NPTS,NP152,IR,HRSPU,HCLRL,HCURV,HGURV,RHCT)
      SUBROUTINE STKPLOT(NPTS,NP152,IR,HRSPU,HCLRL,HCURV,HGURV,RHCT)
      SUBROUTINE STKPLOT C CREATES A PLOT OF CURRENT VECTORS AS A
      FUNCTION OF TIME VS PLANE OF V COMPONENTS, V COMPONENTS,
      AND TEMPERATURE VS TIME. THE USER SHOULD REFER TO THE NAVAL
      PLANT DESIGN SCHOOL TECHNICAL NOTE NC. G141-24 IN REGARDS TO
      PLOTTING PARAMETERS.
      DIMENSION IR(NPTS),HRSPU(NPTS),HOURV(NPTS),HOURU(NPTS),
      1   HCLRL(NPTS)
      NPTS=NP152
      XLEN=(NPTS/20.)*2.
      YLEN=10.*8X,1HJ;11X,2H1R,4X,5HRSPO,SX,
      1   1LNU?>1H9X,1H7X,2H)1,3X,2Y1,2)
      20 J  FURNITURE(I1,I2,I3,I4,I5,I6,I7,I8,I9,I10,I11,I12)
      SET UP THE STICKPLT
      CALL PLCS(0.0,0)
      CALL PLCS(0.3,0)

```

```

PR3P (C*15+1)=740.
HRSP (NFTS+2)=13.
FVAL =HRSPE(NFTS+1)
CALL FLCT (J*10,-3)
SAMPLE (J*10,-3,XLEN,SEC), -13*XLEN,SC.,FVALS,DVS)
CALL AXISE (0,-4,13HSPFEC(CV/SEC),13,YLEN,0,2111)
CALL FLNE (C,C,XLEN,0,2111)
WRIT(E,100)

C PLUT 1E DATA.
DO 10 I=1,NPTS
  CALL FLUT (I,DVS,C.,-3)
X1=4.CJFS (1)/CVS
Y1=CVS
CALL PLUT (X1,Y1,2)
CALL FLNE (J,I,HRSP (1),HRSP (1),HCURV (1),HOLFT (1),X1,Y1
ORTELE200)
CNTFLNE
CALL PLUT (C,C,SS)
SET UP THE (C,C) PLENENT FLCT.
CALL FLCT (C,C)
HFS=C(NFTS+1)=10.
NFTS=C(NFTS+2)=10.
FVAL =HRSPE(NFTS+1)
CVS=HRSPE(NFTS+2)
CALL FLCT (J*10,-3)
FVAL =HRSPE(NFTS+5,-3)
CALL AXISE (J*4,13HSPFEC(CV/SEC),13,XLEN,SEC.,FVALS,DVS)
CALL FLNE (J,XLEN,C.,2111)
CALL FLUT (C.,0.,-3)
D=3.
I=1,NPTS
X1=DCURV (1)/DVS
Y1=DCURV (1)/DVS
CALL PLUT (X1,Y1,2)
CNTFLNE
CALL PLUT (C,C,SS)
SET UP THE (C,C) PLENENT FLUT.
CALL FLCT (C,C)
HFS=C(NFTS+1)=10.
NFTS=C(NFTS+2)=10.
FVAL =HRSPE(NFTS+2)
CVS=HRSPE(NFTS+2)

```

```

CALL PLT(1,10,-1)
CALL AXIS(0,-5,10,SAMPLE(NU18E2),-13,YLEN,9,C,FVALS,DVS)
CALL LINE(0,-4,13,SEC,C,21111)
CALL PLT(0,0,-3)
B=5
PLT 12 1E DATA
DO 12 I=1,NPTS
  B=5+I/25
  X1=5
  Y1=HCCRY(1)/CVS
  CALL PLC(1,X1,Y1,2)
  12  CALL INUE(0,0,SS)
  CALL PLC(0,TEMPERATURE PLT).
C   SET UP THE TEMPERATURE PLT.
  CALL PLC(0,0,0)
  CALL PLC(0,135,-3)
  CALL PLC(0,135,-3)
  CALL AXS(0,135,-3,SAMPLE(NU18E2),-13,YLEN,C,0,,20.)
  CALL AXS(0,135,-4,13,FEATLSE,21111)
  CALL LINE(0,0,XLEN,RFGT,21111)
  CALL PLC(0,RFGT,+3)
B=5
PLT 12 1E DATA
DO 12 I=1,NPTS
  B=5+I/25
  X1=5
  Y1=CHUR((I)*2.0)-14.
  12  CALL PLC(1,X1,Y1,2)
  CALL FINUE(0,0,SS)
  RETURN
END

```

```

C DIVISION REF(1000),C18(10000),SPD(10000),AF(6),
1 ALU(ND(10000)),CSUS(10000),F1(10000),PERIOD(10000),
2 FREQU(10000),V(10000),TRT(10000),INT(10000)

C PROGRAM TO EVALUATE THE ENERGY DENSITY SPECTRA AT
C THROUGH THEIR ALLOWSphere AND CROSS SHELF COMPONENTS.

C IN FORMAT (IX,10,2F10.2)

C DATA IS THE (HOURLY) DATA POINT AT WHICH THE ENERGY SPECTRA
C PROGRAM SHOULD BEGIN TO LOOK AT DATA. IT DOES NOT ALWAYS START AT
C 1 SINCE SOME METERS HAVE A LONG LEADER WITH NO RELEVANT VALUES.

C JCAT 2=5

C READ RAW DATA FROM MAGNETIC TAPE.

C 23 READ(I,END=25) II,AR
    REF(I)=AR(1)
    TEM=AR(2)
    SALES=AR(3)
    DIR(1)=AR(4)
    DIR(1)=AR(5)
    SPD(1)=AR(6)
    CJ(1)=20
    25 CONTINUE

C CREATE ARTIFICIAL VALUES FOR MISSING RECORDS (THIS SUBROUTINE
C LEAVES THE NUMBER ZERO READY IDENTIFICATION OF
C ARTIFICIAL VALUES.)
```

6

```

APTS=NPTS-2
GC3=L-3,APT$)
IF(SPC(I).GE.100) GC TO 6
IF(REF(I).NE.0) GC TO 5
GATEFILLER(I,SFC,DIR,SPD,CIRCUIT)
SPC(I)=SPC(I)
CIR(I)=CIR(I)
CONTINUE
CJ,I=1,NPTS
VAP=32*I
TRT(I)=C(I)+VAR
IF(TRT(I).LT.0) TRT(I)=TRT(I)-360.
IAT(I)=IAT(I)*((017453)
U(I)=SPC(I)*SIN(TH(I))
V(I)=SPC(I)*COS(TH(I))
CHCS(I)=U(I)
```

```

11    ALLINE(J,J=1..Y(1))
      COUNT(1)
      CJ(S,J=1..4) GO TO 40
      IF (J>E(S,2)) GO TO 50
      IF (J>E(S,3)) GO TO 40
      IF (J>E(S,4)) GO TO 60
      CALL SECXCAR(ALONG,NPIS,24,1,NOUT1)
      CALL SECXCAR(ALONG,NPIS,24,1,NOUT1)
      CALL SECXCAR(CROSS,NPIS,24,1,NOUT1)
      CALL SECXCAR(CROSS,NPIS,25,1,NOUT1)
      CALL SECXCAR(CROSS,NPIS,24,1,NOUT1)
      CALL SECXCAR(CROSS,NPIS,25,1,NOUT1)
      N=11
      NS=1
      DT=(1./C.)
      J3=F1=JDATA
      D,J=4,5,I=1..4590
      IF ((J>I)&(J<E(2))) GO TO 41
      YY(Y(1))=ALONG(JSTART)
      GU(TL,43)
      YY(Y(1))=CROSS(JSTART)
      JSTART=JSTART+1
      41    CONTINUE
      IF (J>E(2)) Y(0)=YY,F1,PERI(),FREQUE,NF)
      CALL PKEFA(Y(0),Y(1),GC,TC,8G)
      CALL PLCT(0.0,C,C,SSS)
      GU(TL,43)
      IC CALL PKEFA(M,MS,DI,YY,F1,PERIC),FREQUE,NF)
      80    COUNT(1)
      CALL FILE(1.,0,0,0,4559)
      STOP
      EIC SUBROUTINE FILLER (I,SFC,CIR,SDOUT,CIRCUIT)

SUBROUTINE CIR(I),SFC(I)
J=1
IF (SFC(I+1).LE.100.) ICC TC,
J=J+1

```

SUBROUTINE

SUBROUTINE FILLER CREATES SPEED AND DIRECTION VALUES FOR THE CURRENT METER READING. THIS IS USEFUL TO PROVIDE REASSEMBLED APPROXIMATIONS FOR THE ECCASIGNAL RECCRD WHICH IS SEC CIRCUIT INSTRUMENT (METER) HALF FUNCTION.


```

      C U S P L I F = 1, NF
      F1(I) = 0.
      K=0
      DO 21 IZ=1,27=1,1
        ART(I,IZ)=YY(IZ)
      21  CALL INVALA(ART,N,ANEAR)
      C(IZ)=ART(I,IZ)-ANEAR
      C(IZ)=ART(I,IZ)-ANEAR
      CUN(I,IZ)=ART(I,IZ)-ANEAR
      CO(IZ)=1,MS
      K=K+1
      CO(5)=1,NM
      IZ=IZ+1
      F1S(J-1)=C(IZ)
      WRITE(FEIN,(F1S(N),ET,U21,U21,U41,URNS1))
      CALL SPSC(F1S,N,V1,V2,U21,U21,U41,URNS1)
      WRITE(FE(260),(F1S(1),U21,U21,U41,URMS1)
      DO 240 F1(I)=F1S(I)+FL(I)
      F1(I)=FL(I)
      DO 520 FL(I)=1,1NF
        F1(I)=F1(I)*1/12.*MS)
      IF(I.EQ.1) GO TO 23
      PERIOD(I)=(FLCAT(NY))**CF/(FLAT(I-1))
      FREQUE(I)=1.0/PERIOD(I)
      IF(F1(I).LE.10.0) GO TO 55
      GO TO 24
      PERIOD(I)=FLCAT(NM)
      FREQUE(I)=0.0
      WRITE(FE(270)FL(I),PERIOD(I),FREQUE(I))
      24  CALL INVAL
      550 CALL FLCTG(FREQUE,FL,NF,I,1,1,FREQUENCY(CYCLES PER HOUR),27,FC
      INVERS DENSITY FUNCTION(CYCLE HOUR),36,0,C2,0,0,0,12,0,6,0)
      RETURN
      END
      SUBROUTINE SPEC (FL,N,INV,S,IFER)
      C
      C      SUBROUTINE TO CALCULATE THE FCHER SPECTRUM CF A SIGNAL USING RHEAR
      C
      CIVENSICA INV(S15),S(S15),FL(S15)
      CALL RHEAR(FL,N,INV,S,IFER)
      NF=2#N+1
      NY=2#N+1
      NL=N+1

```



```

U3 = U2*(1-U1)
U4 = U2*(1-U1)
SUMU3 = SUMU2+U2
SUMU4 = SUMU3+U3
COUNT IN U5
FNT5 = M1*U5
U2 = SUMU3/FNT5
URYS = U2*(1-U2)
U3 = FNT5*(U2*URYS)
U4 = SUMU4/(FNT5*(U2*URYS))
RETURN
END
SUBROUTINE PAGE
DIMENSION A(NPTS)
SUM = 0.0
DO 100 I=1,NPTS
SUM = SUM + A(I)
100 COUNT IN U5
MEAN = SUM/NFLOAT(NPTS)
RETURN
END

```

151

1C

100

PROGRAM TRAJEC TO PLCT PROGRESSIVE VECTOR DIAGRAMS OF CURRENT
 METEOR CATASTIC ARE GIVEN. WE SET COMP=1 IF SPEED
 AND DURATION ARE GIVEN. WE SET COMP=2 IF SPEED IS GIVEN AS
 EVERY PLT A SET OF POINTS ARE GIVEN AS
 PLOTTED POINTS CAN NOT EXCEED 900 SO IF DRAW IS CALLED. THE TIME
 INTERVALS ARE USED OBJECT TIME FORMAT. THE
 VECTOR POINTS ARE STORED IN FOUR STUFFED COLUMNS. CVAID CV*IT IS STORABLE THAT NP#N X
 CORRESPONDING TO AN INTEGRAL FRACTION OF CAE DAY. IF PLT IS TRUE,
 READING SUBTRACTS THE DATA AND THE TREATMENT IS REPEATED.
 PROVIDED FOR READING AND DISCARDING TWO MORE FILES IF NFILE
 IS SET TO 2 OR MORE. PROVISION IS MADE FOR READING TWO CARDS AT THE
 SAME TIME FOR EACH FILE. THIS PROVIDES FOR READING FFCCY FILE TO FILE SEQUENTIALLY.
 IF THEY ARE SET AS ONE LESS THAN THE FILE NUMBER WITH WHICH CNE
 STAR IS CAN EINPUT. FILE NUMBER ON WHICH YOU WANT TO STOP.
 DIMENSION L(900) V(SCCG) FM(10),PU(2CC),FV(200),CU(900),
 1 CV(900) FT(900) J(SCCG) * /,LAEEEL2/*
 READ*3 TITLE(12) LAEEEL1/F
 LOCAL CCNP PLT RPT
 NAMELIST/I INPUT/GMF,N,NP,N,DELT,RPT,PLT,NSTRT,MFILE/INPUT1/MFILE
 C
 RAD=1.141552/180.
 AFLTE=1
 RP=FALSE.
 NSTRI=C
 MFILE=C
 READ(5,INPUT)
 4 READ(5,INPUT)
 WRITE(6,INPUT)
 READ PLT TITLE, 96 CHARACTERS INCL. USERS NAME
 READ(5,INPUT)
 6 FORMAT(610) /2A8/
 1C FORMAT(1FC)
 C IREPT=C
 C REAC AND DISCARD NSTRT FCINTS

```

IF (A$TR1 .EQ. 0) GC TC 12C
D:1 J=1 INSTR
READ (2,12) JUNK
112 FORMAT(2,14)
C READ DATA
NJ=J CO 12 N=15 END=200,ERR=353) U(J),V(J)
13C READ (2,12) U(J),V(J)
175 FOR,AT(2,12,5)
NJ=J

C IF GCNF IS FALSE, FIND THE EAST AND NORTH COMPONENTS AND PUT
THE X IN U AND Y IN V
14 IF(GCNF) GC TC 16
DO 15 J=1,N
UX=U(J)
VX=V(J)+XAE
U(J)=UX+CUS(VX)
V(J)=UX-CUS(VX)
15

C PARAMETERS FOR COMPRESSING DATA
16 NPTS=NFX
NXI=N/AFIS
JEVN=NP*NXI
JEVN=N-JEVN*FT
KEVN=JEVN*AF
LEVNE=JEVN-KEVN*NP
WRITE(NESACE
161 WRITE(6,161) NP,NP1$'LEVN' JEVN
      ,PLT'ING IS CNE EVERY '13/5X,? POINTS A CROSS IS PLOTTED AND
      12,13,? POINTS THERE ARE '13/5X,? POINTS NOT PLOTTED AND
      12,13,? POINTS AFTER THE LAST CROSS.')
C SUM THE COMPONENT DISPLACEMENTS IN KILOMETERS AND STORE NP POINTS
IN CU AND CV
17 SUMJ=C*
L=0
K=1
CU(1)=C*
CV(1)=C*
XDELT=L*EL!*3600.*1.E-5
CO 27 N=1,NX
20 CO 26 LL=1,NX
L=L+1
DO 25 KK=1,NP
K=K+1

```

```

25      SUML=SL*U+L*(K)*XDELT
26      SUMV=SL*V+V*(K)*XDELT
27      PU(M)=SL*U
      PV(M)=SL*V
      FLINE(L) LOCSE END
      IF(J>EVN .EQ. 0) GO TO 28
      DO 29 L=1,NX
      CU(L)=SL*U
      CV(L)=SL*V
      K=L+1, NX
      CU(K)=SL*U
      CV(K)=SL*V
      K=K+1, NX
      SUMU=SL*PU+U(K)*XDELT
      SUMV=SL*PV+V(K)*XDELT
      CU(L)=SL*U
      CV(L)=SL*V
      CU(L)=SL*U
      CV(L)=SL*V
      SAVE THE NUMBER OF FLCTED FCNTS
      NT=N
      FILL THE NEXT 3 WITH THE LAST VALUE TC FILL THE END OF THE
      3-COLUMN PRINTOUT IN ALL CASES
      28      DO 31 J=1,3
      L=L+1
      CU(L)=CU(N)
      CV(L)=CV(N)
      31      CU(L)=CV(N)
      C      FORMAT FOR THREE COLUMNS
      NPRINT=N/3
      LEVN=N-3*NPRINT
      IF(LEVN.NE.0) NPRINT=NPRINT+1
      C      PRINT HEADINGS
      WRITE(*,100) T15, 'X(KM)', T24, 'Y(KM)', 'HOURS', '142,
      1      'X(KM)', 'T61, 'Y(KM)', 'T61, 'HOURS', '179, 'Y(KM)', '179
      C      INPUT TIME PARAMETERS
      IOTIM=FLOCAT(N)*DELT
      CELTIME=FLOCAT(NP)*DELT
      TIM1=CELTIM
      TIM2=FLOCAT(NPRI)*CELTIM+CELTIM
      TIM3=2.*TIM2-DELTIM
      CJ5=NPRT
      K2=NPRT+J
      K3=K2+NPRINT
      WRITE(*,155) TIM1,CU(1),CV(1),TIM2,CU(K2),CV(K2),TIM3,CU(K3),CV(K3)

```



```

REAL*8 ICODE,BLANK*8
REAL*8 ITIT,ICAT(16),SHINIDE,SHIGH,EYCODE,X*,SHIXUP,ISV
1,8H ICODE,YAX,'8HRIGHT,'8HUNITS,'8H-SCALE=,'8H UNITS, '8H
2,8H UNITS,I,'8H ALL X,'8H ADD -,,'8H ADD +,'8H VALUES. , '8H-SCALE=
3,8H TEST = 14,8H
C C CHECK PREVIOUS OPERATION OF ROUTINE, IF ANY. CODES ARE
C C TEST = 0 IF PREVIOUS GRAPH, IF ANY, COMPLETED
C C TEST = 1 IF PREVIOUS GRAPH NOT COMPLETED
C C TEST = 2 IF EACH FUNCN WHILE PREVIOUS WAS CNE, CR IF
C C MDCUR WAS ILLEGAL.

IPOINT = ITYPE
IF(IPOINT = 2)LOC1,LOC1,LOC1,LOC1
1001 IF(MDCUR)1003,1002,1003
1002 ITEST = 5
1003 OUTCUCR - 1)1004,1002,1004
1004 LAST = 3
RETURN SET UP EXPCR RETURN ROUTINE. ENTRY AT STATEMENT 1005.

C 1005 IF(IPOINT)1005,1006,1007
1006 IF(MDCUR)1007,1008,1007
1007 PRINT 1,LOC5,9H NO FURTHER GRAPH OUTPUT UNTIL MDCUR NEXT IS ZERO CR
1008 FORMAT 1,LOC5,9H
1009 ITEST = 2
1010 LAST = 2
RETURN PRINT 1,LOC1
1011 IF(MDCUR = 2)1010,1008,1010
1012 LAST = 3
FORMAT 1,LOC8
1013 ITEST = 3
GO TO LOC8
C 1000 IF(IPOINT)1001,201,2,2
1001 PRINT 1,LOC5,32H NUMPTS MUST BE LESS THAN 20.
1002 GO TO LOC5
1003 IF(IPOINT)1004,9994,9991
9994 PRINT 1,LOC5,15H ILLEGAL INPUT.
9995 GO TO LOC5
9996 IF(ILPCNT = 5)9992,9992,9993
9997 IF(NUMPTS = 30)3,9993
9998 PRINT 1,LOC5
9101 FORMAT 1,LOC5,15H ILLEGAL INPUT.
9102 GO TO LOC5
9103 IF(ILPCNT = 5)9992,9992,9993
9104 IF(NUMPTS = 30)3,9993
9105 PRINT 1,LOC5
9106 FORMAT 1,LOC5,15H ILLEGAL INPUT.
9107 GO TO LOC5
9108 IF(ILPCNT = 5)9992,9992,9993
9109 IF(NUMPTS = 30)3,9993
9110 PRINT 1,LOC5
9111 FORMATTED INPUT.

```

```

GO TO 1005
IF(NUPTS - SCC) 3,2,SC05
9005 PRINT S102 28H NUMPTS MUST NOT EXCEED 900.
2
91C2 FORMAT(10F12.5)
CJ TU 10C5
3 IX=10DATA(1)
IY=10DATA(2)
A1AXX=X(1)
A1INY=Y(1)
A1INX=X(1)
A1INY=Y(1)
DC 1 C2C 1=2,1NMP1S
A1AXX=A1AXX(1)(1),A1AXX(1)
A1INY=A1INY(1),A1INY(1)
A1INX=A1INX(1)(1),A1INX(1)
A1INY=A1INY(1)(1),A1INY(1)
1020 AMINX=A1INX(1)(1),A1INY(1)(1)
1022 IF(A1AXX-AMINX) 1025,1024,1025
1023 PRINT 10C3
1024 FCRMA1 1,33# ALL FCINTS HAVE THE SAME COORDINATES.
1
1025 GO TO 10C5
1026 IF(C1TEST14 .754
1027 IF(C1CCCLR-3)6,2240,5
1028 IF(C1CCCLR-3)6,2240,6
1029 PRINT 10C1
1030 FORMAT(1,17H ILLEGAL OCCURR.)
1031 GO TO 10C5
1032 IF(C1CCCLR)6,9,8
1033 IF(C1CCCLR-1)6,9,6
1034 IF(IWIDE10 11,12
1035 IT=ICATE(1)
1036 PRINT 10C2, ITIT ITIT, ITIT
1037 FORMAT(1, 9H ILLEGAL ,AS,29H. GRAPH WILL BE PLOTTED WITH ,AS,
1038 5H = E. ,/),
11 JWIDTH = 3
12 GC TC 14
13 IF(IWIDE - 9)13,12,1C
14 IF(IHIGH15 16,17
15 IT=ICATE(2)
16 PRINT 10C2, ITIT, ITIT
16 JHIGH = E
17 GC TO 19
2240 CCNTLINE 4,
C BACKSPACE 4,
18 GO TO 24
17 IF(IFICH - 15)18,1d,15
18 JHIGH = IFIGH

```

```

19 NOCXAX = NOCXAX
    IF(MOD(xax),20,21,21
20 ITIT=IAT8(3)
    PRINT 104, ITIT, IX
1C4 FORMAT (/ A1, A1, 7HAX = 0.
1C4,1 NOCXAX = C
    GO TO 27
21 IF(MOCXAX - JHIGH)24,24,23
22 ITIT=IAT8(4)
23 ITIT=IAT8(5) ITIT, IX
    NOCXAX = C
    GO TO 27
24 IF(IXLF)23,26,26
25 JXUP = IXLUP
26 NOCYAX = NOCYAX
27 IF(HCX)YAX)25,25,25
28 ITIT=IAT8(5) ITIT, IY
    NOCYAX = C
    GO TO 25
29 IF(MCX)YAX - JWIDE)22,22,21
30 ITIT=IAT8(6) ITIT, IY
31 PRINT 104, ITIT, IY
    NOCYAX = C
    GO TO 25
32 IF(IYRIGHT)21,34,34
33 ITILITLIZE PRICR SCALING AND AXIS IFLAG = 1 FOR PASS WITH YDATA.
34 ITILITLIZE PRICR SCALING AND AXIS IFLAG = 0 FOR PASS WITH XDATA.
C   IFLAG = 0
    BETA = C
    SCALE = C
    SCAL = EXSCAL
    IAXIS = JRIGHT
    MODE = NOCYAX
    ISIZE = JKIDE
    IXY = IX
    IYX = IY
    AMAX = AMAXX
    AMIN = AMINX
    GOTC 52
    IFLAG = 1
    BETA = C
    SCAL = YSCALE
    IAXIS = JXCP
    MODE = NOCXAX

```

```

ISIZE = JRLCH
AMAX = AMAXY
AMIN = AMINY
IYX = IY
IYX = IY SCALE AND GO TO FIXED OR AUTO SCALE ROUTINES.

C 52 IF (SCALE) 59,58
53 PRINT 14, IYX, IYX
54 FORMAT (1H ILLEGAL ,A1,3SH SCALE. GRAPH WILL BE PLOTTED WITH AL
114 TU ,A1,7H-SCALE. ,J)
115 GO TO 55
C 58 CALL SCAL (SCALE, ISCL1, FACTR, 1)
C 59 SCAL FACTOR*10.*#ISCL1
C 60 SCAL CHECK AND COMPUTE AXIS LOCATION IF NECESSARY. FIXED SCALE
CASE. ITAG = 0 IF CR1 IN GRAPH CR1 IF IT IS SUPPRESSED.

1030 IF (ITAG = 2) 1031,1030
1030 GOTO C2
1031 PRINT 11C4 ,IYX, IYX, 14H NUDE,A1,24H AX MUST NOT BE 1 UNLESS A1,5H SCALE IS ,C
1134 FPRINT (1,5H SCALE). GRAPH WILL BE PLOTTED WITH AL ,A1,7H-SCALE. ,J
1135 (AUTOMATIC SCALE).
1 GOTO 55
1032 IF (AMAX - AMIN) 1036,1035,1033
1033 IF (AMAX) 1036,1034,1037
1034 TAXIS = ISIZE/2
1035 GOTO 1032
1036 TAXIS = ISIZE
1037 GOTO 1035
1038 GO TO 1030
1039 IF (SIGN(1.,AMAX)-SIGN(1.,AMIN)) 1040,1039,1040
1040 ASIZE = ISIZE
1041 TAXIS = -AMIN/(AMAX - AMIN)*ASIZE +0.5
1042 GO TO 1030
C 55 IF (MCDE = 1) 60,64,65
60 AMAX=ANAL(0.,AMIN)
61 PRINT 14,AMAX-A1,(C,AMIN)
64 IF (AMAX-A1) 68,65,68
65 PRINT 14, IYX, IYX, 14H ALL VALUES ARE NON-ZERO. AND MCDE,A1,7H AX = 2.,J
116 FORTRAN (1,5H VALU
117 IF (TFC 1,5
68 ASIZE = ISIZE
69 SCALE = (AMAX - AMIN)/ASIZE
70 TFC 13
69 IF (AMAX-A1) 74,7C,74

```

```

7C IF( AMAX ) 74,71,74
71 PRINT 112, 1XY
118 FURNAT( /5H ALL , A1, 2EH VALUES ZERO. AUTIC SCALE NOT POSSIBLE. )
    GD TGC 105
    74 IF( AY1 ) 76,76,75
    75 IF( ISIZE - TAXIS ) 77,76,77
    76 SCAL1 = C.
    GO TO 16
17 AXIS = AXIS
18 ISIZE = ISIZE
SCAL1 = AMAX/ISIZE - 4*ISIZE
19 IF( AXIN ) 79,79,80
79 IF( TAXIS ) 81,8C,81
8C SCAL2 = C.
GO TO C 82
81 AXIS = AXIS
SCAL2 = -AMIN/AXIS
82 IF( SCAL1 + SCAL2 ) 1984,1982,1984
PRINT 152, 1XY,
1982 FORMAT( /,56H NO LINE OF THE PLOT LINES ON THE GRAPH WITH THIS SPECIF
1983 FORMAT( /,47H-AXIS LOCATION. GRAPH WILL BE PLOTTED WITH MOCE,A1,
1984 LINED1,A1,47H-AXIS LOCATION. GRAPH WILL BE PLOTTED WITH MOCE,A1,
2 7HAX = C.
    GO TO C
GO TO C
1984 SCAL1 = AX1(SCALE1,SCAL2)
CALL SCAL1(SCALE1,ISCL1),FACTOR,3)
    IF( FACTOR - 5.C5 ) 85,E5,84
84 FACTOR = 1
ISCL10 = 1 ISCL10+1
GO TO SC
85 IF( FACTOR - 2.02 ) 87,87,86
86 FACTOR = 5
GO TO SC
87 IF( FACTOR - 1.01 ) 85,85,89
88 FACTOR = 2
GO TO SC
89 SCAL1 = FACTOR*10.*ISCL13
CALL SCAL1(SCALE1,SCAL2) IF NECESSARY. AUTIC SCALE CASE.
C   IF( MOCF - 1 ) 92,91,93
91 IF( SIGN( 1.AMAX ) - SIGN( 1.AMIN ) ) 92,S4,92
92 AXIS = -AMIN/SCALE + 0.5
93 ITAG = C.
GO TO C 202
94 IF( AMAX ) 95,95,200
95 AXIS = ISIZE
BETA = -MAX/SCALE
IF( BETA - 1.E+12 ) 99,99,96

```

```

56 PRINT 12C, IXY THE ORIGIN OF , AL, 43H CANNOT BE JFFSET MORE THAN 1
120 FOR IAT (/,15H THE ORIGIN OF , AL, 43H CANNOT BE JFFSET MORE THAN 1
1.0E+12 INCHES.
) GO TO 120
55 I BETA = -I BETA + 0.5
      BETA = -I BETA
      I BETA IS THE NUMBER OF INCHES OF CRIGIN SUPPRESSION, POSITIVE IF
      CRIGIN IS BELCA CR TC LEFT OF THE GRAPH.
C     IF(BETA + 1.0E7, 0.7, 0.3
      IYAX = 1
      GU TO 202
200 IYAX = 0
      IYAX = AXIN/SCALE
      IF(BETA = 1.0E+12) 2C1, 2C1, 66
      IYAX = BETA + 0.5
      BETA = -I BETA
      IF(BETA = 1.0E7, 0.7, 2C2
202 ITAG = 1AG USE RESULTS FOR YVALUES IF NOT YET COMPUTED.
      PASS FOR YVALUES IF NOT YET COMPUTED. START SECOND
C     203 IF(IFLAG) 2C5, 2C4, 2C5
      2C4 SCALEX = SCALER
      IXFACT = FACTOR
      IXSC10 = IXCL10
      IXAXIS = IAXIS
      ITAXX = ITAG
      ISIZEX = ISIZE
      BETA = BETA
      GO TO 15C
      SCALEY = SCALER
      IYFACT = FACTOR
      IYSC10 = IXCL10
      IYAXIS = IAXIS
      ITAYY = ITAG
      ISIZELY = ISIZE
      ISCALEY = SCALER
      IXFACT = IXFACT
      IXSC10 = IXCL10
      IYFACT = IYFACT
      IXSC10 = IYSC10
      BETA = SCALER
      SCALERY = SCALER
      IYFACT = IYFACT
      IXSC10 = IYSC10
      BETA = SCALEX/SCALEY
      SCALERY = SCALEX
      IYFACT = IXFACT
      IYSC10 = IXCL10
      EETAY = BETA*SCALEY/SCALEY
      END OF CHANGES
C

```

THIS COMPLETELY CALCULATES OF SCALE FACTORS ETC. NOW GENERATE
 RECORDS FIRST, THE SCALE FACTOR TITLES.
 C 206 JX1 I(1)=ICCODE(SCALEX)
 JX1 I(2)=ICDATE(8)
 JX1 I(3)=ICDATE(9)
 JX1 I(4)=ICDATE(10)
 JY1 I(1)=ICCODE(SCALEY)
 JY1 I(2)=ICDATE(8)
 JY1 I(3)=ICDATE(9)
 DO 926 I(4)=ICDATE(9)
 JXT IT(1)=BLANK
 JYT IT(1)=BLANK
 IF(IETAGX)>11,211,207
 207 IF(IETAY)>208,208
 208 GOTO 210
 209 JXT IT(5)=ICDATE(14)
 210 JXT IT(6)=ICCODE(BEAX*SCALEX)
 JXT IT(7)=ICDATE(11)
 JXT IT(8)=ICDATE(12)
 JXT IT(9)=ICDATE(15)
 JIF(IETAGY)>16,216,
 211 JIF(IETAY)>13,214
 212 JYT IT(5)=ICDATE(13)
 213 GOTO 215
 214 JYT IT(6)=ICDATE(14)
 215 JYT IT(7)=ICCODE(BEAY*SCALEY)
 JYT IT(8)=ICDATE(11)
 JYT IT(9)=ICDATE(16)
 JYT IT(10)=ICDATE(15)
 216 CONTINUE
 C TEST FOR ALL BLANK TITLE RECORDS.
 C NOW GENERATE AXES RECORDS.
 C 9091 LEFTMGN =
 LEFTMGN = LEFTMGN + IXAXIS*1CC
 LH = LEFTMGN + ISIZE*1CC - 107
 JL = JL - 13
 IHL2 = -1CC
 IYH2 = -(ISIZEX - IXAXIS - 1)*IXFACT
 NH = ISIZEX
 ISH = ICATE(17)
 IV = LEFTMGN + IXAXIS*103

```

JY = I3YGN
JYL = IY1GN * 3
JYL = IY1GN + IYSIZEY * IGC - 107
JYL2 = -IC1
JYL2 = (ISIZEY - IYAXIS - 1) * IYFACT
JY2 = ISIZEY
I3Y = IUDAT(18)
I3Y = NOX GENERATE CURVES.
SCX = ILC * SCALEx
SCY = ILC * SCALy
EXAXIS = IYAXIS * 100
YAXIS = IYAXIS * 100
ALFTMGN = LEFTMGN
SHIFIX = EXAXIS - BEIAXIS * 100 * + ALFTMGN
SHIFEY = ISIZEX * 100 + LEFTMGN * + 6J
SIZEX = LEFTMGN - 6C
SIZEY = ISIZEY * 100 + IB1GN + 7J
SIZEY = IEPMCN - 70
240 IF(C1 < 1) THEN C1 = 90C7, SC10
2007 IF(C1 < 1) THEN C1 = 97C1, SC11, S70C
97C C0 TQ 242
9701 IS4 = 2
242 INUM = ((LNU + 1) / 2) * 4
C1 = X((L+1)/2)*SCX + SHIFTx
C2 = Y((L+1)/2)*SCY + SHIFTy
1F (L+1)-INUM) 241, C241, C1
9241 GUTC (S242, 241), ISK TCH
9242 C3=C1
C4=C2
C0 TQ 242
9243 C3=X((L+1)/2+1)*SCX + SHIFTx
C4=Y((L+1)/2+1)*SCY + SHIFTy
9243 C1=ANIN1(C1, EXSIZE)
C1=ANIN1(C1, YSIZE)
C2=ANIN1(C2, EXSIZE)
C2=ANIN1(C2, YSIZE)
C3=ANIN1(C3, EXSIZE)
C3=ANIN1(C3, YSIZE)
C4=ANIN1(C4, EXSIZE)
C4=ANIN1(C4, YSIZE)
ICURV((L+1)=IC2

```

```

ICURV(1+2)=IC3
244 ICURV(1+3)=IC4
246 COUNT INDE
C 9010 ACAL WRITE RECORDS
260 CALL PFLCT(10,0,0)
XAXIS=0
YAXIS=G
CALL SYNBL(XAXIS,YAXIS,.14,JXTIT,0.,72)
YAXIS=SYNBL(XAXIS,YAXIS,.14,JYTIT,0.,72)
261 CALL SYNBL(XAXIS,YAXIS,.14,JYTIT,0.,72)
YAXIS=SYNBL(XAXIS,YAXIS,.21,ITITLE,0.,48)
9268 CALL SYNBL(XAXIS,YAXIS,.21,ITITLE,0.,48)
YAXIS=SYNBL(XAXIS,YAXIS,.21,ITITLE(13),0.,48)
9270 CALL SYNBL(XFLOAT(IH)/LOC.
YAXIS=FLLCAT(JH)/LOC.
CALL FLLCAT(XAXIS,YAXIS,3)
XAXIS=FLLCAT(IH+LH)/LOC.
CALL FLLCAT(XAXIS,YAXIS,2)
CALL SPECOUT(IH2,NH,YAXIS,1)
XAXIS=FLLCAT(IH)/LOC.
YAXIS=FLLCAT(JY)/LOC.
CALL FLLCAT(XAXIS,YAXIS,3)
YAXIS=FLLCAT(JY+LY)/LOC.
CALL FLLCAT(XAXIS,YAXIS,2)
CALL FLLCAT(IY,IY2,INV,YAXIS,2)
9015 IF(FCIN19020,270,9020
270 CALL SCLE1ICURV(IY,IY)
CALL MFLERE(XAXIS,YAXIS)
CALL SYNBL(XAXIS,YAXIS,G7,LAEEL,0.,4)
9020 IF(MOLCUR-1)9025,9025
272 IF(IGRIDE-1)9025,9025
C 273 IX10GE=ISIZEX*LOC
NEXT1=ISIZEY*LOC
NEXT2=ISIZEN
ED1274=LEFTMGN+IX100
ED1274=LEFTMGN+80,8
JGRI(G(J+2))=NEXT2
JGRI(G(J+2))=NEXT2
IF(NEXT1-NEXT1-1)9TMGN-IX10C
NEXT1=NEXT1+10C
1272 NEXT1=NEXT1+10C
JGRI(G(J+4))=NEXT12
JGRI(G(J+6))=LEFTMGN

```

```

JGRIC(J+7)=NEXT1      LYLOC)1274,1276,1276
1275 JGRIC(J+4)=NEXT1+100
NEXT1=JGRIC(J+5)=NEXT12
JGRIC(J+6)=NEXT1
JGRIC(J+7)=NEXT1
1276 CCNTINUE
        NUMGRID=J+7
        CALL SLE1(JCRID,NUMRD)
1277 NEXT1=LFTMGN
        NEXT2=LFTMGN+LY1C0
        D1=1*7.9-J=1*48.9
        JGRIC(J+J)=NEXT1
        JGRIC(J+J+1)=NEXT1
        JGRIC(J+J+2)=NEXT1
        JGRIC(NEXT1)=NEXT2-LFTMGN-LCC
        NEXT1=NEXT1+LCC
        JGRIC(J+4)=NEXT1
        JGRIC(J+5)=NEXT12
        JGRIC(J+6)=NEXT1
        JGRIC(J+7)=IBTMGN
        IF(NEXT1-NEXT1)=LFTMGN
        NEXT1=NEXT1+LCC
        JGRIC(J+4)=NEXT11
        JGRIC(J+5)=NEXT12
        JGRIC(J+6)=NEXT1
        JGRIC(J+7)=NEXT12
1278 CCNTINUE
        NUMRD=4+7
        CALL SLE1(JCRID,NUMRD)
1279 IF(LPCINT(S030,276,SC2C
C GENERATE POINT PLOT RECORDS IF CALLED FCH.
1280 IOUT=C
1281 CCNTINUE
        NUMRD=4+7
        CALL SLE1(JCRID,NUMRD)
1282 IF(LPCINT(S030,276,SC2C
C GENERATE POINT PLOT RECORDS IF CALLED FCH.
1283 IOUT=C
        CD,050,I=1,NUMPTS
        C1=X(I)*SCX+SHIFIX
        C2=Y(I)*SCY+SHIFTY
        IF(C1-EXSIZE19031,SC31,SC34
9031 IF(C2-YSIZE19032,SC32,SC34
9032 IF(C1-SIZE19034,SC34,SC32
9033 IF(C2-SIZE19034,SC34,SC32
9034 IOUT=LCI+1
        GO TO SC35
9035 ICI=C1
        IC2=C2
        GO TO GENERATE CROSSES,
C

```

9036 ICURV(1)=IC1-5
ICURV(2)=IC2-5
ICURV(3)=IC1+5
ICURV(4)=IC2+5
ICURV(5)=IC1-5
ICURV(6)=IC2+5
ICURV(7)=IC1+5
ICURV(8)=IC2-5
ICURV(9)=IC1+5
ICURV(10)=IC2+5
ICURV(11)=IC1-5
ICURV(12)=IC2-5
INUM=12

GO TO SC41
CREATE PLUS.

C 9037 ICURV(1)=IC1-5
ICURV(2)=IC2-5
ICURV(3)=IC1+5
ICURV(4)=IC2+5
ICURV(5)=IC1-5
ICURV(6)=IC2-5
ICURV(7)=IC1+5
ICURV(8)=IC2+5
ICURV(9)=IC1-5
ICURV(10)=IC2+5
ICURV(11)=IC1+5
ICURV(12)=IC2-5
INUM=12

GO TO SC41
CREATE SQUARE.

C 9038 ICURV(1)=IC1+4
ICURV(2)=IC2-4
ICURV(3)=IC1+4
ICURV(4)=IC2+4
ICURV(5)=IC1-4
ICURV(6)=IC2+4
ICURV(7)=IC1-4
ICURV(8)=IC2-4
ICURV(9)=IC1+4
ICURV(10)=IC2-4
ICURV(11)=IC1+4
ICURV(12)=IC2-4
INUM=12

GO TO SC41
CREATE DIAMOND.

C 9039 ICURV(1)=IC1+5
ICURV(2)=IC2
ICURV(3)=IC1

```

ICURV(4)=IC2+5
ICURV(5)=IC1-5
ICURV(6)=IC2
ICURV(7)=IC1
ICURV(8)=IC2-5
ICURV(9)=IC1+5
ICURV(10)=IC2
ICURV(11)=IC1+5
ICURV(12)=IC2
INUM=12
GO TO SC41
C 994C ICURV(1)=IC1+5
ICURV(2)=IC2-2
ICURV(3)=IC1
ICURV(4)=IC2+6
ICURV(5)=IC1-5
ICURV(6)=IC2-3
ICURV(7)=IC1+5
ICURV(8)=IC2-3
INUM=3
SUB1(ICURV,INUM)
9041 CALL INUE1(ICURV,INUM)
9042 CALL WFESE(XAXIS,YAXIS)
CALL SYNECL(XAXIS,YAXIS,.C7,LABEL(2),0.,4)
9043 IF(I-SC49,SC45,SC44,SC45
CALL WFESE(XAXIS,YAXIS)
CALL SYNECL(XAXIS,YAXIS,.C7,LABEL(1),0.,4)
GO TO SC46
9045 COUNTINUE
9046 COUNTINUE
CALL CCNTINUE(SC4E,276,SC4E
IF(IOUT,SC4E,IOUT,SC4E
9048 PRINT(12,29H FINISH) WHERE CFF THE GRAPH.,/)
31C4 FJRMAT(/,IX,12,29H RETURN.
C 276 IF(MSECCL,277,278,277
277 IF(MSECCL,278,277,277
278 ITESI=0
YAXIS=YAXIS+IGT+4
CALL PLC1(0.0,C,YAXIS,-3)
CALL PLC1(0.0,C,YAXIS,-3)
KRITE1(13C1)ITLE
12C FORMAT(1/13H GRAPHITTLEC/2(5X,12A4/),18H HAS BEEN PLOTTED.)
6J TO 2EC

```

```

275 ITESI = 1
28C LAST=C
C RETURN THESE ARE THE NORMAL RETURNS.
C
C ENDO LINE SCALIT (ANUMBR,ISCL10,FACTOR,MCEE)
C   FINALS FACTOR (BETWEEN 1.0 AND 9.999999999999999) AND SCALE OF 10 AS
C   DEFINED BY ANUMBR = FACTOR*10.**ISCL10
C   MCEE IS THE NUMBER OF SIGNIFICANT FIGURES REQUIRED. THIS MUST
C   BE BETWEEN 1 AND 10 OR ISCL10 WILL BE PUT EQUAL TO SIX.
C
C ISCL10 = ALG(ANUMBR)*4.2425448
C FACTOR = ANUMBR/10.*ISCL10
C IF(FACTOR - 0.1)1,2,2
1  ISCL10 = FACTOR*10C.
GO TO 6
2  IF(FACTOR = 1.0)3,4,4
3  ISCL10 = FACTOR - 1
GO TO 6
4  IF(FACTOR = FACTOR*10C - 1
5  ISCL10 = ISCL10 + 2
GO TO 6
6  IF(FACTOR = FACTOR*10C,5,5
7  FACTOR = FACTOR/10C
8  ISCL10 = ISCL10 + 1
9  NODE = 6
GO TO 11
10 IF(1CCE - 10)11,11,9
11 IF(FACTOR = FACTOR*10.**ISCL10 - 1) + 0.5
12 FACTOR = 1FACTR
FACTOR = FACTOR/10.**ISCL10 - 1
IF(FACTOR = 10.)13,12,12
12 FACTOR = 1
ISCL10 = ISCL10 + 1
13 RETURN
C
C FUNC ICODE (ANUMBR)
C   CODES ABSOLUTE VALUE OF A FLOATING POINT NUMBER BETWEEN
C   1.0E-100 AND 1.0E+100 INTO 8-C CHARACTER FCD IN THE FORM
C   1.23E+45.ICODE = 8HCE.CE+0, IF MAGNITUDE OUT OF RANGE.
C
C LINE 11(8)
DATA IFLUS/4HCC00+/,IMINUS/4H000C-,IE/4H000E,IPER/4H000./
BNL1R = 4E5(ANUMBR)

```

```

2 CALL SCALIT(BNUMLR,ISCLIC,FACTCR,3)
  ISIGNSC=SIGN(1,ISCL10)
  ISCL1C=LABS(ISCL1C)
  IFAC=FACTOR*100*CC1
  II(3)=YCC((ISCL10,10)
  II(7)=ISCL10/10
  IF((ISNSC))4,3,3
  II(6)=IFLLS
3 GO TO E
4 II(6)=IVINL5
  II(5)=IE
  II(4)=YCC(IFACT*10)
  II(3)=(YCC(IFACT,10C))/10
  II(2)=IFFR
  II(1)=IFACT/100
  CALL ENCODE(3,ICCDE,II)
  RETURN
END
FUNCTION I1YP2 (ICLMMY)
TYPE KERD GRAPH.
RETURN
END
SUBROUTINE SUB1(IA,N)
DIMENSION IA(2)
IPEN=2
DO 100 I=1,N,2
X=IA(I)
X=X/10C
Y=IA(I+1)
Y=Y/10C
CALL PLET(X,Y,IPEN)
IPEN=2
100 CONTINUE
RETURN
END
SUBROUTINE SPECNO (IVF,IVF2,NH,XAXIS,YAXIS,IA)
DATA MINL/4HOOC/-/
DIMEN$ICN II(4)
MIN$=-252645280
GJTG (100,200),IA
100 TH=0.0 3C2
200 TH=SIN (TR*.0174533)
300 CTB=COS (TH*.C174533)
X=XAXI*-1.*CTB-1.*STB
Y=YAXI*-1.*1.*CTB-1.*STB
INCA$=IVF

```


LITERATURE REFERENCES

- Allen, J. S., "Models of wind-driven currents on the continental shelf", Annual Review of Fluid Mechanics, v. 12, pp. 389-433, 1980.
- Bakun, A., "Coastal upwelling indices, west coast of North America, 1946-71, U.S. Department of Commerce", NOAA Technical Report NMFS SSRF-671, pp. 193.
- Bakun, A., Personal communication, 1981.
- Coddington, K., "Measurement of the California Countercurrent", M.S. Thesis, Naval Postgraduate School, Monterey, June 1979.
- Dreves, D. A., "Sea levels and metered currents off central California", M.S. Thesis, Naval Postgraduate School, Monterey, September 1980.
- Ekman, V. W., "On the influence of the earth's rotation on ocean currents", Arkiv for Matematik, Astronomi, och Fysik, 2(11), pp. 1-52, 1905.
- Halpern, D., et al., "Oceanographic observations of the 1982 warming of the Tropical Eastern Pacific", Science, v. 221, pp. 1173-1175 16 September 1983.
- Hamilton, P. and N. Rattray, "A numerical model of the depth dependent wind-driven upwelling circulation on a continental shelf", Journal of Physical Oceanography, v. 8, pp. 437-457, May 1978.
- Hickey, B. M. and P. Hamilton, "A spin-up model as a diagnostic tool for interpretation of current and density measurements on the continental shelf of the Pacific Northwest", Journal of Physical Oceanography, v. 10, pp. 12-24, 1980.
- Hickey, B. M., "The California Current System - Hypothesis and Facts", Contribution Number 1038 of the Department of Oceanography, University of Washington, 24 April 1978.
- Hickey, B. M., A. Huyer and R. L. Smith, "The alongshore coherence and generation of fluctuations in currents and sea level on the Pacific Northwest continental shelf, winter and spring 1975", Journal of Physical Oceanography, v.11, pp. 822-835, June 1981.

Havoc, A., F. J. C. Sobeck and R. L. Smith, "The spring transition in currents over the Oregon continental shelf", Journal of Geophysical Research, v. 84, pp. 6993-7011, 20 November 1979.

Janowitz, G. S., "A model and observations of time-dependent upwelling over the mid-shelf and slope", Journal of Physical Oceanography, v. 10, pp. 1574-1583, July 1980.

Munk, W. H., "On the wind driven ocean circulation", Journal of Meteorology, v. 7, pp. 79-93, 1950.

O'Brien, J. J. and H. E. Hurlburt, "A numerical model of coastal upwelling", Journal of Physical Oceanography, v. 2, pp. 14-26, January 1972.

O'Brien, J. J., "Upwelling in the ocean: Two and three dimensional models of upper ocean dynamics and variability", Modeling and Prediction of the Upper Layers of the Ocean, Pergamon Press, 1977.

Reid, J. L., G. I. Roden and J. G. Wyllie, "Studies of the California Current System", Progress Report of the California Cooperative Oceanic Fisheries Investigations, 1 July 1956 to 1 January 1958, pp. 28-56, Scripps Institution of Oceanography, La Jolla, California, 1958.

Reid, J. L., Jr. and R. A. Schwatzlose, "Direct measurements of the Davidson Current off central California", Journal of Geophysical Research, v. 67, pp. 559-565, June 1962.

Reid, J. L., Jr., "Measurements of the California Countercurrent at a depth of 250 meters", Journal of Marine Research, v. 20, pp. 134-137, 15 July 1962.

Ryther, J. H., "Photosynthesis and fish production in the sea", Science, v. 166, pp. 72-76, 30 October 1969.

Smith, R. L., "Peru coastal currents during El Nino: 1976 and 1982", Science, v. 221, pp. 1397-1399, 30 September 1983.

Stewart, R. W., "The influence of friction on inertial models of oceanic circulation", Studies on Oceanography, University of Washington Press, 1965.

Suginohara, N., "Coastal upwelling: onshore - offshore circulation, equatorward coastal jet and poleward undercurrent over a continental shelf slope", Journal of Physical Oceanography, v. 12, pp. 272-284, March 1982.

Sverdrup, H. U., M. M. Johnson and R. H. Fleming, The Ocean, their Physics, Chemistry, and general Biology, Prentice-Hall, Inc., Englewood Cliffs, N. J., 1942.

Sverdrup, H. U. and R. H. Fleming, "The waters off the coast of Southern California", Scripps Institute of Oceanography Bulletin, v. 4, pp. 261-375, 9 October 1941.

Wickham, J. B., "Observations of the California Undercurrent", Journal of Marine Research, v. 33, pp. 325-340, September 1975.

INITIAL DISTRIBUTION LIST

	No. Copies
1. Chairman Code 68 Department of Oceanography Naval Postgraduate School Monterey, CA 93943	2
2. Director Naval Oceanography Division (OP952) Navy Department Washington, DC 20350	1
3. Office of Naval Research Code 480 Naval Ocean Research and Development Activity NSFL Station, NSD 39529	1
4. Dr. Robert E. Stevenson Scientific Liaison Office, ONR Scripps Institution of Oceanography La Jolla, CA 92037	1
5. SIO Library University of California, San Diego P.O. Box 2367 La Jolla, CA 92037	1
6. Department of Oceanography Library University of Washington Seattle, WA 98105	1
7. Department of Oceanography Library Oregon State University Corvallis, OR 97331	1
8. Commanding Officer Fleet Numerical Weather Central Monterey, CA 93940	1
9. Commanding Officer Naval Environmental Prediction Research Facility Monterey, CA 93940	1
10. Commander Oceanographic Systems Pacific Box 1390 Pearl Harbor, Hawaii 96860	1

11.	Defense Technical Information Center Camelot Station Alexandria, VA 22314	2
12.	Library Code 0142 Naval Postgraduate School Monterey, CA 93943	2
13.	Commanding Officer Naval Ocean Research and Development Activity NSFL Station, MS 39529	1
14.	Commander Naval Oceanography Command NSFL Station, MS 39529	1
15.	Commanding Officer Naval Oceanographic Office NSFL Station, MS 39529	1
16.	Dr. S. P. Tucker, Code 68Tx Department of Oceanography Naval Postgraduate School Monterey, CA 93943	3
17.	Professor J. B. Wickham, Code 68Wk Department of Oceanography Naval Postgraduate School Monterey, CA 93943	3
18.	Lt. K. Coddington Department of Ocean Sciences U.S. Coast Guard Academy New London, Ct 06320	1
19.	LCDR R. L. Harrod IAGS, Blgd. 144 Ft. Sam Houston, TX 78234	3

END

FILMED

3-85

DTIC